

Fault Diagnosis of Inclined Edge Cracked Cantilever Beam Using Vibrational Analysis and Artificial Intelligence Techniques



Ranjan Kumar Behera

Fault Diagnosis of Inclined Edge Cracked Cantilever Beam Using Vibrational Analysis and Artificial Intelligence Techniques

*A Thesis Submitted to the
Department of Mechanical Engineering
National Institute of Technology, Rourkela
In Partial Fulfillment of the Requirements*

For

The Award of the Degree

Of

Master of Technology
(Machine Design & Analysis)

By

Ranjan Kumar Behera
Roll No. 212ME1273

Under the guidance of
Prof. Dayal R. Parhi



National Institute of Technology, Rourkela

राष्ट्रीय प्रौद्योगिकी संस्थान, राउरकेला

Odisha (India)-769008

May 2014

Declaration

I do, hereby, declare that this submission is my own work and that, to the best of my knowledge and belief, it contains no material previously published or written by another person nor material which to a substantial extent has been accepted for the award of any other degree or diploma of the university or other institute of higher learning, except where due acknowledgement has been made in the text.

Place: NIT Rourkela

(Ranjan Kumar Behera)

Date:



NATIONAL INSTITUTE OF TECHNOLOGY, ROURKELA -769008, ODISHA, INDIA

Certificate

*This is to certify that the thesis entitled, “Fault Diagnosis of Inclined Edge Cracked Cantilever Beam Using Vibrational Analysis and Artificial Intelligence Techniques”, being submitted by Mr. Ranjan Kumar Behera to the Department of Mechanical Engineering, National Institute of Technology, Rourkela, for the partial fulfillment of award of the degree of **Master of Technology** with specialization in **Machine Design & Analysis**, is a record of bona fide research work carried out by him under our supervision and guidance.*

This thesis in our opinion, is worthy of consideration for award of the degree of Master of Technology in accordance with the regulation of the institute. To the best of our knowledge, the results embodied in this thesis have not been submitted to any other University or Institute for the award of any degree or diploma.

Prof. Dayal Ramakrushna Parhi
(Supervisor)
Dept. of Mechanical Engineering
National Institute of Technology
Rourkela-769008, Odisha, India

AREA OF RESEARCH CERTIFICATE

This is to certify that the thesis entitled “**Fault Diagnosis of Inclined Edge Cracked Cantilever Beam Using Vibrational Analysis and Artificial Intelligence Techniques**” submitted for the award of Master of Technology in Mechanical Engineering of National Institute of Technology, Rourkela has been prepared by Ranjan Kumar Behera under my guidance and is original.

Prof. Dayal Ramakrushna Parhi
Supervisor

To my Parents

*Anant koti brahmand nayak rajadhiraj yogiraj parambrahma shri
sachidanand sadguru Shree Sai Nath maharaj Ki
jai.....*

ACKNOWLEDGEMENTS

Foremost, I would like to express my heartfelt gratitude & warm regards to Prof. Dayal Ramakrushna Parhi, my research supervisor, for his patience, continuous support, encouragement, timely guidance, discussions and suggestions. His guidance, great moral support and inspiration helped me throughout the journey of my research and the improvement of writing the thesis. He lives in my heart for ever.

Besides my supervisor, I would like to thank to Prof. Sunil Kumar Sarangi, Director of National Institute of Technology, Rourkela and Prof. K. P. Maity, Head of the Department, Department of Mechanical Engineering, for their insightful comments, encouragement and valuable suggestions regarding the research work. Also, special thanks to the Mechanical Engineering Department of National Institute of Technology, Rourkela for the different facilities they offered.

No words are sufficient to express my heartfelt gratitude to beloved Mr Prases Kumar Mohanty, senior research scholar, for the rock solid support he has rendered at the time of adversity during my research work and preparation of the thesis. The technical assistance of Mr. Maheswar Das is gratefully acknowledged.

My sincere thanks go to all research scholars in Robotics Laboratory, Department of Mechanical Engineering for their invaluable support towards realization of my goal. I would like to thank my best friend Mr. Durjyodhan Sethi for his financial support, kindness & friendship.

Last but not the least; I would greatly indebted to thank my family: my parents Mr. Bidyadhar Behera & Mrs. Jayanti Behera, for giving birth to me at the first place and supporting me spiritually throughout my life; and my loving younger brother Somanath Behera for his constant support.

For any errors or inadequacies that may remain in this work, of course, the responsibility is entirely my own.

Ranjan Kumar Behera

ABSTRACT

Damage is one of the vital characteristics in structural analysis because of safety cause as well as economic prosperity of the industries. Identification of faults in dynamic structures and components are a significant aspect in judgment creating about their overhaul and retirement. Failure to identify the damages has various significances, and they change based on the use, and significance of the vibrating structures and elements. Premature identification of faults in engineering structure during their service period is the great challenge to the engineers because of its importance. Though dynamic based fault diagnosis has been advanced for last three decades and there is large number of literatures, still there are so many problems avoid doing it from application.

The existence of cracks which influence the performance of structures as well as the vibrational parameters like modal natural frequencies, mode shapes, modal damping and stiffness. In this research paper, the effect of crack parameters (relative crack location & crack depth, and crack inclination) on the vibrational parameters of a single inclined edge crack cantilever beam are examined by different techniques using numerical method, finite element analysis (FEA), AI techniques (FUZZY inference method and Artificial Neural Network). Experimental analysis is carried out for verifying the results.

Analytical study has been executed on the cantilever beam with inclined edge crack to get the vibration parameters of the structure by using the derivation of strain energy release rate and stress intensity factor. The existence of inclined crack in a structural element leads a local stiffness that changes its vibration response. The local stiffness matrices at inclined crack position have been calculated using the inverse of local compliance matrices. Suitable boundary conditions are used for predict the variation in the vibration parameters of the cracked cantilever beam from that of the uncrack beam.

Finite Element Method has been accomplished to derive the vibration signatures of the inclined cracked cantilever beam. The results obtained analytically are validated with the results obtained from the FEA. The simulations of FEA have done with the help of ANSYS software. Different artificial intelligent techniques based on Fuzzy controller and Artificial Neural Network controller have been formulated using the computed vibrational parameters for inclined edge crack identification in cantilever beam elements with more precision and significantly low computational period.

CONTENTS

Declaration	i
Certificate	ii
Area of Research Certificate.....	iii
Acknowledgements	v
Abstract.....	vi
Contents	vii
List of Tables	x
List of Figures.....	xi
Nomenclature	xv

1	INTRODUCTION	1
1.1	Theme of Thesis	2
1.2	Motivation of Work	2
1.3	Thesis Layout	3
2	LITERATURE REVIEW	4
2.1	Introduction	5
2.2	Overview	5
2.3	Techniques usages for fault detection	6
	2.3.1 <i>Classical method</i>	6
	2.3.2 <i>Finite element method</i>	9
	2.3.3 <i>Artificial Intelligence (AI) techniques</i>	12
	2.3.3.1 <i>Fuzzy inference method</i>	12
	2.3.3.2 <i>Artificial Neural network method</i>	12
2.4	Objective	13
3	THEORETICAL VIBRATION ANALYSIS FOR IDENTIFICATION OF CRACK	14
3.1	Introduction	15
3.2	Theoretical Analysis	15
	3.2.1 <i>Inclined Crack Model in Cantilever Beam</i>	15

3.2.2	<i>Evaluation of local Flexibility of an Inclined Cracked Cantilever Beam under Axial and Bending Loading</i>	18
3.2.3	<i>Vibration analysis of inclined crack cantilever beam</i>	22
4	FINITE ELEMENT ANALYSIS FOR IDENTIFICATION OF CRACK	27
4.1	Introduction	28
4.2	Steps for Finite Element Analysis	28
4.3	Analysis of Finite Element by ANSYS	29
4.4	Process of Crack Identification	29
4.5	Modal Analysis of cracked beam using finite element analysis (FEA)	30
4.5.1	<i>Variation of relative crack location with relative natural frequencies for particular relative crack depth and crack inclination</i>	35
4.5.2	<i>Variation of relative crack depth with relative natural frequencies for particular relative crack location and crack inclination</i>	32
4.5.3	<i>Variation of relative crack inclination with relative natural frequencies for particular relative crack location and relative crack depth</i>	33
4.5.4	<i>First three mode shapes at different crack location, crack depth & crack angle</i>	33
4.6	Results and discussion of finite element analysis	36
4.6.1	<i>Comparing Results of Finite Element Analysis with Numerical Analysis</i>	36
5	EXPERIMENTAL ANALYSIS FOR IDENTIFICATION OF CRACK	39
5.1	Introduction	40
5.2	Experimental Setup	40
5.3	Experimental Results	41
5.4	Comparison between the results of numerical, finite element and experimental analysis	42
5.5	Discussion	43
6	ANALYSIS OF FUZZY INFERENCE SYSTEM (FIS) FOR IDENTIFICATION OF CRACK	44
6.1	Introduction	45
6.2	Fuzzy inference system (FIS)	45
6.3	Analysis of fuzzy controller used for inclined crack identification	46

6.3.1	<i>Fuzzy mechanism for inclined crack identification</i>	48
6.3.2	<i>Results of fuzzy model</i>	53
6.3.3	<i>Summary</i>	56
7	ANALYSIS OF ARTIFICIAL NEURAL NETWORK FOR IDENTIFICATION OF CRACK	57
7.1	Introduction	58
7.2	Development of an ANN Model	59
7.3	Model Building	61
7.4	Architecture of Neural Networks	63
7.5	Back propagation Algorithm	64
7.6	Analysis of Artificial Neural Network model for crack identification	66
7.7	Results and discussion of neural controller	70
7.8	Summary	74
8	INSTALLATION AND DESCRIPTION OF EXPERIMENTAL SETUP FOR IDENTIFICATION OF CRACK	75
8.1	Introduction	76
8.2	Detail specifications of the vibration measuring instruments	76
8.3	Experimental procedure and its architecture	78
9	CONCLUSIONS AND FUTURE WORK	80
9.1	Contributions	81
9.2	Conclusions	81
9.3	Application	83
9.3	Scope for Future work	84
	REFERENCES	85
	PUBLICATIONS	91
	APPENDIX	93

LIST OF TABLES

Table 4.1	Comparison the results of modal analysis between numerical and FEA	38
Table 5.1	Comparison the results of modal analysis between numerical, FEA and Experimental	43
Table 6.1	Description of Linguistic terms in fuzzy controllers	52
Table 6.2	Comparison between Triangular, Trapezoidal, Gaussian, Bell Shape & Hybrid Fuzzy Controllers results of inclined edge crack in cantilever beams	54
Table 6.3	Comparison between Gaussian, Bell Shape & Hybrid Fuzzy Controllers with FEA & Experimental results of inclined edge crack in cantilever beams	55
Table 7.1	The results of modal analysis obtained from ANN Controller	70
Table 7.2	Comparing the results of modal analysis between numerical, FEA, ANN and Experimental	71
Table 7.3	Comparing the results of modal analysis between Fuzzy Controller, numerical, FEA, ANN and Experimental	72
Table 7.4	Comparing the results of modal analysis between Fuzzy Controller, numerical, FEA, ANN and Experimental	73

LIST OF FIGURES

Figure 2.1	Representation of open cracked cantilever beam with cross-section	7
Figure 2.2	Representation of cracked by rotational spring of cracked cantilever	7
Figure 2.3	Finite element meshing of an open cracked	10
Figure 3.1	Cantilever beam having inclined crack	16
Figure 3.2	Geometry of inclined crack cantilever beam	16
Figure 3.3	Magnified view at the inclined crack section of the beam	16
Figure 3.4	Magnified view at the inclined crack section having equal no. of small division	18
Figure 3.5	Inclined crack cantilever beam, subjected to axial load (P1) and bending moment (P2)	19
Figure 3.6	Magnified view at the inclined crack section having equal no. of division	19
Figure 3.7	Cantilever beam model with inclined edge crack	22
Figure 4.1	Element type SOLID 187	29
Figure 4.2	Relative first mode natural frequencies Vs. Relative crack location from fixed end at crack angle (θ) 30^0	31
Figure 4.3	Relative second mode natural frequencies Vs. Relative crack location from fixed end at crack angle (θ) 30^0	31
Figure 4.4	Relative third mode natural frequencies Vs. Relative crack location from fixed end at crack angle (θ) 30^0	31
Figure 4.5	Relative first mode natural frequencies Vs. Relative crack location from fixed end at relative crack depth (α) 0.3	31
Figure 4.6	Relative Second mode natural frequencies Vs. Relative crack location from fixed end at relative crack depth (α) 0.3	31
Figure 4.7	Relative third mode natural frequencies Vs. Relative crack location from fixed end at relative crack depth (α) 0.3	31
Figure 4.8	Relative first mode natural frequencies Vs. Relative crack depth at crack angle (θ) 35^0	32
Figure 4.9	Relative second mode natural frequencies Vs. Relative crack depth at crack angle (θ) 35^0	32
Figure 4.10	Relative third mode natural frequencies Vs. Relative crack depth at crack angle (θ) 35^0	32
Figure 4.11	Relative first mode natural frequencies Vs. Relative crack depth at relative crack location (β) 0.4	32
Figure 4.12	Relative second mode natural frequencies Vs. Relative crack depth at relative crack location (β) 0.4	32
Figure 4.13	Relative third mode natural frequencies Vs. Relative crack depth at relative crack location (β) 0.4	32
Figure 4.14	Relative natural frequencies Vs. Crack angles at $\beta = 0.3, \alpha = 0.25$	33

Figure 4.15	Relative first mode natural frequencies Vs. Crack angles at $\beta = 0.3, \alpha = 0.25$	33
Figure 4.16	Relative second mode natural frequencies Vs. Crack angles at $\beta = 0.3, \alpha = 0.25$	33
Figure 4.17	Relative third mode natural frequencies Vs. Crack angles at $\beta = 0.3, \alpha = 0.25$	33
Figure 4.18	First mode relative amplitude Vs. Relative location from fixed end at $\beta = 0.25, \alpha = 0.3$ and $\theta = 30^\circ$	33
Figure 4.19	Magnified view of First mode relative amplitude Vs. Relative location from fixed end at $\beta = 0.25, \alpha = 0.3$ and $\theta = 30^\circ$	33
Figure 4.20	Second mode relative amplitude Vs. Relative location from fixed end at $\beta = 0.25, \alpha = 0.3$ and $\theta = 30^\circ$	34
Figure 4.21	Magnified view of Second mode relative amplitude Vs. Relative location from fixed end at $\beta = 0.25, \alpha = 0.3$ and $\theta = 30^\circ$	34
Figure 4.22	Third mode relative amplitude Vs. Relative location from fixed end at $\beta = 0.25, \alpha = 0.3$ and $\theta = 30^\circ$	34
Figure 4.23	Magnified view of Third mode relative amplitude Vs. Relative location from fixed end at $\beta = 0.25, \alpha = 0.3$ and $\theta = 30^\circ$	34
Figure 4.24	Magnified view of First mode relative amplitude Vs. Relative location from fixed end at $\beta = 0.7, \alpha = 0.3$ and $\theta = 30^\circ$	34
Figure 4.25	Magnified view of Second mode relative amplitude Vs. Relative location from fixed end at $\beta = 0.7, \alpha = 0.3$ and $\theta = 30^\circ$	34
Figure 4.26	Magnified view of Third mode relative amplitude Vs. Relative location from fixed end at $\beta = 0.7, \alpha = 0.3$ and $\theta = 30^\circ$	35
Figure 4.27	Magnified view of First mode relative amplitude Vs. Relative location from fixed end at $\beta = 0.25$ and $\theta = 30^\circ$	35
Figure 4.28	Magnified view of Second mode relative amplitude Vs. Relative location from fixed end at $\beta = 0.25$ and $\theta = 30^\circ$	35
Figure 4.29	Magnified view of Third mode relative amplitude Vs. Relative location from fixed end at $\beta = 0.25$ and $\theta = 30^\circ$	35
Figure 4.30	Magnified view of First mode relative amplitude Vs. Relative location from fixed end at $\beta = 0.5$ and $\theta = 30^\circ$	35
Figure 4.31	Magnified view of Second mode relative amplitude Vs. Relative location from fixed end at $\beta = 0.5$ and $\theta = 30^\circ$	35
Figure 4.32	Magnified view of Third mode relative amplitude Vs. Relative location from fixed end at $\beta = 0.5$ and $\theta = 30^\circ$	36
Figure 4.33	Magnified view of First mode relative amplitude Vs. Relative location from fixed end at $\beta = 0.7$ and $\theta = 30^\circ$	36
Figure 4.34	Magnified view of Second mode relative amplitude Vs. Relative location from fixed end at $\beta = 0.7$ and $\theta = 30^\circ$	36
Figure 4.35	Magnified view of Third mode relative amplitude Vs. Relative location from	36

	fixed end at $\beta = 0.7$ and $\theta = 30^\circ$	
Figure 4.36	First mode relative amplitude Vs. Relative location from cantilever end at $\beta = 0.3, \alpha = 0.35$ and $\theta = 35^\circ$	36
Figure 4.37	Magnified view of First mode relative amplitude Vs. Relative location from cantilever end at $\beta = 0.3, \alpha = 0.35$ and $\theta = 35^\circ$	36
Figure 4.38	Second mode relative amplitude Vs. Relative location from cantilever end at $\beta = 0.3, \alpha = 0.35$ and $\theta = 35^\circ$	37
Figure 4.39	Magnified view of Second mode relative amplitude Vs. Relative location from cantilever end at $\beta = 0.3, \alpha = 0.35$ and $\theta = 35^\circ$	37
Figure 4.40	Third mode relative amplitude Vs. Relative location from cantilever end at $\beta = 0.3, \alpha = 0.35$ and $\theta = 35^\circ$	37
Figure 4.41	Magnified view of Third mode relative amplitude Vs. Relative location from cantilever end at $\beta = 0.3, \alpha = 0.35$ and $\theta = 35^\circ$	37
Figure 5.1	Schematic Block Diagram of Experimental set-up	41
Figure 5.2	First mode relative amplitude Vs. Relative location from cantilever end at $\beta = 0.3, \alpha = 0.35$ and $\theta = 35^\circ$	41
Figure 5.3	Magnified view of First mode relative amplitude Vs. Relative location from cantilever end at $\beta = 0.3, \alpha = 0.35$ and $\theta = 35^\circ$	41
Figure 5.4	Second mode relative amplitude Vs. Relative location from cantilever end at $\beta = 0.3, \alpha = 0.35$ and $\theta = 35^\circ$	42
Figure 5.5	Magnified view of Second mode relative amplitude Vs. Relative location from cantilever end at $\beta = 0.3, \alpha = 0.35$ and $\theta = 35^\circ$	42
Figure 5.6	Third mode relative amplitude Vs. Relative location from cantilever end at $\beta = 0.3, \alpha = 0.35$ and $\theta = 35^\circ$	42
Figure 5.7	Magnified view of Third mode relative amplitude Vs. Relative location from cantilever end at $\beta = 0.3, \alpha = 0.35$ and $\theta = 35^\circ$	42
Figure 6.1	Fuzzy inference system	46
Figure 6.2	Triangular Fuzzy Controller	47
Figure 6.3	Trapezoidal Fuzzy Controller	47
Figure 6.4	Gaussian Fuzzy Controller	47
Figure 6.5	Bell-Shaped Fuzzy Controller	48
Figure 6.6	Hybrid Fuzzy Controller	48
Figure 6.7	Triangular Membership functions for RFNF, RSNF and RTNF of vibration respectively	49
Figure 6.8	Triangular Membership functions for RFMD, RSMD and RTMD of vibration respectively	49
Figure 6.9	Triangular Membership functions for RCL, RCD and CA of vibration respectively	50

Figure 6.10	Trapezoidal Membership functions for RFNF, RSNF and RTNF of vibration respectively	50
Figure 6.11	Trapezoidal Membership functions for RFMD, RSMD and RTMD of vibration respectively	50
Figure 6.12	Trapezoidal Membership functions for RCL, RCD and CA of vibration respectively	50
Figure 6.13	Gaussian Membership functions for RFNF, RSNF and RTNF of vibration respectively	50
Figure 6.14	Gaussian Membership functions for RFMD, RSMD and RTMD of vibration respectively	50
Figure 6.15	Gaussian Membership functions for RCL, RCD and CA of vibration respectively	51
Figure 6.16	Bell-Shape Membership functions for RFNF, RSNF and RTNF of vibration respectively	51
Figure 6.17	Bell-Shape Membership functions for RFMD, RSMD and RTMD of vibration respectively	51
Figure 6.18	Bell-Shape Membership functions for RCL, RCD and CA of vibration respectively	51
Figure 6.19	Hybrid Membership functions for RFNF, RSNF and RTNF of vibration respectively	51
Figure 6.20	Hybrid Membership functions for RFMD, RSMD and RTMD of vibration respectively	51
Figure 6.21	Hybrid Membership functions for RCL, RCD and CA of vibration respectively	52
Figure 7.1	Schematic representation of neural network	62
Figure 7.2	Mathematical representation of neural network	62
Figure 7.3	A learning cycle in the ANN model	63
Figure 7.4	Schematic Representation of Neural Model	66
Figure 7.5	Schematic Representation of Neural Model	67

NOMENCLATURE

L	= Length of the beam
b	= Width of the beam
A	= cross-sectional area of the beam
t	= Thickness of the beam
L_1	= Length of the beam from fixed end up to crack section
L_2	= Length of the beam at crack section
L_3	= Length of the beam from free end up to crack section
x	= Crack location or distance from fixed end
a	= Crack depth
θ	= Crack inclination angle
θ'	= Modified crack inclination angle
$\beta (= x/L)$	= Relative crack location
$\alpha (= a/t)$	= Relative crack depth
J	= Strain energy release rate
$K_{1,i} (i = 1, 2)$	= Stress intensity factors for P_i loads
E	= Young's modulus of elasticity of the beam material
ν	= Poisson's ratio
C_{ij}	= Flexibility influence co-efficient
C_{11}	= Axial compliance

$C_{12}= C_{21}$	= Coupled axial and bending compliance
C_{22}	= Bending compliance
\bar{C}_{11}	= Dimensionless form of C_{11}
$\bar{C}_{12}= \bar{C}_{21}$	= Dimensionless form of $C_{12}= C_{21}$
\bar{C}_{22}	= Dimensionless form of C_{22}
A_i (i = 1 to 12)	= Unknown coefficients of matrix A
F_i (i = 1, 2)	= Experimentally determined function
i, j	= Variables
K_{ij}	= Local flexibility matrix elements
P_i (i=1,2)	= Axial force (i=1), Bending moment (i=2)
Q	= Stiffness matrix for free vibration.
u_i (i=1,2)	= Normal functions (longitudinal) $u_i(x)$
x	= Co-ordinate of the beam
y	= Co-ordinate of the beam
y_i (i=1,2)	= Normal functions (transverse) $y_i(x)$
ω	= Natural circular frequency
ρ	= Mass-density of the beam
Λ	= Aggregate (union)
\wedge	= Minimum (min) operation
\forall	= For every

CHAPTER 01

INTRODUCTION

- 1.1. Theme of Thesis**
- 1.2. Motivation of Work**
- 1.3. Thesis Layout**

CHAPTER 01

Introduction

1.1. Theme of the Thesis

In the present research, an effort has been prepared to formulate and develop an inclined edge crack diagnostic tool using the dynamic behavior of cracked and un-cracked cantilever beam element using analytical analysis, finite element analysis, experimental analysis and artificial intelligence techniques.

The different stages for the current analysis are listed below:

1. Analytical analysis for the cantilever beam having single inclined edge crack has been achieved to calculate the modal parameters (natural frequencies and mode shapes).
2. Finite Element Analysis (FEA) has been executed to calculate the vibration signatures of the inclined crack and un-cracked cantilever beam with different crack parameters.
3. Experimental set up has been improved and is being used to get the values of first three relative natural frequencies and average relative mode shape differences of the inclined cracked cantilever member.
4. The modal parameters obtained from analytical, finite element and experimental analysis have been used to formulate and train the artificial intelligence (AI) techniques.

1.2. Motivation of Work

The objective of this paper is to model the beam structures having inclined edge crack at different locations with different crack inclination by taking Euler Bernoulli beam elements. Firstly the modelling and simulation of the crack has done by the help of finite element method using commercial available FEA software ANSYS 12 and estimates the crack position, crack depth and crack angle from the calculated modal data. After that the results come from ANSYS are compared with the analytical results. In the present research, a methodical effort has been made to improve AI based intelligent system for

structural health monitoring of inclined cracked cantilever beam model. The parameters required to formulate and train the AI model have been obtained by using the analytical, finite element and experimental analysis of the inclined cracked cantilever beam structure.

1.3. Thesis Layout

The content of the thesis is organized as follows:

Chapter 1 is the introductory one; it states about the effect of crack on the functionality of different engineering structure and also discuss about the methodologies being adopted by the scientific community to diagnosis faults in different industrial applications.

Chapter 2 followed the literature survey which contains the previous studies had been made in the analysis of cracked structure using vibrational techniques, finite element analysis, fuzzy logic techniques, neuro network techniques.

Chapter 3 introduces the analytical model to calculate the modal parameters (natural frequencies and mode shapes) by using strain energy release rate and putting down different boundary conditions.

Chapter 4 defines the finite element analysis being applied on the cracked beam structure to calculate the dynamic response of the inclined cracked cantilever beams, afterward the measured values are used to identify the crack parameters.

Chapter 5 presents the experimental procedure along with the instruments used for validating the results from techniques being implemented in the present analysis for inclined crack identification.

Chapter 6 shows the applicability of fuzzy inference system for fault diagnosis in cracked structure. The Gaussian, triangular and trapezoidal, bell shape and hybrid membership function based intelligent model with their detail architecture are briefly discussed.

Chapter 7 introduces an inverse technique based on the artificial neural network technique for effective identification of crack damage in a cracked cantilever structure containing inclined crack. Chapter 8 discusses the conclusions drawn from the research carried out on the current topic and gives the recommendations for scope of future work in the same domain.

CHAPTER 02

LITERATURE SURVEY

- 2.1 Introduction**
- 2.2 Overview**
- 2.3 Techniques usages for fault detection**
 - 2.3.1 Classical method*
 - 2.3.2 Finite element method*
 - 2.3.3 Artificial Intelligence (AI) techniques*
 - 2.3.3.1 Fuzzy inference method*
 - 2.3.3.2 Artificial Neural network method*
- 2.4 Objective**

CHAPTER 02

Literature survey

2.1. Introduction

Damage or fault diagnosis, as determined by variation in the dynamic characteristics of structures, is a major issue that has focused in the literature. Most of the researchers are doing their research work related to crack detection using various techniques. A crack in the dynamic structures can lead to untimely failure if it is not identified in early time. The existence of a crack in a structural member leads a local flexibility that changes its vibration response. The main objective is that modal parameters like modal frequencies, mode shapes and modal damping are the functions of the structural properties like damping, stiffness and mass of the structure. So, the variation of structural properties will cause the variation in the modal properties.

According to Doebling et al. [1], one damage identification system commonly classifies four levels of damage assessment:

- Level 1: Determining the presence of damage,
- Level 2: Locating the damage,
- Level 3: Quantifying the damage severity,
- Level 4: Prediction of the remaining serviceability of the structure.

This section emphasizes the various techniques usages by researchers in their research work in the last three decades. The area of research basically includes the analytical approach, FEA approach, experimental validation and the artificial intelligent techniques.

2.2. Overview

Many researchers have used the free and forced vibration techniques for developing procedures for crack detection. The eventual goal of this research is to establish new methodologies which will predict the crack location, crack depth and crack inclination in a dynamically vibrating structure with the help of intelligence technique with considerably less

computational time and high precision. This chapter recapitulates the previous works, mostly in computational methods for structures, and discusses the possible ways for research.

2.3. Techniques usages for fault detection

In the current research paper explain to understand different methods for fault analysis of damaged structures exposed to vary dynamic loading. There mainly following three methods are briefly described for fault diagnoses which are pioneer for all the researchers. They are

2.3.1. Classical Method

2.3.2. Finite element Method

2.3.3. Artificial intelligence (AI) Techniques

2.3.3.1. Fuzzy Inference Method

2.3.3.1.1. Triangular Fuzzy Controller

2.3.3.1.2. Trapezoidal Fuzzy Controller

2.3.3.1.3. Gaussian Fuzzy Controller

2.3.3.1.4. Bell-shaped Fuzzy Controller

2.3.3.1.5. Hybrid Fuzzy Controller

2.3.3.2. Neural Network Method

2.3.4. Experimental Techniques

2.3.1. Classical Method:

In this method contains mainly explain the theoretical model for crack identification. To derive this method by help of using either energy based method, modal response method, algorithm based method or analytical method.

Narkis [2] has used the crack as an equivalent massless spring (as shown in Fig. 1 and Fig. 2) which joins the two parts of the beam. Result from this approximate model in algebraic equations which compare the natural frequencies to beam and crack features. Muller et al. [3] used the theory of Lyapunov exponents to identify the crack of the nonlinear dynamics of a cracked rotating shaft. Chinchalkar [4] has determined the location of a crack in a beam of varying depth by the help of known lowest three natural frequencies of the cracked beam. Here crack is behaved as a rotational spring and graphs are plotted between

spring stiffness and crack location for each natural frequency. The point of intersection of three curves gives the location of the crack.

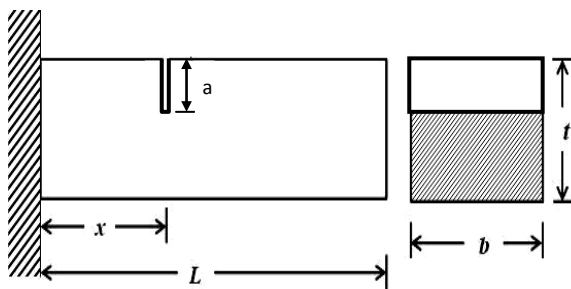


Fig.2.1. Representation of open cracked cantilever beam with cross-section

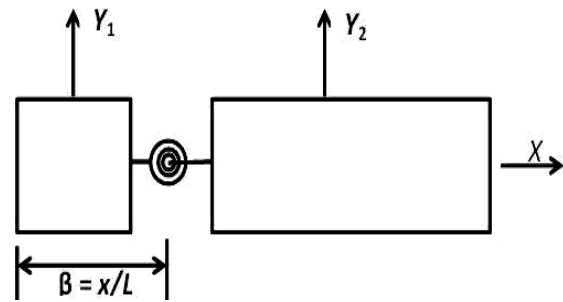


Fig.2.2. Representation of cracked by rotational spring of cracked cantilever

Dado et al. [5] examined the ratio between the natural frequencies of the cracked and uncracked cantilever beam which carrying end mass and rotary inertia and appeared high crack depth ratios to increase the coupling effects. Song et al. [6] evaluated the bending free vibration of cantilevered laminated composites beams having surface crack with based on Laplace transform technique. Majumder and Manohar [7] have developed the damage detection of localized or distributed damages in a beam using a time-domain approach. Lin [8] has explained the direct and inverse problems of simply supported beams having an open crack by the use of analytical transfer matrix method. Here crack size can be calculated by using the correlation among the sectional flexibility and the crack size. Douka et al. [9, 10] calculated instantaneous frequency (IF) by relating empirical mode decomposition and Hilbert transform with the help of both simulated and experimental response data. The variation of IF acts as indicator of the crack size and also help to improve vibration based crack identification techniques. Law and Lu [11] have stated a time domain methods in which detect the crack parameters from strain or displacement measurements. Chondros [12, 13] has determined the circumferential crack due to torsional vibration by the use of Hu–Washizu–Barr variational formulation which improve the differential equation and the boundary conditions of the cracked shaft. Loya et al. [14] found the natural frequencies of Timoshenko cracked beams due to bending vibrations. Here the beam is demonstrated as two segments joined by two massless springs (extensional and rotational) and helps break in both vertical displacement and rotation which are proportional to shear force and bending moment respectively where transmitted by the cracked section.

Viola et al. [15] examined the variations in modal response and the magnitude of natural frequencies of a cracked uniform . They used different and appropriate method which based on the combination of line-spring element and dynamic stiffness matrix to design the cracked beam. Curadelli et al. [16] used wavelet transfer to identify structural damage by the help of the instantaneous damping coefficient identification. Faverjon and Sinou [17] have identified the size and location of the cracks in a simply supported beam by use of a robust damage assessment technique which based on the Constitutive Relation Error (CRE) updating method and crack depth error function. Lee [18] has used easy and effective method to identify the multiple cracks in a beam in which the crack is used as a massless rotational spring. Here finite element method is used as for solving forward problem based on the Euler–Bernoulli beam theory and inverse problem is solved iteratively for the crack positions and dimensions by the Newton–Raphson method. Shih et al. [19] determined damage identification in beams and plates by using multi-criteria approach which includes two methods, one is modal flexibility and another is modal strain energy method. Behzad [20] has developed a continuous model for flexural vibration of beams with an edge crack perpendicular to the neutral plane and used J-integral concept from fracture mechanics and solved by using Hamilton principle and modified Galerkin method. Ryvkin and Slepyan [21] have expressed the resistance of the crack of the square bending beam in the terms of bending moment. The relation is founded on the solutions resulting for the lattice with a semi-infinite original crack and for the associated incessant anisotropic bending plate. Rezaee and Hassannejad [22] have used energy balance method for study of a cracked cantilever beam where both structural damping and crack damping are taken into account and also crack opening and closing during vibration are taken into account. Prasad et al. [23] investigated that the effect of crack position from free end to fixed end of the vibrating cantilever beam at each of the frequency on the resolve of crack growth rate. Rezaee and Hassannejad [24, 25] have examined a new analytical method (perturbation method) for vibrational study of fatigue cracked simply supported beam. Mazanoglu and Sabuncu [26] have presented an algorithm for crack detection from searching over the frequency map and minimizing the measurement errors. Also a statistical approach called ‘recursively scaled zoomed frequencies (RSZF)’ is used for reducing the deviations. Zheng and Ji [27] have calculated the natural frequencies with a variable stiffness distribution along the length of the cracked beam by using improved Rayleigh method. Yan et al. [28] have suggested an algorithm which based on closed form of element modal strain energy sensitivity that helps for detection of statistical structural

damage on simply supported beam with different damage. Mostafa Attar [29] has exemplified a new analytical method to determining both natural frequency and mode shapes of stepped beam having random number of transverse cracks and also calculating the general form of boundary conditions. This method helps to solve the inverse problem of calculating the crack location and crack depth of multiple cracks in the stepped beam. Maghsoodi et al. [30] have formulated a simple method for determining the location of cracks, size of cracks and number of cracks in a multi-stepped beam. They have used natural frequencies and mode shapes of un-cracked beam for determine the above parameters. Behzad et al. [31] have used a simple method for identification of number of edge cracks in beam having different types of cracks. They have taken two types of edge cracks for their verification and solved by energy method and LEFM (Linear Elastic Fracture Mechanics) theory. Using above theory they have demonstrated a relationship among natural frequencies, crack position and stiffness of beam.

2.3.2. Finite Element Method:

Apart from the classical methods, finite element method is also have been used for crack detection in cracked structures. Various research papers from this field are explained in this section.

B. P. Nandwana and S. K. Maiti [32] have calculated the crack position, crack depth and crack inclination by using numerical and experimental method. The inclined crack used as a rotational spring for vibrational analysis which helps to determine the crack location and depth, according to the changes of vibration signatures. The governing equation obtained from the vibration analysis of the beam is manipulated to give a relationship between the stiffness of the spring and the location of the crack. Saavedra and Cuitino [33] have used to calculate the dynamic response of a cracked free-free beam and a U-frame after a harmonic force is applied. For calculating the equations of motion using different integration techniques like Taylor, Hilbert and Hughes which are applied using Matlab software platform. Viola et al. [34] examined the effect of the crack on the stiffness matrix and mass matrix for a cracked Timoshenko beam. Here mass matrix is obtained from the shape function for rotational and translational displacements of the beam and detection of the cracks in beam using modal test data.

Zheng and Kessissoglou [35] have calculated the mode shapes and natural frequencies of cracked beam using finite element method. Here global additional flexibility matrix is used instead of local additional flexibility matrix to determine the total flexibility matrix of a cracked beam. From this total flexibility matrix, the stiffness matrix is obtained. Kisa and Gurel [36, 37] have used both finite element method and component mode synthesis method to analyse the modal analysis of multi-cracked beams. The main feature of this paper is that the mode shapes and natural frequencies of multi-cracked beam can be calculated by knowing two end conditions. To verify their results they have taken a number of numerical examples. Potirniche et al. [38] used two-dimensional element having an implanted edge crack which is not physically designed within the element. Here the element is executed as a User Element (UEL) in the field of commercial finite element code ABAQUS (as shown in Fig. 3). The stiffness matrix of the components for the cracked element is determined from the Castigliano's first theorem with the help of fracture mechanics. This UEL produces good results as compare to experimental results.

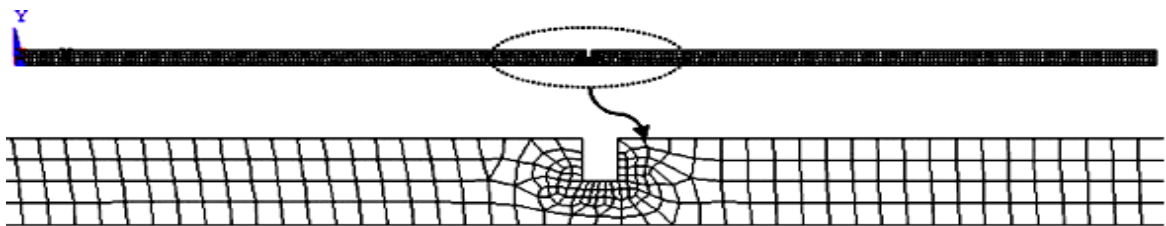


Fig. 3. Finite element meshing of an open cracked

Dong et al. [39] used novel technique, wavelet finite element (WFE) model, having best accuracy modal parameter which represents to identify the position and depth of the transverse crack in a shaft. Here crack itself behaves as a massless rotational spring. Identify the crack position and depth is measured from the intersection of the three natural frequencies curves. Ariaei et al. [40] used both approaches, called finite element method (FEM) and discrete element technique (DET), to find the dynamic response of the Euler–Bernoulli beam having cracks with un-damped and subjected to carrying moving masses. Initially formulate the DET by considering both centrifugal forces and effects of Coriolis on beam then formulate the beam with breathing cracks. Kalanad and Rao [41] have measured relative crack depth up to 0.9 times of total element depth and natural frequency of cracked beam more accurately using two dimensional finite element approaches. The function of frequency response and function of crack size and location are approached by means of surface-fitting techniques. Calculated natural frequencies are used in a crack

identification process and the crack position and depth can be determined by finding the point of intersection of three natural frequencies lines. Karaagac et al. [42] have calculated natural frequencies and stability of the edge cracked circular curved beam using finite element method. The effect of crack size and its location in the cracked beam due to buckling load are calculated by the use of energy principle. They have derived governing matrix equations based on local flexibility concept. Cheng et al. [43] have used p-version finite element method to determine the vibration parameters of cracked rotating tapered beam. They have taken fracture mechanics for calculating stiffness matrix of the crack elements and also have taken Lagrange equation for calculating p-version finite element model of beam. The mode shapes of the cracked beam are found from the spatial wavelet transform approach. Kalanad and Rao [44] have upgraded the two-dimensional finite element who proposed by Potirniche et al. [45] with an embedded edge crack. Here crack depth ratios extending up to 0.9 and for calculating natural frequency of a cracked beam high precisely. The calculated crack position and crack sizes are in good agreement with the experimental data.

Sutar [46] has defined the finite element analysis of a cracked cantilever and examined the relation among the natural frequencies with crack size and crack position. He used single crack at different depth and at different location in the beam and found the relationship between crack depth and natural frequency. For verification he used ALGOR analysis software. Bing et al. [47] identified the multiple crack of beam by using a three-step-meshing method with less subdivision and more precision. It can be used to detection of multiple cracks of complicated structure. Khan and Parhi [48] have determined the variation of crack size on natural frequency and mode shape of cantilever beam by using ANSYS software. Here increasing the natural frequency and decrease the mode shape, the crack size will increase. The experimental results are good agreement with results of finite element analysis. Bouboulas and Anifantis [49] have derived three-dimensional finite element model for analysis the modal behaviour of non-propagating surface crack cantilever beam with dynamic loading. The crack characteristics like location, depth and geometry are extracted from that response. Silani et al. [50] investigated small open crack over shaft by using new finite element approach. In this approach the co-efficient of flexible matrix or the stiffness matrix of elements of crack is calculated with changed integration limits which gives more precise than conventional method.

2.3.3. Artificial Intelligence (AI) Techniques:

There are different types of AI Techniques for identification of fault in damage structures.

2.3.3.1. Fuzzy Inference Method

Sazonov et al. [51] have designed fuzzy expert system based on a finite element (FE) model of a simple beam and have provided reliable detection of damage for every tested damage scenario. Kim et al. [52] have conferred a computer based crack detection system for concrete structures using Fuzzy set theory. They have taken the crack parameters and characteristics to build the rooms for the proposed fuzzy inference system. Boutros et al. [53] have developed four condition monitoring indicators for detection of transient and gradual abnormalities using fuzzy logic approach. Ganguli et al. [54] have used Monte Carlo simulation to study the changes in the damage indicator due to uncertainty in the geometric properties of the beam. The results obtained from the simulation are used for developing and testing the fuzzy logic system. Dash & Parhi [55] have used the fuzzy logic based techniques to detect the cracks in a cantilever beam of uniform cross section. They have utilized the dynamic characteristics such as change in natural frequencies and mode shapes as input to the fuzzy model to predict the crack position and severity, which is subsequently validated by finite element and experimental methods. Sugumaran et al. [56] described the use of decision tree of a fuzzy classifier for selecting best few features that will discriminate the fault condition of the bearing from given trained samples.

2.3.3.2. Neural Network Method

Suresh et al. [57] have described a method considering the flexural vibration in a cantilever beam having transverse crack. They have executed modal frequency parameters analytically for various crack locations and depths and these parameters are used to train the neural network to identify the damage location and size. Mehrjoo et al. [58] have presented a fault detection inverse algorithm to estimate the damage intensities of joints in truss bridge structure using back propagation neural network method. Das & Parhi [59] have presented an artificial neural network (ANN) technique to predict crack location and crack depth in a cracked cantilever beam. They have used first three relative natural frequencies and relative mode shapes as input parameters to the ANN. Paviglianiti et al. [60] have devised a scheme for detecting and isolating sensor faults in industrial robot manipulators. The dynamics of the proposed scheme has been enriched by using radial

basis functions neural network. Eski et al. [61] have presented a fault detection based on neural network for an experimental industrial welding robot. Parhi & Dash [62] have analyzed the cantilever beam with multiple cracks for its vibrational characteristics, which in turn is being utilized to train the neural network controller complemented with back propagation technique.

2.4. Objective

The objective of this paper is to model the beam structures having inclined edge crack at different locations with different crack inclination by taking Euler Bernoulli beam elements. Secondly the modeling and simulation of the crack has done by the help of finite element method using commercial available FEA software ANSYS 12 and estimates the crack position and crack depth from the calculated modal data. After that the results come from ANSYS are compared with the analytical results. In the present analysis, a methodical effort has been made to improve AI based intelligent system for structural health monitoring of cracked cantilever beam model. The parameters required to formulate and train the AI model have been obtained by using the theoretical, finite element and experimental analysis of the cracked cantilever beam element.

CHAPTER 03

THEORETICAL VIBRATION ANALYSIS FOR IDENTIFICATION OF CRACK

3.1. Introduction

3.2. Theoretical Analysis

3.2.1. *Inclined Crack Model in Cantilever Beam*

3.2.2. *Evaluation of local Flexibility of an Inclined Cracked Cantilever Beam under Axial and Bending Loading*

3.2.3. *Vibration analysis of inclined crack cantilever beam*

CHAPTER 03

THEORETICAL VIBRATION ANALYSIS FOR IDENTIFICATION OF CRACK

3.1. Introduction

In this present research work it has been analysed that the crack can be detected in the various structures through visual inspection or by the method of measuring natural frequency, mode shape and structural damping. As the measurement of natural frequency and mode shape is quite easy as compared to other parameters, so in this chapter a logical approach has been adopted to develop the expression to calculate the natural frequency and the mode shape of the cantilever beam with the presence of a transverse crack and the effect of natural frequency in the presence of crack. Experimental analysis has been done over cracked cantilever beam specimen for validation of the theory established.

3.2. Theoretical Analysis

In this analysis, theoretical modeling of un-cracked cantilever beam for calculating the modal parameters i.e. modal frequencies and mode shapes and also modeling of cracked cantilever beam for calculating the modal parameters of the crack beam having inclined edge crack for different crack parameters i.e. crack locations, crack depths and crack inclinations. The proposed theoretical method has been established by comparing the results with both finite element analysis and the experimental analysis.

3.2.1. Inclined Crack Model in Cantilever Beam

A cantilever beam of length 'L' ($=L_1+L_2+L_3$), width 'b', thickness 't' having inclined crack at a distance 'L₁' from the fixed end as shown in Fig.3.1 and Fig. 3.2. The Fig. 3.3 represents magnified view at crack region. Let Δ MNP which is very small which doesn't affect the stiffness of the whole beam, i.e. neglect the mass of Δ MNP.

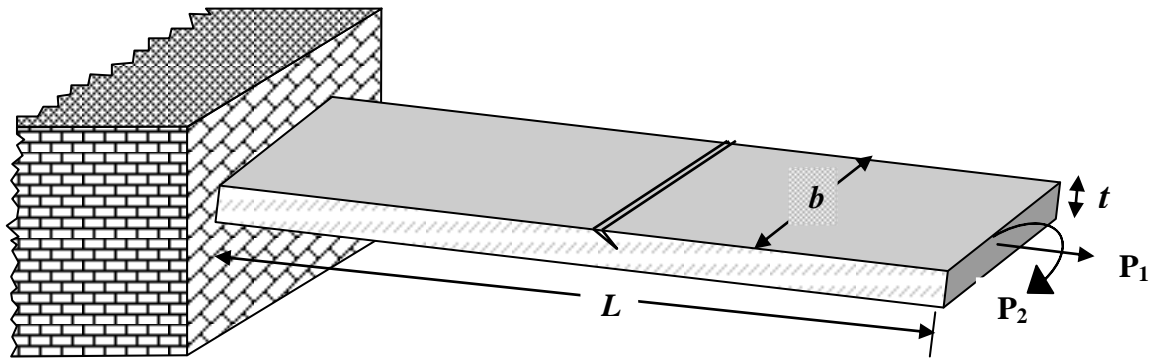


Fig.3.1. Cantilever beam having inclined crack

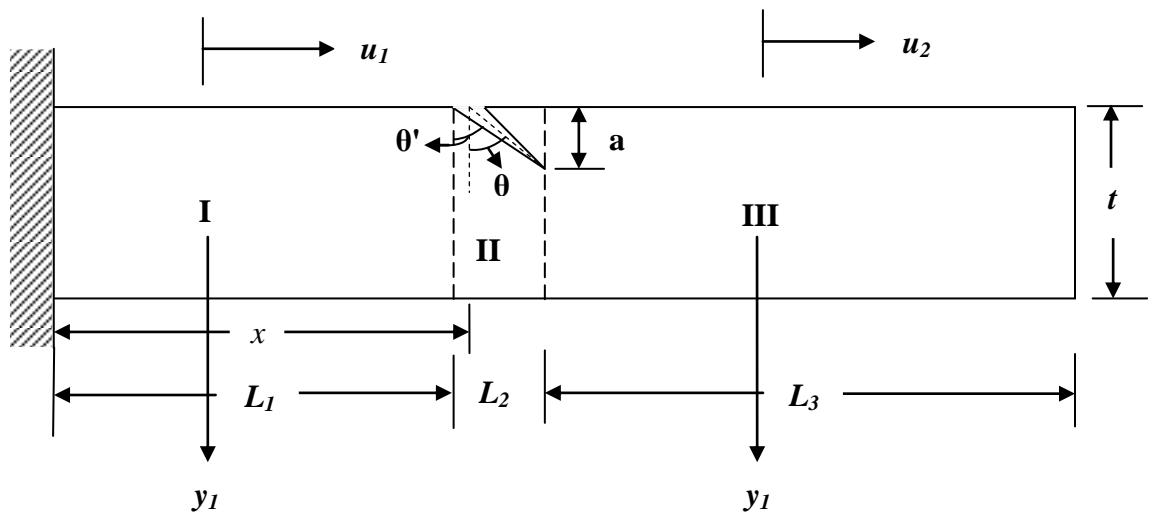


Fig.3.2. Geometry of inclined crack cantilever beam

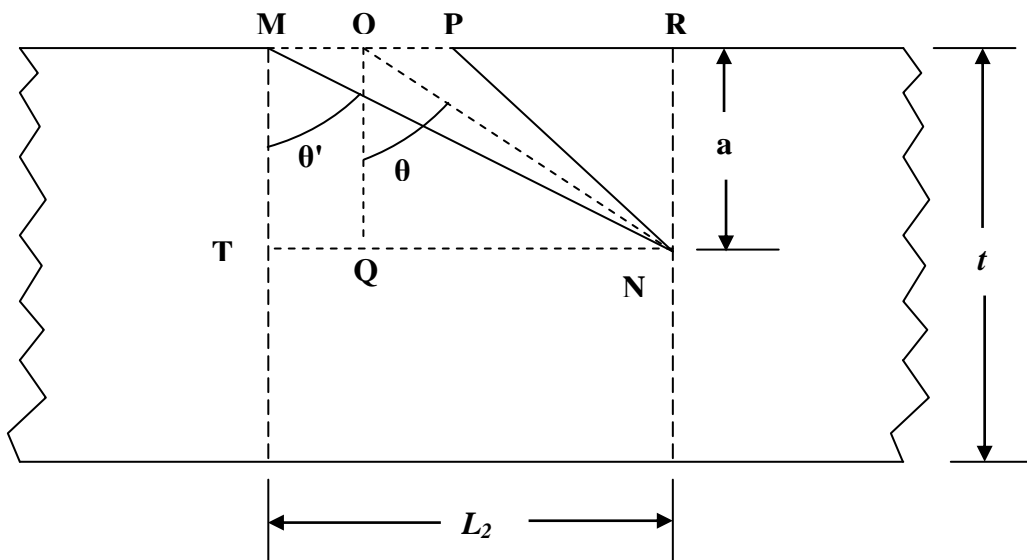


Fig. 3.3. Magnified view at the inclined crack section of the beam

Let $\angle QON=\theta$ and $\angle TMN=\theta'$, where θ and θ' are the crack inclination angle and modified crack inclination angle respectively. Here we assume crack opening (=MO+OP) is 0.0008 m = 0.8 mm.

In ΔQON and ΔMNT ,

$$\begin{aligned} \tan\theta &= \frac{QN}{OQ} = \frac{QN}{a} = \frac{L_2 - 0.0004}{a} = \frac{a \times \tan\theta' - 0.0004}{a} \\ \Rightarrow \theta &= \tan^{-1} \left[\frac{a \times \tan\theta' - 0.0004}{a} \right] \end{aligned} \quad (3.1)$$

$$\tan\theta' = \frac{TN}{MT} = \frac{TQ+QN}{a} = \frac{0.0004+a \times \tan\theta}{a} = \frac{L_2}{a} \quad (3.2)$$

$$\theta' = \tan^{-1} \left[\frac{L_2}{a} \right] = \tan^{-1} \left[\frac{0.0004+a \times \tan\theta}{a} \right] \quad (3.3)$$

The beam is divided into three parts I, II and III as shown in Fig. 3.2. Consider the whole beam is an Euler-Bernoulli's beam. Here

$$\left. \begin{aligned} L_1 &= x - 0.0004 \\ L_2 &= 0.0004 + a \times \tan\theta \\ L_3 &= L - (x + a \times \tan\theta) \end{aligned} \right\} \quad (3.4)$$

Let $\alpha = \frac{a}{t}$ = Relative Crack Depth and $\beta = \frac{x}{L}$ = Relative Crack Location. Put these values in eq. (3.4), we get

$$\left. \begin{aligned} L_1 &= \beta L - 0.0004 \\ L_2 &= 0.0004 + \alpha t \times \tan\theta \\ L_3 &= L - (\beta L + \alpha t \times \tan\theta) \end{aligned} \right\} \quad (3.5)$$

Put the values of $L = 0.8$ m and $t = 0.006$ m in eq. (3.5). At crack position, we take 'N' number of equal divisions i.e. $n=1,2,3,4,\dots,N$ as shown in Fig.3.4. So, each division having length

$$L_n = \frac{L_2}{N} \quad (3.6)$$

Now thickness of 1st section is

$$\left. \begin{aligned} t_1 &= t - MM' \\ \Rightarrow t_1 &= t - \frac{L_2}{N \times \tan \theta'} \end{aligned} \right\} \quad (3.7)$$

In general thickness of each section will be

$$t_n = t - \frac{n \times L_2}{N \times \tan \theta'} \quad (3.8)$$

The crack depth and relative crack depth of each section are given in eq. (3.5).

$$\left. \begin{aligned} a_n &= \frac{n \times L_2}{N \times \tan \theta'} \\ \alpha_n &= \frac{n \times L_2}{t \times N \times \tan \theta'} \end{aligned} \right\} \quad (3.9)$$

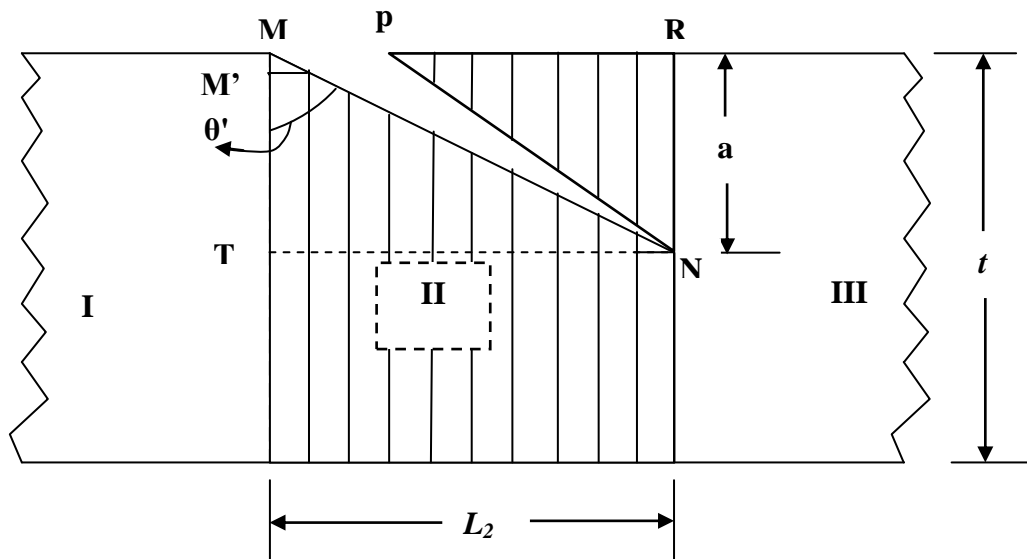


Fig. 3.4. Magnified view at the inclined crack section having equal no. of small division

3.2.2. Evaluation of local Flexibility of an Inclined Cracked Cantilever Beam under Axial and Bending Loading:

Below Fig. 3.5 and Fig. 3.6 represent inclined crack cantilever beam, subjected to axial load (P_1) as well as bending moment (P_2). The loading provides a coupling effect resulting

in both longitudinal and transverse motion of the beam. The beam contains inclined crack having length 'L', maximum crack depth 'a', crack depth at nth section of crack 'a_n', width 'b' and thickness 't'.

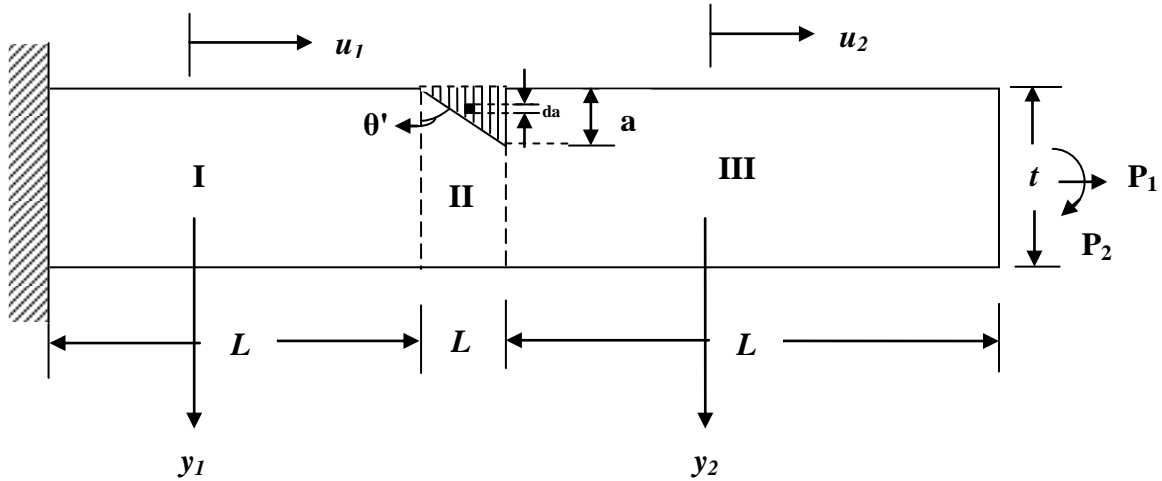


Fig. 3.5. Inclined crack cantilever beam, subjected to axial load (P1) and bending moment (P2)

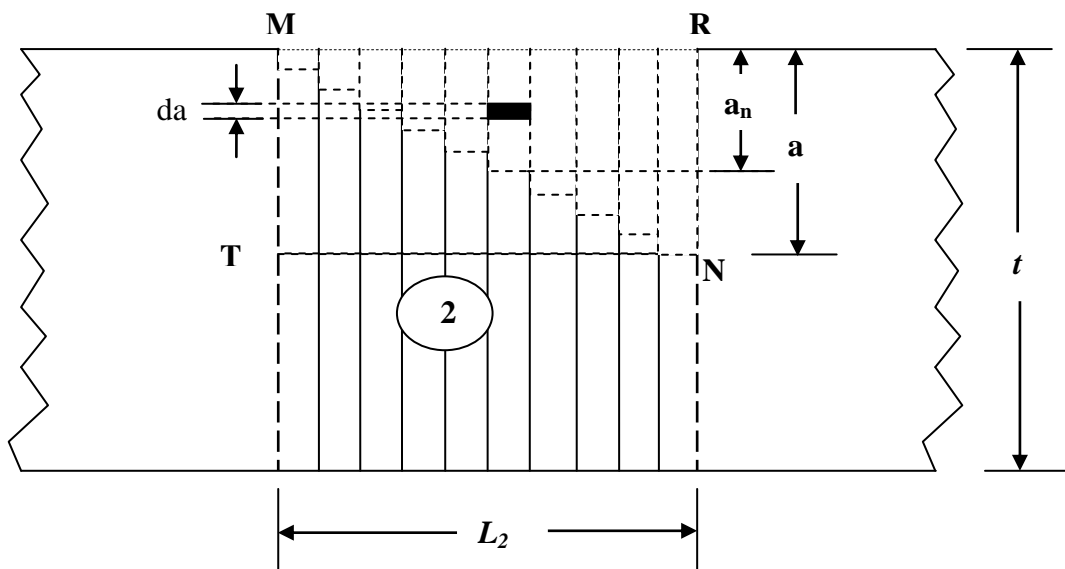


Fig. 3.6. Magnified view at the inclined crack section having equal no. of division

Due to the presence of crack in the beam a local stiffness will be introduced and 2×2 matrix is considered, which represent the stiffness of the beam. At the section strain energy release rate can be explained as [63];

$$J = \frac{1}{E'} (K_{I1} + K_{I2})^2 \quad (3.10)$$

$$\text{Where } \frac{1}{E'} = \frac{1-\nu^2}{E} \text{ (for plane strain)} \quad (3.11)$$

$$\frac{1}{E'} = \frac{1}{E} \text{ (For plane stress)} \quad (3.12)$$

$(K_{I1})_n$, $(K_{I2})_n$ are the stress intensity factors of mode I (opening of the crack) for load P_1 and P_2 respectively at “nth” section of the crack. The values of stress intensity factors from earlier studies [63] are;

$$\left. \begin{aligned} (K_{I1})_n &= \frac{P_1}{bt} \sqrt{\pi a_n} \left(F_1 \left(\frac{a_n}{t} \right) \right) \\ (K_{I2})_n &= \frac{6P_2}{bt^2} \sqrt{\pi a_n} \left(F_2 \left(\frac{a_n}{t} \right) \right) \end{aligned} \right\} \quad (3.13)$$

The expression for F_1 and F_2 are given below

$$\left. \begin{aligned} F_1 \left(\frac{a_n}{t} \right) &= \left(\frac{2t}{\pi a_n} \tan \left(\frac{\pi a_n}{2t} \right) \right)^{0.5} \left\{ \frac{0.752 + 2.02(a_n/t) + 0.37(1 - \sin(\pi a_n/2t))^3}{\cos(\pi a_n/2t)} \right\} \\ F_2 \left(\frac{a_n}{t} \right) &= \left(\frac{2t}{\pi a_n} \tan \left(\frac{\pi a_n}{2t} \right) \right)^{0.5} \left\{ \frac{0.923 + 0.199(1 - \sin(\pi a_n/2t))^4}{\cos(\pi a_n/2t)} \right\} \end{aligned} \right\} \quad (3.14)$$

Let U_t be the strain energy due to the crack. According to Castigliano’s theorem, the additional displacement along the force P_i is:

$$u_i = \frac{\partial U_t}{\partial P_i} \quad (3.15)$$

The form of strain energy will have,

$$U_t = \int_0^{a_n} J da_n = \int_0^{a_n} \frac{\partial U_t}{\partial a} da_n, \quad n = 1, 2, 3, 4, \dots, N \quad (3.16)$$

Where $J = \frac{\partial U_t}{\partial a_n}$ the strain energy density function.

From eq. (3.10) and (3.16), we can have

$$u_i = \frac{\partial}{\partial P_i} \left[\int_0^{a_n} J(a_n) da_n \right] \quad (3.17)$$

$(C_{ij})_n$ = Flexibility influence co-efficient at n^{th} crack section. According to definition,

$$(C_{ij})_n = \frac{\partial u_i}{\partial P_j} = \frac{\partial^2}{\partial P_i \partial P_j} \int_0^{a_n} J(a_n) da_n \quad (3.18)$$

and can be expressed as,

$$(C_{ij})_n = \frac{b}{E'} \frac{\partial^2}{\partial P_i \partial P_j} \int_0^{a_n} [(K_{11})_n + (K_{12})_n]^2 da_n \quad (3.19)$$

Putting $\alpha_n = a_n/t$ and $da_n = \frac{da_n}{t}$ in eq. (3.19), we get

$$(C_{ij})_n = \frac{bt}{E'} \frac{\partial^2}{\partial P_i \partial P_j} \int_0^{\alpha_n} [(K_{11})_n + (K_{12})_n]^2 d\alpha_n \quad (3.20)$$

Where $\alpha_n = a_n/t$ and when $a=0; \alpha=0$. Using eq. (3.20), the compliance

$(C_{11})_n, (C_{12})_n$ [= $(C_{21})_n$] and $(C_{22})_n$ we get,

$$\left. \begin{aligned} (C_{11})_n &= \frac{bt}{E'} \int_0^{\alpha_n} \frac{\pi a_n}{b^2 t^2} 2(F_1(\alpha_n))^2 d\alpha_n \\ &= \frac{2\pi}{bE'} \int_0^{\alpha_n} [\alpha_n (F_1(\alpha_n))]^2 d\alpha_n \end{aligned} \right\} \quad (3.21)$$

$$(C_{12})_n = (C_{21})_n = \frac{12\pi}{E'bt} \int_0^{\alpha_n} [\alpha_n (F_1(\alpha_n)F_2(\alpha_n))] d\alpha_n \quad (3.22)$$

$$(C_{22})_n = \frac{72\pi}{E'bt^2} \int_0^{\alpha_n} [\alpha_n (F_2(\alpha_n))^2] d\alpha_n \quad (3.23)$$

The dimensionless form of the influence co-efficient will be;

$$\overline{(C_{11})}_n = (C_{11})_n \frac{bE'}{2\pi} ; \overline{(C_{12})}_n = \overline{(C_{21})}_n = (C_{12})_n \frac{E'bt}{12\pi} ; \overline{(C_{22})}_n = (C_{22})_n \frac{E'bt^2}{72\pi} \quad (3.24)$$

The inversion of compliance matrix will get local stiffness matrix and can be written as;

$$\mathbf{K} = \begin{bmatrix} (C_{11})_n & (C_{12})_n \\ (C_{21})_n & (C_{22})_n \end{bmatrix}^{-1} = \begin{bmatrix} (K_{11})_n & (K_{12})_n \\ (K_{21})_n & (K_{22})_n \end{bmatrix} \quad (3.25)$$

3.2.3. Vibration analysis of inclined crack cantilever beam:

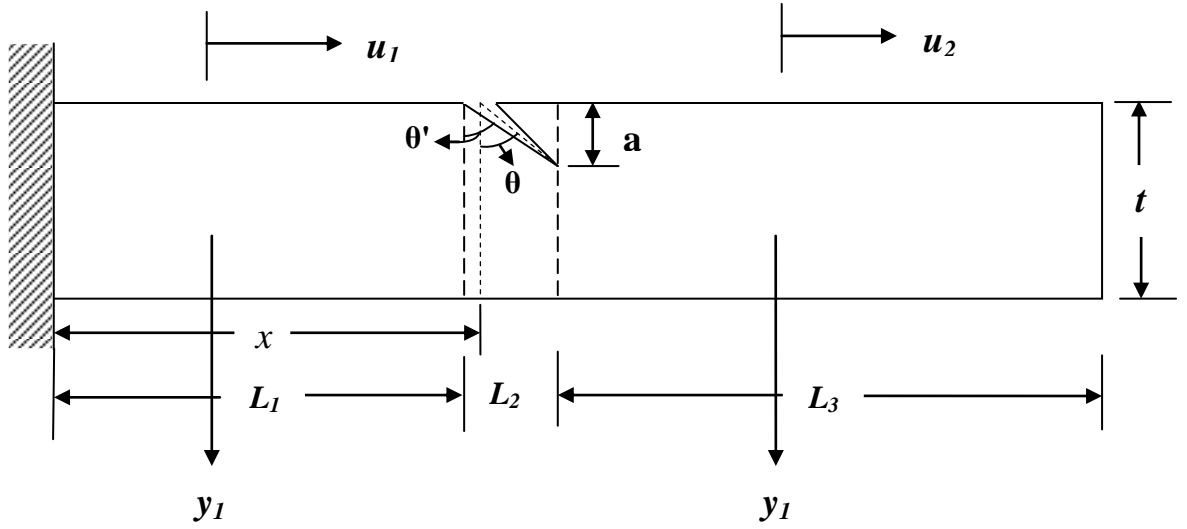


Fig. 3.7. Cantilever beam model with inclined edge crack

A cantilever beam of length 'L' ($=L_1+L_2+L_3$), width 'b', thickness 't' having inclined crack at a distance ' L_1 ' from the fixed end as shown in Fig.3.7. Here L_2 is length of the inclined crack region which is very much small as compared to length of the beam. The amplitude of the longitudinal vibration have been taken $u_1(x,t)$ and $u_2(x,t)$, and amplitudes of bending vibration have been considered as $y_1(x,t)$ and $y_2(x,t)$ for the section before and after the crack as shown in Fig. 3.16. The expressions of the normal function for the system can be defined as

$$\bar{u}_1(\bar{x}) = A_1 \cos(\bar{K}_u \bar{x}) + A_2 \sin(\bar{K}_u \bar{x}) \quad (3.26)$$

$$\bar{u}_2(\bar{x}) = A_3 \cos(\bar{K}_u \bar{x}) + A_4 \sin(\bar{K}_u \bar{x}) \quad (3.27)$$

$$\bar{y}_1(\bar{x}) = A_5 \cosh(\bar{K}_y \bar{x}) + A_6 \sinh(\bar{K}_y \bar{x}) + A_7 \cos(\bar{K}_y \bar{x}) + A_8 \sin(\bar{K}_y \bar{x}) \quad (3.28)$$

$$\bar{y}_2(\bar{x}) = A_9 \cosh(\bar{K}_y \bar{x}) + A_{10} \sinh(\bar{K}_y \bar{x}) + A_{11} \cos(\bar{K}_y \bar{x}) + A_{12} \sin(\bar{K}_y \bar{x}) \quad (3.29)$$

$$\text{Where } \bar{x} = x/L; \bar{u} = u/L; \bar{y} = y/L; \beta = L_1/L; \bar{K}_u = \frac{\omega \times L}{\left(\frac{E}{\rho}\right)^{0.5}}; \bar{K}_y = \left[\frac{\omega \times L^2}{\left(\frac{E \times I}{A \times \rho}\right)^{0.5}} \right]^{0.5} \quad (3.30)$$

The constants A_i , (i=1 to 12) are to be determined from boundary conditions. The boundary conditions of the cantilever beam is considered are;

At fixed end $x = \bar{x} = 0$;

$$\bar{u}_1(0) = 0 \quad (3.31)$$

$$\bar{y}_1(0) = 0 \quad (3.32)$$

$$\bar{y}'_1(0) = 0 \quad (3.33)$$

At free end $x = L, \bar{x} = 1$;

$$\bar{u}'_2(1) = 0 \quad (3.34)$$

$$\bar{y}''_2(1) = 0 \quad (3.35)$$

$$\bar{y}'''_2(1) = 0 \quad (3.36)$$

At the crack section;

$$\bar{u}'_1(\beta) = \bar{u}'_2(\beta) \quad (3.37)$$

$$\bar{y}_1(\beta) = \bar{y}_2(\beta) \quad (3.38)$$

$$\bar{y}''_1(\beta) = \bar{y}''_2(\beta) \quad (3.39)$$

$$\bar{y}'''_1(\beta) = \bar{y}'''_2(\beta) \quad (3.40)$$

We take ‘N’ number of small equal divisions at crack section. Here we compare two crack positions i.e. middle of the crack region ($n = N/2$ section) which is crack prominent and end of the crack region ($n = N$) is more prominent. Because our assumption crack depth at $n = 1$ to $n = N$ goes on increase.

Also at the cracked section (due to the discontinuity of axial deformation to the left and right of the crack location at the distance L_1 from the fixed end of the beam), we have:

$$AE \frac{du_1(L_1)}{dx} = (K_{11})_N [u_2(L_1)] - (K_{11})_{N/2} [u_1(L_1)] + (K_{12})_N \left[\frac{dy_2(L_1)}{dx} \right] - (K_{12})_{N/2} \left[\frac{dy_1(L_1)}{dx} \right] \quad (3.41)$$

Similarly at the crack section (due to discontinuity of slope to the left and right of the crack), we have:

$$EI \frac{d^2y_1(L_1)}{dx^2} = (K_{21})_N [u_2(L_1)] - (K_{21})_{N/2} [u_1(L_1)] + (K_{22})_N \left[\frac{dy_2(L_1)}{dx} \right] - (K_{22})_{N/2} \left[\frac{dy_1(L_1)}{dx} \right] \quad (3.42)$$

By using normal functions, eq. (3.26), eq.(3.27), eq.(3.28) and eq.(3.29) along with boundary conditions as mention above (eq. (3.31) to eq.(3.40)), yield characteristic equations (eq. (3.41) & eq.(3.42)) of the system as:

$$|Q|=0 \quad (3.43)$$

Where Q is the 12X12 matrix and is expressed as following 12 boundary conditions, i.e. the value of eq. (3.31) to (3.42), we get the values A_1 to A_{12} .

$$\begin{bmatrix} 1 & 0 & 0 & 0 & 0 & 0 & 0 & 0 & 0 & 0 & 0 & 0 \\ 0 & 0 & 0 & 0 & 1 & 0 & 1 & 0 & 0 & 0 & 0 & 0 \\ 0 & 0 & 0 & 0 & 0 & 1 & 0 & 1 & 0 & 0 & 0 & 0 \\ 0 & 0 & -R_1 & R_2 & 0 & 0 & 0 & 0 & 0 & 0 & 0 & 0 \\ 0 & 0 & 0 & 0 & 0 & 0 & 0 & 0 & S_1 & S_2 & -S_3 & -S_4 \\ 0 & 0 & 0 & 0 & 0 & 0 & 0 & 0 & S_5 & S_6 & S_7 & -S_8 \\ T_1 & -T_2 & T_1 & T_2 & 0 & 0 & 0 & 0 & 0 & 0 & 0 & 0 \\ 0 & 0 & 0 & 0 & T_3 & T_4 & T_5 & T_6 & -T_3 & -T_4 & -T_5 & -T_6 \\ 0 & 0 & 0 & 0 & T_7 & T_8 & -T_9 & -T_{10} & -T_7 & -T_8 & T_9 & T_{10} \\ 0 & 0 & 0 & 0 & T_{11} & T_{12} & T_{13} & -T_{14} & -T_{11} & -T_{12} & -T_{13} & T_{14} \\ M_1 & -M_2 & M_3 & M_4 & -M_5 & -M_6 & M_7 & -M_8 & M_9 & M_{10} & -M_{11} & M_{12} \\ N_1 & -N_2 & -N_3 & N_4 & -N_5 & -N_6 & N_7 & N_8 & N_9 & N_{10} & -N_{11} & N_{12} \end{bmatrix} \begin{Bmatrix} A_1 \\ A_2 \\ A_3 \\ A_4 \\ A_5 \\ A_6 \\ A_7 \\ A_8 \\ A_9 \\ A_{10} \\ A_{11} \\ A_{12} \end{Bmatrix} = 0 \quad (3.44)$$

$$|Q| = \begin{vmatrix} 1 & 0 & 0 & 0 & 0 & 0 & 0 & 0 & 0 & 0 & 0 & 0 \\ 0 & 0 & 0 & 0 & 1 & 0 & 1 & 0 & 0 & 0 & 0 & 0 \\ 0 & 0 & 0 & 0 & 0 & 1 & 0 & 1 & 0 & 0 & 0 & 0 \\ 0 & 0 & -R_1 & R_2 & 0 & 0 & 0 & 0 & 0 & 0 & 0 & 0 \\ 0 & 0 & 0 & 0 & 0 & 0 & 0 & 0 & S_1 & S_2 & -S_3 & -S_4 \\ 0 & 0 & 0 & 0 & 0 & 0 & 0 & 0 & S_5 & S_6 & S_7 & -S_8 \\ T_1 & -T_2 & T_1 & T_2 & 0 & 0 & 0 & 0 & 0 & 0 & 0 & 0 \\ 0 & 0 & 0 & 0 & T_3 & T_4 & T_5 & T_6 & -T_3 & -T_4 & -T_5 & -T_6 \\ 0 & 0 & 0 & 0 & T_7 & T_8 & -T_9 & -T_{10} & -T_7 & -T_8 & T_9 & T_{10} \\ 0 & 0 & 0 & 0 & T_{11} & T_{12} & T_{13} & -T_{14} & -T_{11} & -T_{12} & -T_{13} & T_{14} \\ M_1 & -M_2 & M_3 & M_4 & -M_5 & -M_6 & M_7 & -M_8 & M_9 & M_{10} & -M_{11} & M_{12} \\ N_1 & -N_2 & -N_3 & N_4 & -N_5 & -N_6 & N_7 & N_8 & N_9 & N_{10} & -N_{11} & N_{12} \end{vmatrix} = 0 \quad (3.45)$$

Where

$$\bar{K}_y = \left[\frac{\omega \times L^2}{\left(\frac{E \times I}{A \times \rho} \right)^{0.5}} \right]^{0.5}; \quad \bar{K}_u = \frac{\omega \times L}{\left(\frac{E}{\rho} \right)^{0.5}}; \quad \beta = L_1 / L$$

$$P = \bar{K}_y$$

$$R_1 = \bar{K}_u \times \sin(\bar{K}_u); \quad R_2 = \bar{K}_u \times \cos(\bar{K}_u)$$

$$S_1 = \bar{K}_y^2 \times \cosh(\bar{K}_y); \quad S_2 = \bar{K}_y^2 \times \sinh(\bar{K}_y); \quad S_3 = \bar{K}_y^2 \times \cos(\bar{K}_y); \quad S_4 = \bar{K}_y^2 \times \sin(\bar{K}_y)$$

$$S_5 = \bar{K}_y^3 \times \sinh(\bar{K}_y); \quad S_6 = \bar{K}_y^3 \times \cosh(\bar{K}_y); \quad S_7 = \bar{K}_y^3 \times \sin(\bar{K}_y); \quad S_8 = \bar{K}_y^3 \times \cos(\bar{K}_y)$$

$$T_1 = \bar{K}_u \times \sin(\bar{K}_u \beta); \quad T_2 = \bar{K}_u \times \cos(\bar{K}_u \beta);$$

$$T_3 = \cosh(\bar{K}_y \beta); \quad T_4 = \sinh(\bar{K}_y \beta); \quad T_5 = \cos(\bar{K}_y \beta); \quad T_6 = \sin(\bar{K}_y \beta)$$

$$T_7 = \bar{K}_y^2 \cosh(\bar{K}_y \beta); \quad T_8 = \bar{K}_y^2 \sinh(\bar{K}_y \beta); \quad T_9 = \bar{K}_y^2 \cos(\bar{K}_y \beta); \quad T_{10} = \bar{K}_y^2 \sin(\bar{K}_y \beta)$$

$$T_{11} = \bar{K}_y^3 \sinh(\bar{K}_y \beta); \quad T_{12} = \bar{K}_y^3 \cosh(\bar{K}_y \beta); \quad T_{13} = \bar{K}_y^3 \sin(\bar{K}_y \beta); \quad T_{14} = \bar{K}_y^3 \cos(\bar{K}_y \beta)$$

$$M_1 = AE\bar{K}_u \sin(\bar{K}_u \beta) - (K_{11})_5 L \cos(\bar{K}_u \beta) ; M_2 = AE\bar{K}_u \cos(\bar{K}_u \beta) + (K_{11})_5 L \sin(\bar{K}_u \beta) ;$$

$$M_3 = (K_{11})_{10} L \cos(\bar{K}_u \beta) ; M_4 = (K_{11})_{10} L \sin(\bar{K}_u \beta) ; M_5 = (K_{12})_5 \bar{K}_y \sinh(\bar{K}_y \beta) ;$$

$$M_6 = (K_{12})_5 \bar{K}_y \cosh(\bar{K}_y \beta) ; M_7 = (K_{12})_5 \bar{K}_y \sin(\bar{K}_y \beta) ; M_8 = (K_{12})_5 \bar{K}_y \cos(\bar{K}_y \beta) ;$$

$$M_9 = (K_{12})_{10} \bar{K}_y \sinh(\bar{K}_y \beta) ; M_{10} = (K_{12})_{10} \bar{K}_y \cosh(\bar{K}_y \beta) ; M_{11} = (K_{12})_{10} \bar{K}_y \sin(\bar{K}_y \beta) ;$$

$$M_{12} = (K_{12})_{10} \bar{K}_y \cos(\bar{K}_y \beta)$$

$$N_1 = (K_{21})_5 L \bar{K}_u \sin(\bar{K}_u \beta) ; N_2 = (K_{21})_5 L \bar{K}_u \cos(\bar{K}_u \beta) ; N_3 = (K_{21})_{10} L \bar{K}_u \sin(\bar{K}_u \beta) ;$$

$$N_4 = (K_{21})_{10} L \bar{K}_u \cos(\bar{K}_u \beta) ; N_5 = EI/L \times \bar{K}_y^{-2} \cosh(\bar{K}_y \beta) + (K_{22})_5 \bar{K}_y \sinh(\bar{K}_y \beta) ;$$

$$N_6 = EI/L \times \bar{K}_y^{-2} \sinh(\bar{K}_y \beta) + (K_{22})_5 \bar{K}_y \cosh(\bar{K}_y \beta) ;$$

$$N_7 = EI/L \times \bar{K}_y^{-2} \cos(\bar{K}_y \beta) + (K_{22})_5 \bar{K}_y \sin(\bar{K}_y \beta) ;$$

$$N_8 = EI/L \times \bar{K}_y^{-2} \sin(\bar{K}_y \beta) - (K_{22})_5 \bar{K}_y \cos(\bar{K}_y \beta) ; N_9 = (K_{22})_{10} \bar{K}_y \sinh(\bar{K}_y \beta) ;$$

$$N_{10} = (K_{22})_{10} \bar{K}_y \cosh(\bar{K}_y \beta) ; N_{11} = (K_{22})_{10} \bar{K}_y \sin(\bar{K}_y \beta) ; N_{12} = (K_{22})_{10} \bar{K}_y \cos(\bar{K}_y \beta)$$

This determinant is a function of natural frequency (ω_n), the relative location of the crack (L_1/L) and the local stiffness matrix (K) which in turn is a function of the relative crack depth (a_n/t).

CHAPTER 04

FINITE ELEMENT ANALYSIS FOR IDENTIFICATION OF CRACK

- 4.1 Introduction**
- 4.2 Steps for Finite Element Analysis**
- 4.3 Analysis of Finite Element by ANSYS**
- 4.4 Process of Crack Identification**
- 4.5 Modal Analysis of cracked beam using finite element analysis (FEA)**
 - 4.5.1 Variation of relative crack location with relative natural frequencies for particular relative crack depth and crack inclination*
 - 4.5.2 Variation of relative crack depth with relative natural frequencies for particular relative crack location and crack inclination*
 - 4.5.3 Variation of relative crack inclination with relative natural frequencies for particular relative crack location and relative crack depth*
 - 4.5.4 First three mode shapes at different crack location, crack depth & crack angle*
- 4.6 Results and discussion of finite element analysis**
 - 4.6.1 Comparing Results of Finite Element Analysis with Numerical Analysis*

CHAPTER 04

FINITE ELEMENT ANALYSIS FOR IDENTIFICATION OF CRACK

Premature identification of damages in dynamic structures during their service period is the key challenge to the researchers because of its importance. At early stage of damages, it is very difficult to find out damages using visual inspection. It may be identified by Non-Destructive Techniques (NDT) such as ultrasonic, magnetic particle, radiography or shaft voltage drop etc. Though dynamic based damage diagnosis has been advanced for last three decades and there are many literatures, still there are so many problems avoid doing it from application. There are many techniques to solve the problem of a cracked beam such as numerical, wavelet, artificial intelligence, analytical, semi-analytical, experimental etc. FEA (Finite Element Analysis) is a common technique to obtain the stiffness matrix of the cracked beam element.

4.1. Introduction

The finite element method (FEM) is a numerical method for analysing structures. It is firmly established as a powerful popular analysis tool. It is most widely used in structural mechanics. The finite element procedure produces many simultaneous algebraic equations, which are generated and solved on a digital computer. In this chapter FEA is carried out to identify crack location, crack depth and crack inclination in a cracked beam having inclined crack. The results from FEA have been compared with that of numerical analysis and it is found that finite element method can be suitable used for inclined crack detection in faulty elements.

4.2. Steps for Finite Element Analysis

Due to the orderly and suitable modeling of the complicated structure, FEA finds extensive applications in several technical fields. Different analysis can be done for different dynamic structures by applying the suitable boundary conditions. Commercial

finite element software packages (e.g. ANSYS, ALGOR, ABAQUS etc.) are available to solve the various problems occurred in many engineering applications.

The procedure of computational modeling of the structure for finding out the natural frequencies and mode shapes of the cracked beam using FEM broadly consists of following steps:

- Selecting the Element Type
- Defining Material Properties
- Creating Geometrical Model of the Structure
- Discretization of the Structure (or Meshing of the structure)
- Apply the boundary, initial and loading conditions
- Setting up an Analysis

4.3. Analysis of Finite Element by ANSYS

ANSYS is universal software, which is used on simulation of the structural elements, fluid dynamics, vibration, thermal transfer and electro mechanics for engineers. We can simulate with ANSYS structures and then test them in the virtual environment. Mesh on the beam is generated automatically by ANSYS, while is used the spatial element type SOLID187 as shown in Figure 4.1. The element (SOLID 187) is defined by 10 nodes while each node has three degrees of freedom. The SOLID187 has a quadratic shifting behaviour and is suitable for modelling of the finite element irregular mesh. The maximum size of the element is 5 mm.

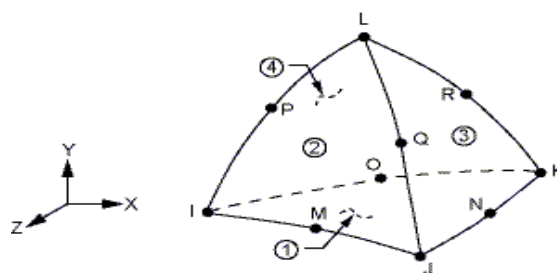


Fig.4.1. Element type SOLID 187

4.4. Process of Crack Identification

In this chapter identification of inclined crack in a cracked cantilever beam has been executed in two ways. Firstly, the finite element model of the inclined crack cantilever

beam is developed and the cracked beam is discretized into a number of elements, and the crack location is supposed to be in each of the elements. Next, for particular location of the crack in each element, the crack depth and crack inclination are varied. Modal analysis for each crack location, crack depth and crack inclination is then executed to determine the natural frequencies and mode shapes of the cracked beam.

4.5. Modal Analysis of cracked beam using finite element analysis (FEA)

The modal analysis deals with the dynamics behaviour of dynamic structures under the dynamics excitation. The modal analysis helps to decrease the noise produced from the system to the environment. It helps to point out the reasons of vibrations that cause fault/damage of the integrity of system components. Using it, we can develop the overall performance of the system in certain operating situations. We know two basic methods of the modal analysis, namely the numerical modal analysis and the experimental modal analysis. The experimental modal analysis deals with measurement input data from which a mathematical model is derived. However, it has to take different levels of analysis, from which the model is constructed.

We can effect computational period of the modal analysis, when a range of frequencies or number of mode shapes is defined. The type of solution and the solver method in software package ANSYS is selected automatically. In direct solver method, the block Lanczos method is used for the modal analysis. The variation of first three relative natural frequencies with respect to relative crack locations, relative crack depths and crack inclinations as shown in Fig. 4.2 to Fig. 4.17. The first three mode shapes are shown in Fig. 4.18 to Fig. 4.44. All the results are compared with the numerical results.

The relative natural frequency (RNF) and relative mode shape difference (RMD) used in different analysis can be defined as given.

$$\text{RNF} = \frac{\text{Natural Frequency of Cracked Beam}}{\text{Natural Frequency of Uncracked Beam}}$$

$$\text{RMD} = \frac{\text{Modal Amplitude of Uncracked Beam} - \text{Modal Amplitude of Cracked Beam}}{\text{Modal Amplitude of Uncracked Beam}}$$

4.5.1. Variation of relative crack location with relative natural frequencies for particular relative crack depth and crack inclination

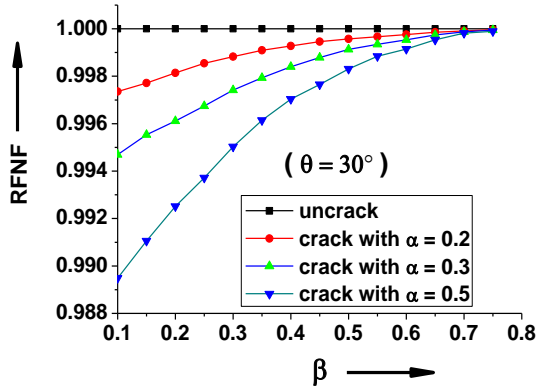


Fig.4.2. Relative first mode natural frequencies Vs. Relative crack location from fixed end at crack angle (θ) 30°

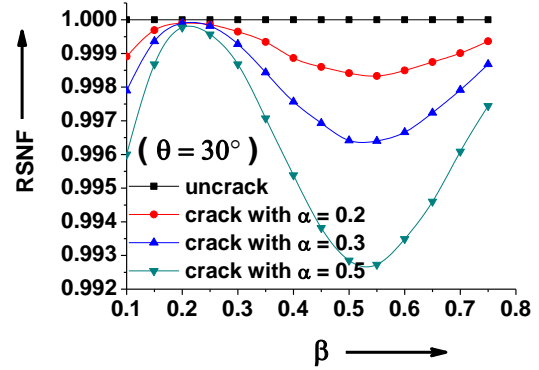


Fig.4.3. Relative second mode natural frequencies Vs. Relative crack location from fixed end at crack angle (θ) 30°

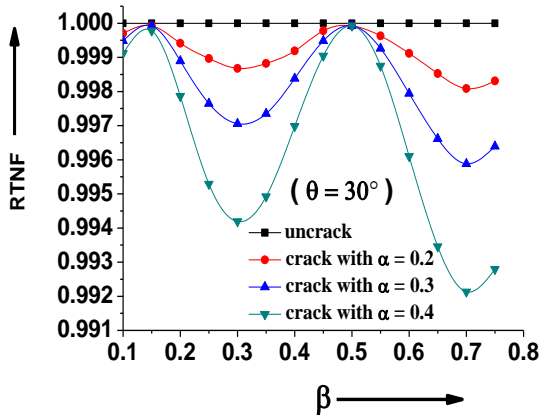


Fig.4.4. Relative third mode natural frequencies Vs. Relative crack location from fixed end at crack angle (θ) 30°

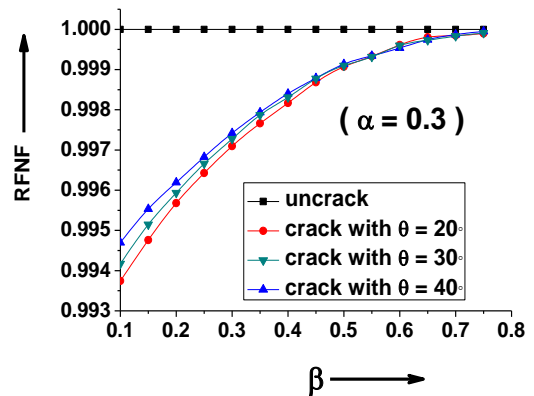


Fig.4.5. Relative first mode natural frequencies Vs. Relative crack location from fixed end at relative crack depth (α) 0.3

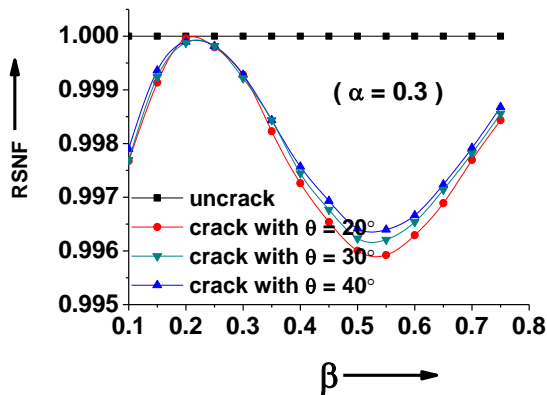


Fig.4.6. Relative Second mode natural frequencies Vs. Relative crack location from fixed end at relative crack depth (α) 0.3

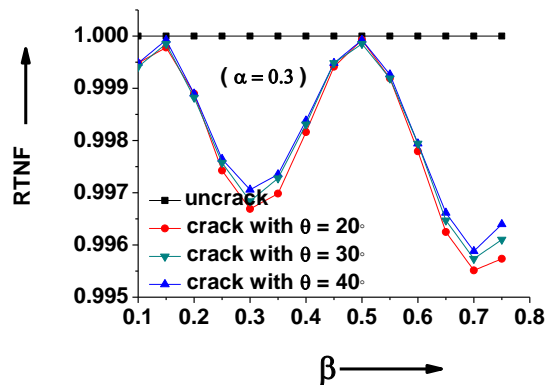


Fig.4.7. Relative third mode natural frequencies Vs. Relative crack location from fixed end at relative crack depth (α) 0.3

4.5.2. Variation of relative crack depth with relative natural frequencies for particular relative crack location and crack inclination

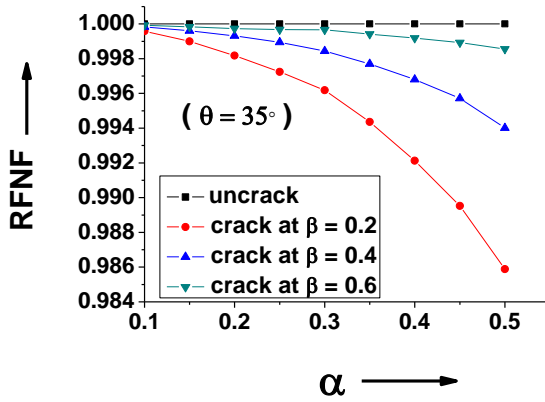


Fig.4.8. Relative first mode natural frequencies Vs. Relative crack depth at crack angle (θ) 35°

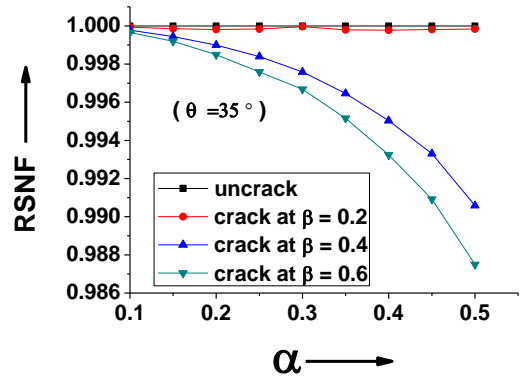


Fig.4.9. Relative second mode natural frequencies Vs. Relative crack depth at crack angle (θ) 35°

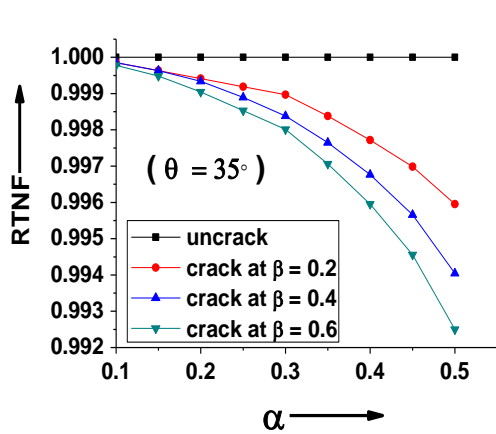


Fig.4.10. Relative third mode natural frequencies Vs. Relative crack depth at crack angle (θ) 35°

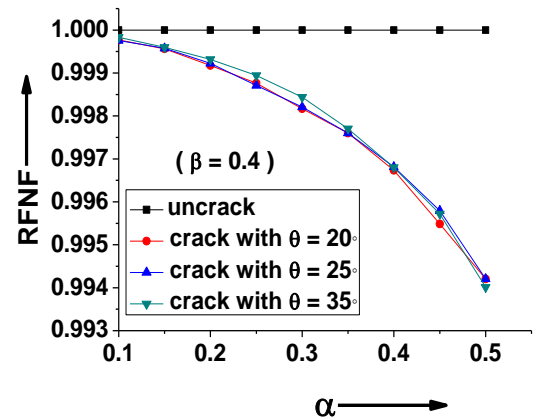


Fig.4.11. Relative first mode natural frequencies Vs. Relative crack depth at relative crack location (β) 0.4

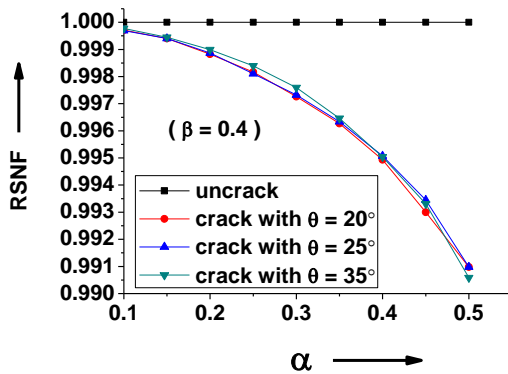


Fig.4.12. Relative second mode natural frequencies Vs. Relative crack depth at relative crack location (β) 0.4

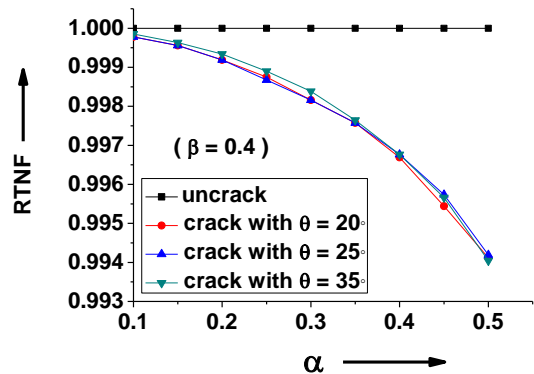


Fig.4.13. Relative third mode natural frequencies Vs. Relative crack depth at relative crack location (β) 0.4

4.5.3. Variation of relative crack inclination with relative natural frequencies for particular relative crack location and relative crack depth

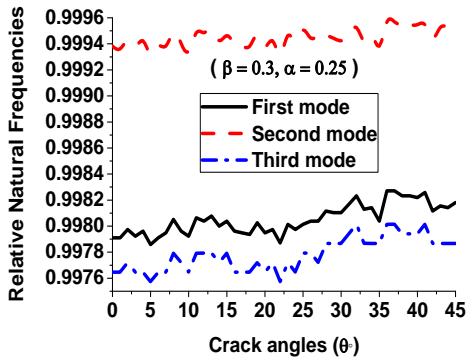


Fig.4.14. Relative natural frequencies Vs. Crack angles at $\beta = 0.3, \alpha = 0.25$

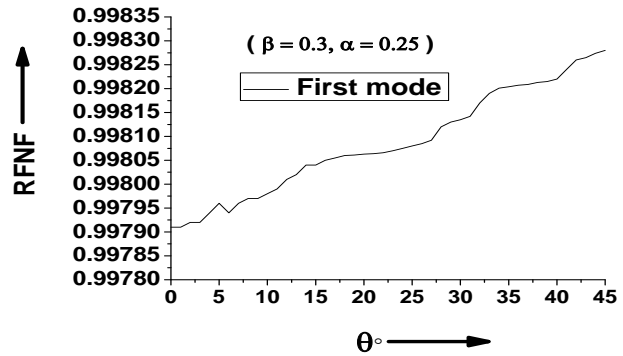


Fig.4.15. Relative first mode natural frequencies Vs. Crack angles at $\beta = 0.3, \alpha = 0.25$

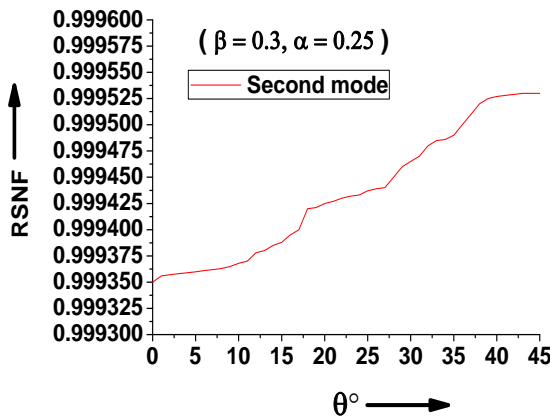


Fig. 4.16. Relative second mode natural frequencies Vs. Crack angles at $\beta = 0.3, \alpha = 0.25$

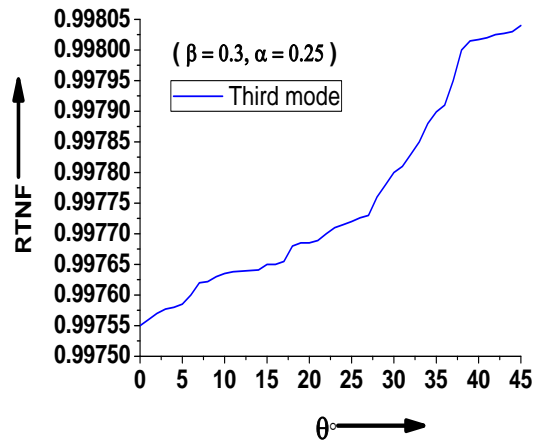


Fig. 4.17. Relative third mode natural frequencies Vs. Crack angles at $\beta = 0.3, \alpha = 0.25$

4.5.4. First three mode shapes at different crack location, crack depth & crack angle

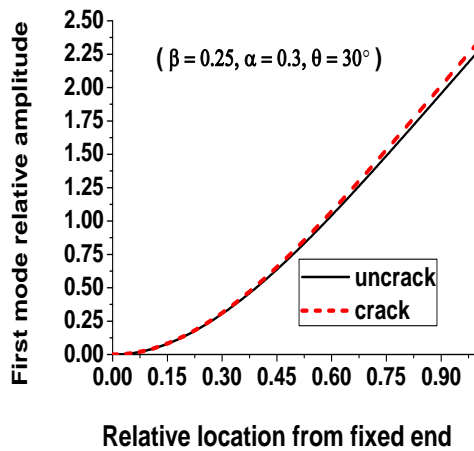


Fig.4.18. First mode relative amplitude Vs. Relative location from fixed end at $\beta = 0.25, \alpha = 0.3$ and $\theta = 30^\circ$

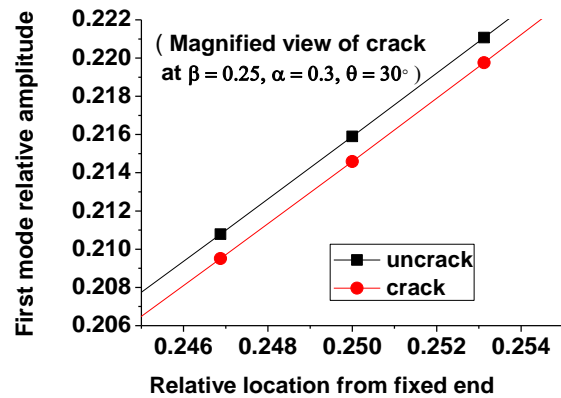


Fig.4.19. Magnified view of First mode relative amplitude Vs. Relative location from fixed end at $\beta = 0.25, \alpha = 0.3$ and $\theta = 30^\circ$

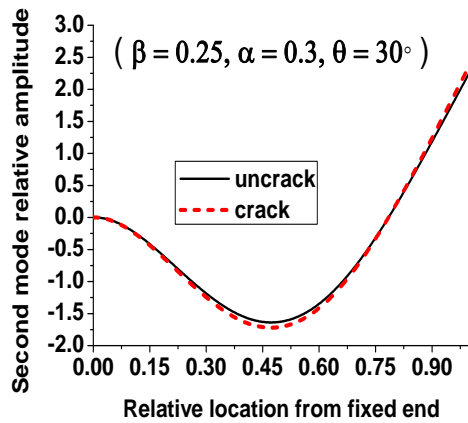


Fig.4.20. Second mode relative amplitude Vs. Relative location from fixed end at $\beta = 0.25$, $\alpha = 0.3$ and $\theta = 30^\circ$

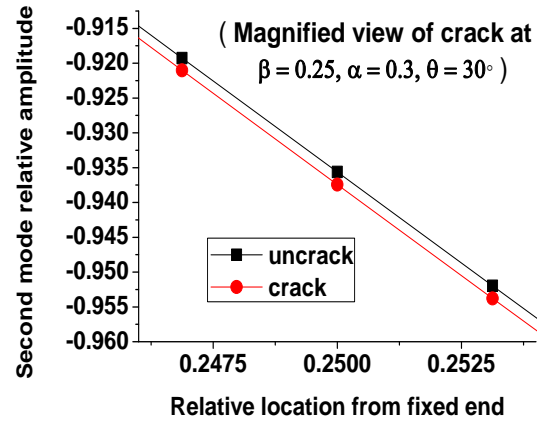


Fig.4.21. Magnified view of Second mode relative amplitude Vs. Relative location from fixed end at $\beta = 0.25$, $\alpha = 0.3$ and $\theta = 30^\circ$

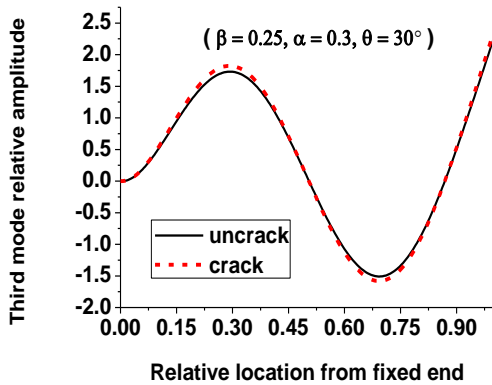


Fig.4.22. Third mode relative amplitude Vs. Relative location from fixed end at $\beta = 0.25$, $\alpha = 0.3$ and $\theta = 30^\circ$

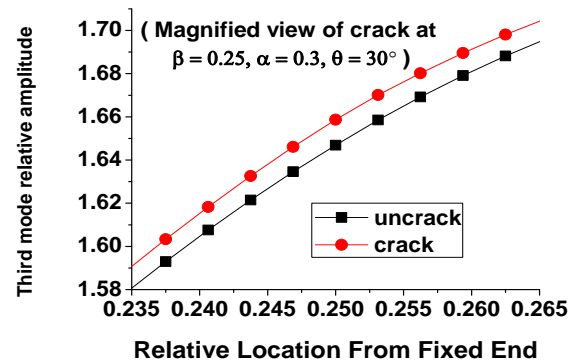


Fig.4.23. Magnified view of Third mode relative amplitude Vs. Relative location from fixed end at $\beta = 0.25$, $\alpha = 0.3$ and $\theta = 30^\circ$

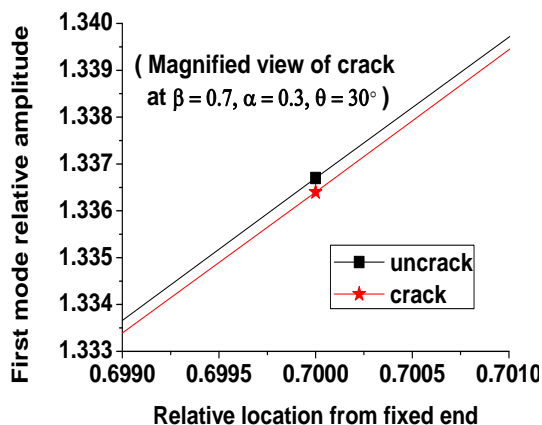


Fig.4.24. Magnified view of First mode relative amplitude Vs. Relative location from fixed end at $\beta = 0.7$, $\alpha = 0.3$ and $\theta = 30^\circ$

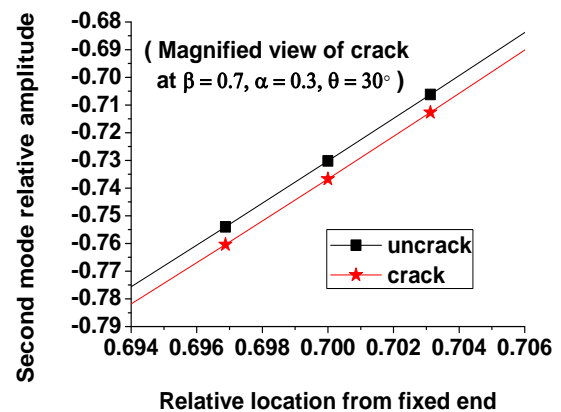


Fig.4.25. Magnified view of Second mode relative amplitude Vs. Relative location from fixed end at $\beta = 0.7$, $\alpha = 0.3$ and $\theta = 30^\circ$

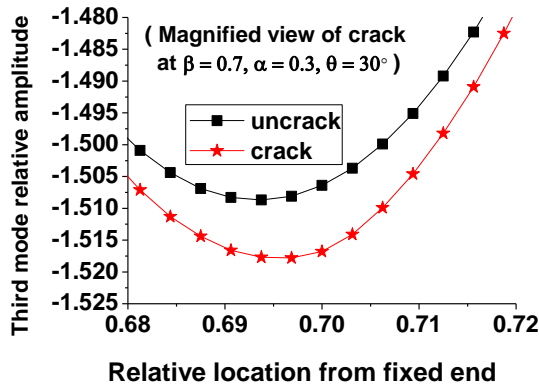


Fig.4.26. Magnified view of Third mode relative amplitude Vs. Relative location from fixed end at $\beta = 0.7, \alpha = 0.3$ and $\theta = 30^\circ$

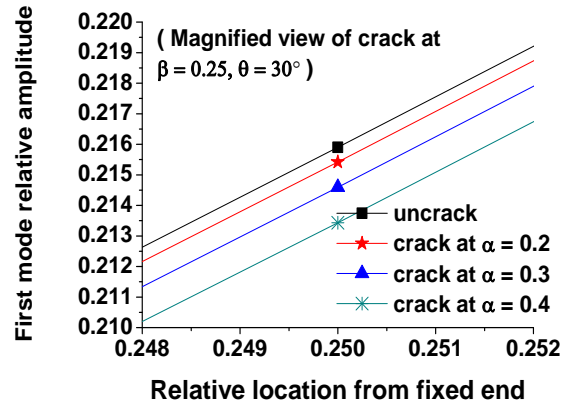


Fig.4.27. Magnified view of First mode relative amplitude Vs. Relative location from fixed end at $\beta = 0.25$ and $\theta = 30^\circ$

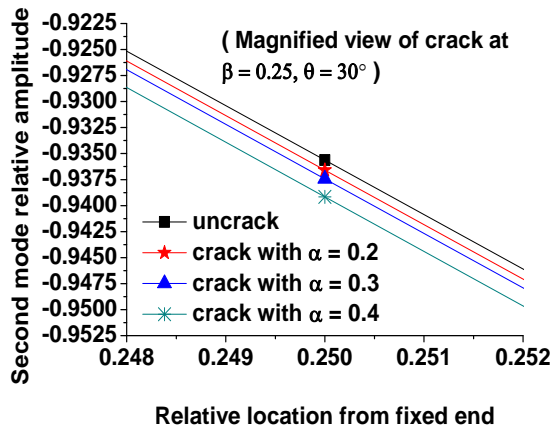


Fig.4.28. Magnified view of Second mode relative amplitude Vs. Relative location from fixed end at $\beta = 0.25$ and $\theta = 30^\circ$

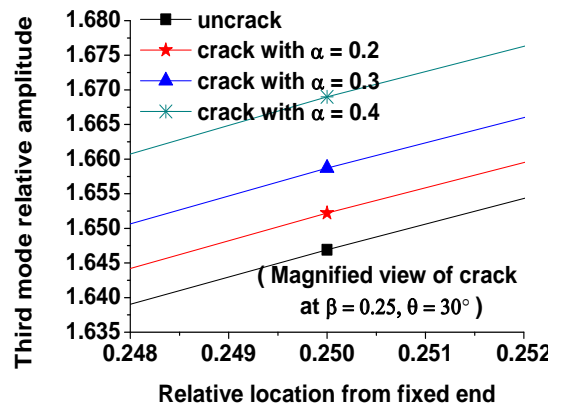


Fig.4.29. Magnified view of Third mode relative amplitude Vs. Relative location from fixed end at $\beta = 0.25$ and $\theta = 30^\circ$

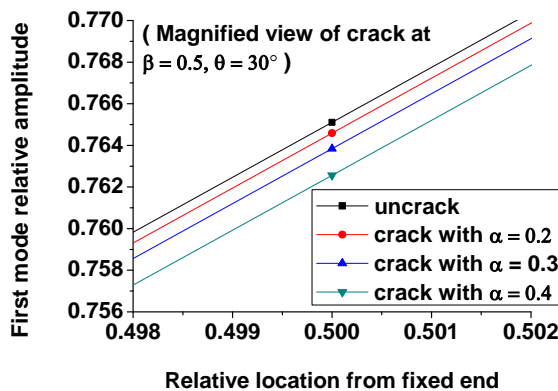


Fig.4.30. Magnified view of First mode relative amplitude Vs. Relative location from fixed end at $\beta = 0.5$ and $\theta = 30^\circ$

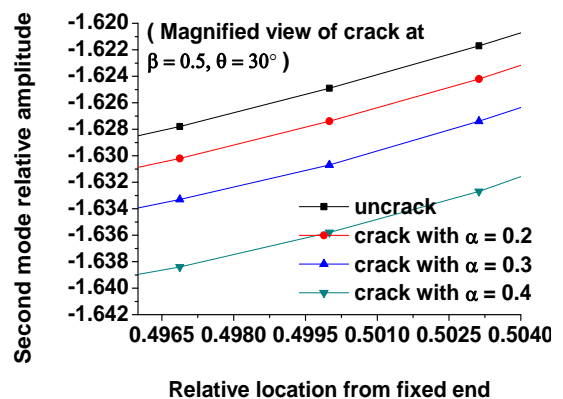


Fig.4.31. Magnified view of Second mode relative amplitude Vs. Relative location from fixed end at $\beta = 0.5$ and $\theta = 30^\circ$

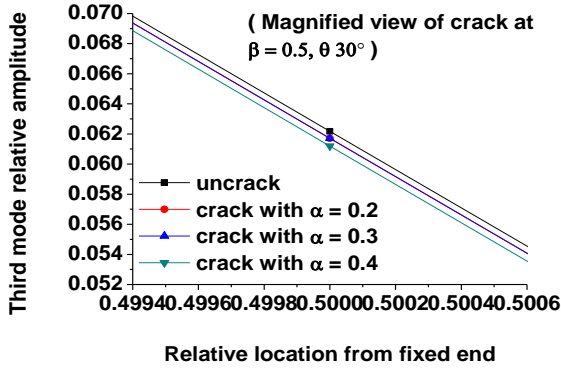


Fig.4.32. Magnified view of Third mode relative amplitude Vs. Relative location from fixed end at $\beta = 0.5$ and $\theta = 30^\circ$

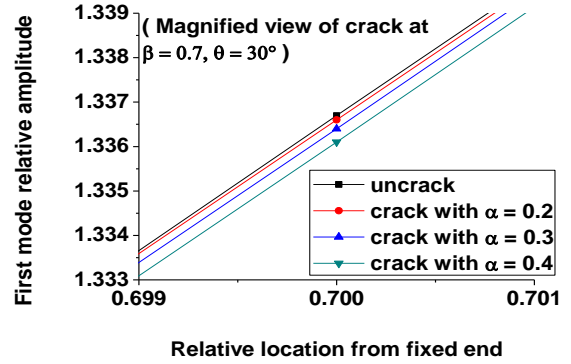


Fig.4.33. Magnified view of First mode relative amplitude Vs. Relative location from fixed end at $\beta = 0.7$ and $\theta = 30^\circ$

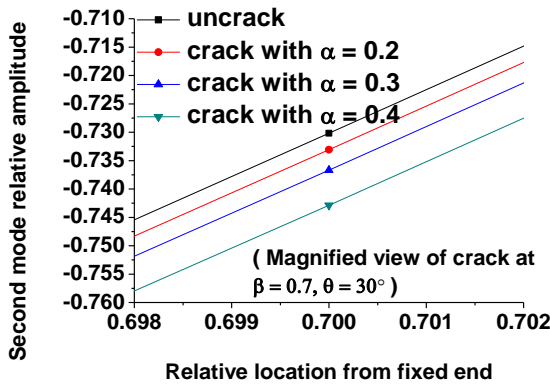


Fig.4.34. Magnified view of Second mode relative amplitude Vs. Relative location from fixed end at $\beta = 0.7$ and $\theta = 30^\circ$

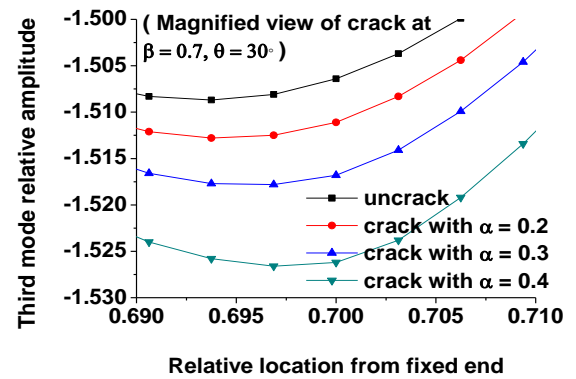


Fig.4.35. Magnified view of Third mode relative amplitude Vs. Relative location from fixed end at $\beta = 0.7$ and $\theta = 30^\circ$

4.6. Results and discussions of finite element analysis

4.6.1. Comparing Results of Finite Element Analysis with Numerical Analysis

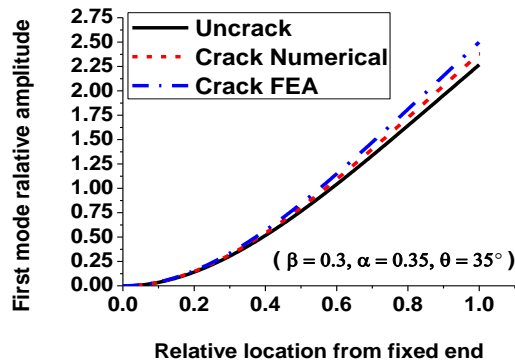


Fig.4.36. First mode relative amplitude Vs. Relative location from cantilever end at $\beta = 0.3$, $\alpha = 0.35$ and $\theta = 35^\circ$

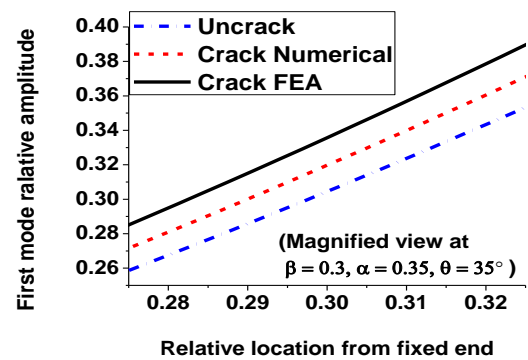


Fig.4.37. Magnified view of First mode relative amplitude Vs. Relative location from cantilever end at $\beta = 0.3$, $\alpha = 0.35$ and $\theta = 35^\circ$

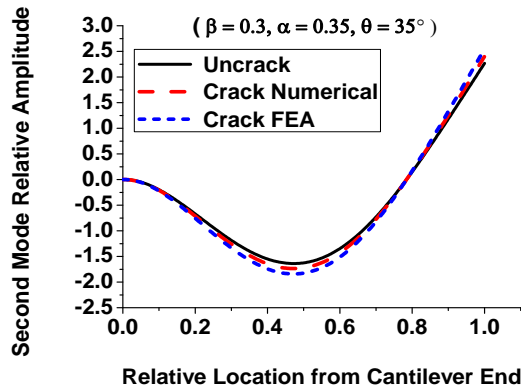


Fig.4.38. Second mode relative amplitude Vs. Relative location from cantilever end at $\beta = 0.3$, $\alpha = 0.35$ and $\theta = 35^\circ$

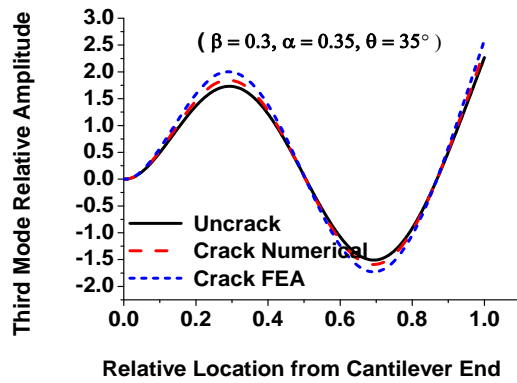


Fig.4.40. Third mode relative amplitude Vs. Relative location from cantilever end at $\beta = 0.3$, $\alpha = 0.35$ and $\theta = 35^\circ$

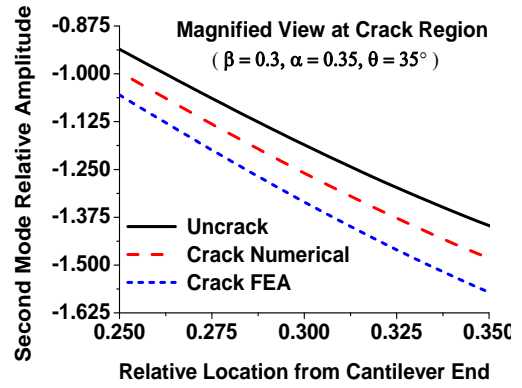


Fig.4.39. Magnified view of Second mode relative amplitude Vs. Relative location from cantilever end at $\beta = 0.3$, $\alpha = 0.35$ and $\theta = 35^\circ$

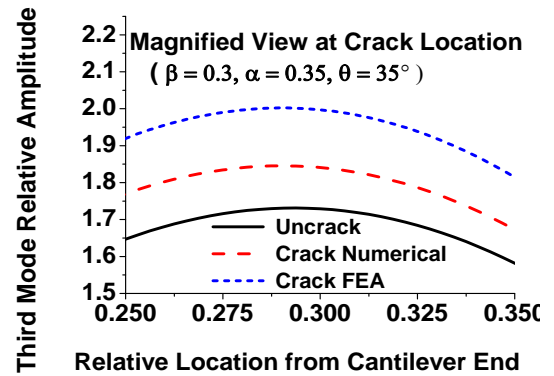


Fig.4.41. Magnified view of Third mode relative amplitude Vs. Relative location from cantilever end at $\beta = 0.3$, $\alpha = 0.35$ and $\theta = 35^\circ$

The results obtained from theoretical analysis and finite element analysis in the form of mode shapes are compared in Fig. 4.36 to Fig. 4.41. Also the results obtained from theoretical analysis and finite element analysis due to different crack parameters in form of modal frequencies are given in Table 4.1.

Table 4.1 represents the comparison study of modal analysis between numerical and finite element analysis (FEA). First three columns present first three relative natural frequencies, columns four to six present first three relative mode shape differences, columns seven and nine present relative crack locations and columns eight and ten presents relative crack depths.

Table 4.1 Comparison the results of modal analysis between numerical and FEA

SL NO.	1	2	3	4	5	6	7	8	9	10
	RFNF	RSNF	RTNF	RFMD	RSMD	RTMD	Numerical		FEA	
							β	α	β	α
Crack inclination (θ) 0°										
1	0.99968	0.99998	0.99978	0.0006	-0.00017	-0.00073	0.245	0.0985	0.25	0.1
2	0.99846	0.99988	0.9989	0.00259	-0.00093	-0.00328	0.24625	0.195	0.25	0.2
3	0.99893	0.99582	0.99985	0.00187	-0.00394	0.01222	0.49125	0.294	0.5	0.3
4	0.99809	0.99182	0.99993	0.00391	-0.00788	0.00928	0.4875	0.389	0.5	0.4
5	0.99999	0.99703	0.9914	0.00013	-0.03827	-0.02445	0.72938	0.392	0.75	0.4
6	0.99992	0.99491	0.98529	0.00034	-0.06516	-0.04052	0.73125	0.4875	0.75	0.5
Crack inclination (θ) 15°										
1	0.99966	0.99998	0.99978	0.0006	-0.00019	-0.00073	0.24625	0.0988	0.25	0.1
2	0.99852	0.99992	0.99897	0.00269	-0.00088	-0.00328	0.24563	0.1963	0.25	0.2
3	0.99908	0.99609	0.99993	0.00186	-0.00382	0.00767	0.49375	0.2933	0.5	0.3
4	0.99817	0.99215	0.99993	0.00375	-0.00757	0.01086	0.49	0.3898	0.5	0.4
5	0.99999	0.99714	0.99162	0.00013	-0.0371	-0.02377	0.73313	0.3906	0.75	0.4
6	0.99981	0.99483	0.98514	0.00034	-0.06545	-0.04119	0.73688	0.4894	0.75	0.5
Crack inclination (θ) 30°										
1	0.99959	0.9999	0.99971	0.00032	-0.00036	-0.00079	0.24638	0.0987	0.25	0.1
2	0.99855	0.99988	0.99897	0.00245	-0.0009	-0.0031	0.2455	0.1957	0.25	0.2
3	0.99908	0.99633	0.99985	0.00165	-0.00357	0.00753	0.4925	0.2929	0.5	0.3
4	0.99832	0.99294	0.99993	0.00327	-0.00671	0.01007	0.48935	0.3906	0.5	0.4
5	0.99999	0.99745	0.99272	6.7E-05	-0.03106	-0.01996	0.73395	0.3904	0.75	0.4
6	0.99988	0.99543	0.98669	0.00027	-0.05856	-0.03671	0.73598	0.4911	0.75	0.5
Crack inclination (θ) 45°										
1	0.99963	0.99994	0.99971	0.00046	-0.00028	-0.00079	0.2447	0.0979	0.25	0.1
2	0.99861	0.99996	0.99904	0.00278	-0.00078	-0.00316	0.24513	0.1952	0.25	0.2
3	0.99893	0.99588	0.99978	0.00178	-0.00382	0.01317	0.48825	0.293	0.5	0.3
4	0.9981	0.99191	0.99993	0.00375	-0.00763	0.01217	0.48935	0.3901	0.5	0.4
5	0.99999	0.99714	0.99184	0.00013	-0.03492	-0.02265	0.73583	0.3915	0.75	0.4
6	0.99992	0.99491	0.98492	0.00034	-0.06586	-0.04142	0.73508	0.4911	0.75	0.5

CHAPTER 05

EXPERIMENTAL ANALYSIS FOR IDENTIFICATION OF CRACK

- 5.1. Introduction**
- 5.2. Experimental Setup**
- 5.3. Experimental Results**
- 5.4. Comparison between the results of numerical, finite element and experimental analysis**
- 5.5. Discussion**
- 5.6. Summary**

CHAPTER 05

EXPERIMENTAL ANALYSIS FOR IDENTIFICATION OF CRACK

5.1. Introduction

In order to support the validation of the results from the theoretical analysis and finite element analysis discussed in chapter-3 and chapter-4, which are used in different artificial intelligence controller proposed to forecast crack location, crack depth and crack inclination discussed in chapter-6 and chapter-7, Experimental analysis is carried out. For the analysis, the experimental setup is made to measure the natural frequency and mode shapes and to observe the response of cantilever beam with the presence of inclined crack.

An aluminium cantilever beam specimen of dimension (800 x 60 x 6 mm³) has been taken for the experimental analysis. A number of experiments have been done on the cracked beam with different configurations of crack parameters (crack locations, crack depths and crack inclinations) to measure the first three natural frequencies and mode shapes.

5.2. Experimental Setup

The schematic block diagram of the complete experimental setup is shown in Figure: 5.1. An experimental set-up contains following devices for performing the experiment.

1. Vibration Analyser
2. Accelerometer
3. Power Distribution
4. Vibration Exciter
5. Power Amplifier
6. Test Specimen-beam
7. Vibration Indicator (PULSE Labshop software)
8. Function Generator

Before the experimental study the beams surface has been cleaned and organized for straightness. Subsequently, transverse inclined crack is created at different location from fixed end in different specimens with the help of Wire EDM machine. The natural

frequencies corresponding to 1st, 2nd and 3rd mode are noted with different crack depth at different crack locations and different crack inclinations in the cracked cantilever beam.

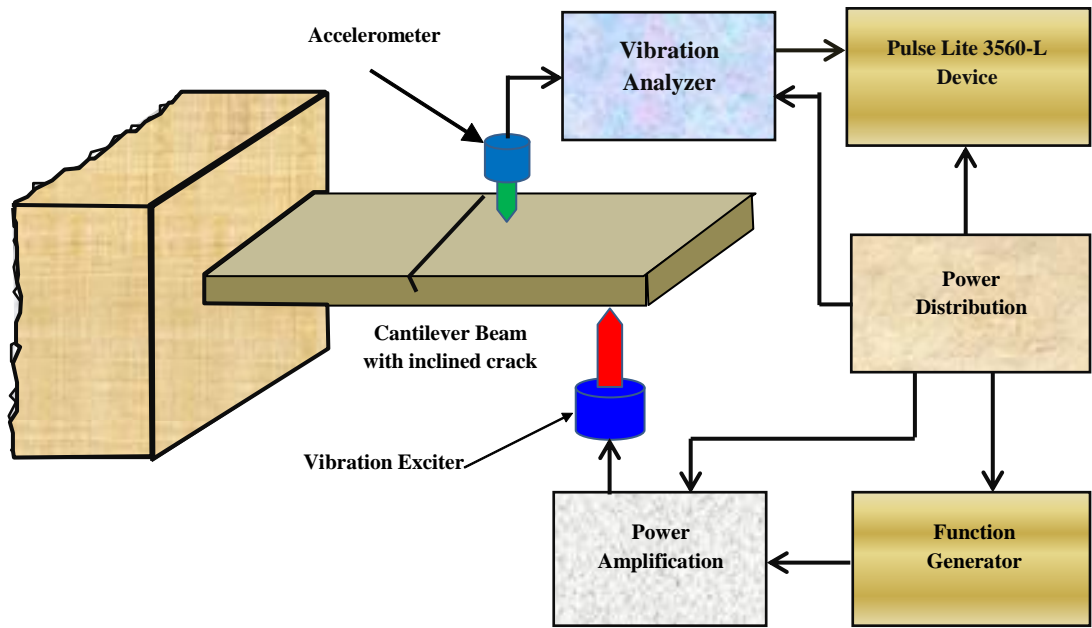


Fig.5.1. Schematic Block Diagram of Experimental set-up

5.3. Experimental Results

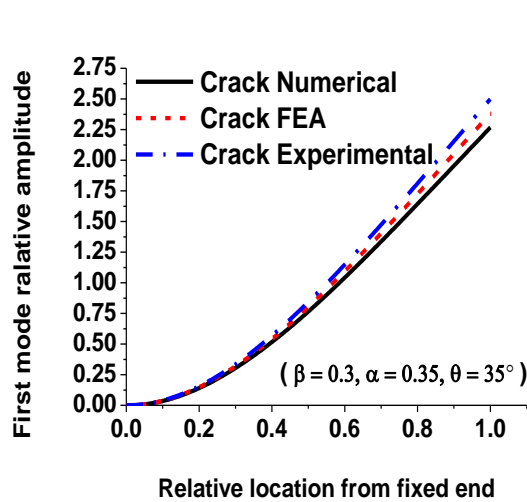


Fig.5.2. First mode relative amplitude Vs. Relative location from cantilever end at $\beta = 0.3$, $\alpha = 0.35$ and $\theta = 35^\circ$

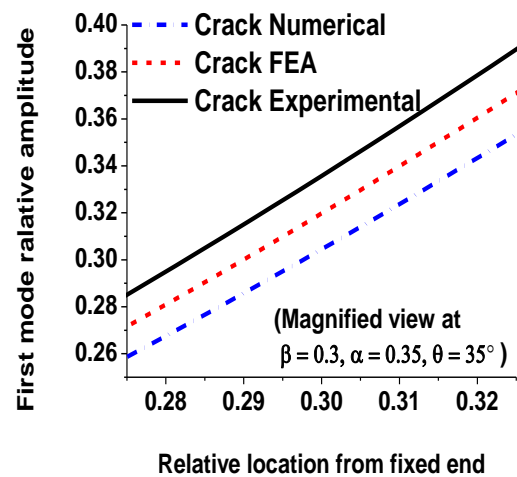


Fig.5.3. Magnified view of First mode relative amplitude Vs. Relative location from cantilever end at $\beta = 0.3$, $\alpha = 0.35$ and $\theta = 35^\circ$

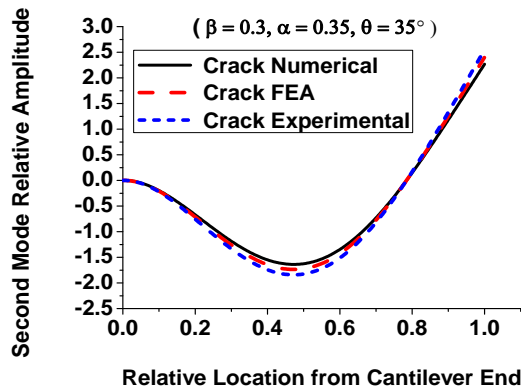


Fig.5.4. Second mode relative amplitude Vs. Relative location from cantilever end at $\beta = 0.3$, $\alpha = 0.35$ and $\theta = 35^\circ$

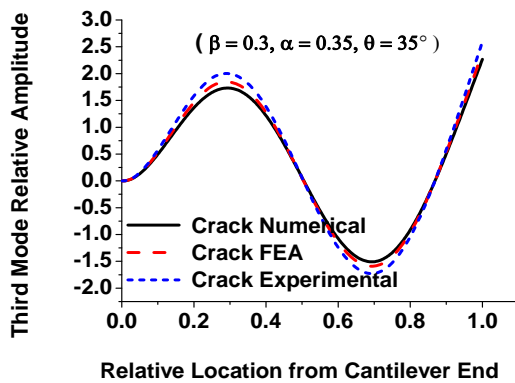


Fig.5.6. Third mode relative amplitude Vs. Relative location from cantilever end at $\beta = 0.3$, $\alpha = 0.35$ and $\theta = 35^\circ$

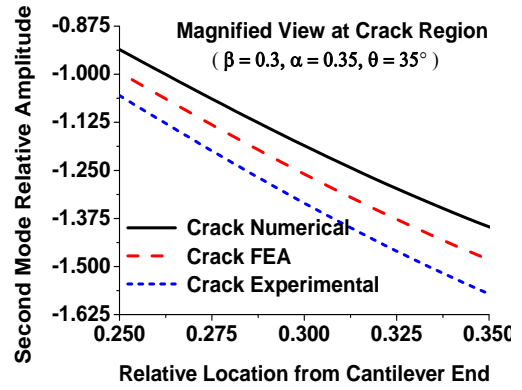


Fig.5.5. Magnified view of Second mode relative amplitude Vs. Relative location from cantilever end at $\beta = 0.3$, $\alpha = 0.35$ and $\theta = 35^\circ$

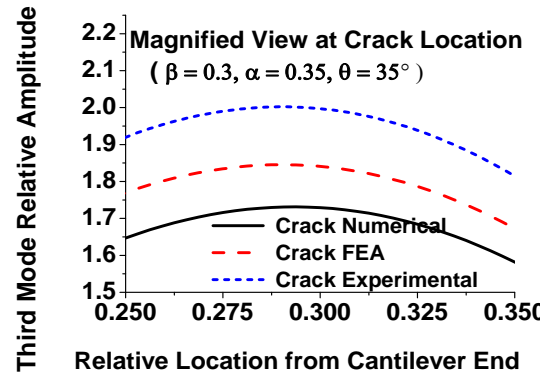


Fig.5.7. Magnified view of Third mode relative amplitude Vs. Relative location from cantilever end at $\beta = 0.3$, $\alpha = 0.35$ and $\theta = 35^\circ$

5.4. Comparison between the results of numerical, finite element and experimental analysis

The results obtained from theoretical analysis, finite element analysis and experimental analysis in the form of mode shapes are compared in Fig. 5.2 to Fig. 5.7. Also the results obtained from theoretical analysis, finite element analysis and experimental analysis due to different crack parameters in form of modal frequencies are given in Table 5.1.

Table 5.1 Comparison the results of modal analysis between numerical, FEA and Experimental

RFNF	RSNF	RTNF	RFMD	RSMD	RTMD	Numerical		FEA		Experiment	
						β	α	β	α	β	α
Crack inclination (θ) 0°											
0.99968	0.99998	0.99978	0.0006	-0.00017	-0.00073	0.245	0.0985	0.25	0.1	0.2575	0.104
0.99846	0.99988	0.9989	0.00259	-0.00093	-0.00328	0.24625	0.195	0.25	0.2	0.2588	0.207
0.99893	0.99582	0.99985	0.00187	-0.00394	0.01222	0.49125	0.294	0.5	0.3	0.5125	0.311
0.99809	0.99182	0.99993	0.00391	-0.00788	0.00928	0.4875	0.389	0.5	0.4	0.52	0.41
0.99999	0.99703	0.9914	0.00013	-0.03827	-0.02445	0.72938	0.392	0.75	0.4	0.7799	0.411
0.99992	0.99491	0.98529	0.00034	-0.06516	-0.04052	0.73125	0.4875	0.75	0.5	0.7838	0.515
Crack inclination (θ) 15°											
0.99966	0.99998	0.99978	0.0006	-0.00019	-0.00073	0.24625	0.0988	0.25	0.1	0.258	0.103
0.99852	0.99992	0.99897	0.00269	-0.00088	-0.00328	0.24563	0.1963	0.25	0.2	0.2594	0.207
0.99908	0.99609	0.99993	0.00186	-0.00382	0.00767	0.49375	0.2933	0.5	0.3	0.521	0.312
0.99817	0.99215	0.99993	0.00375	-0.00757	0.01086	0.49	0.3898	0.5	0.4	0.5138	0.41
0.99999	0.99714	0.99162	0.00013	-0.0371	-0.02377	0.73313	0.3906	0.75	0.4	0.7826	0.4411
0.99981	0.99483	0.98514	0.00034	-0.06545	-0.04119	0.73688	0.4894	0.75	0.5	0.7743	0.517
Crack inclination (θ) 30°											
0.99959	0.9999	0.99971	0.00032	-0.00036	-0.00079	0.24638	0.0987	0.25	0.1	0.2538	0.103
0.99855	0.99988	0.99897	0.00245	-0.0009	-0.0031	0.2455	0.1957	0.25	0.2	0.2563	0.207
0.99908	0.99633	0.99985	0.00165	-0.00357	0.00753	0.4925	0.2929	0.5	0.3	0.5225	0.306
0.99832	0.99294	0.99993	0.00327	-0.00671	0.01007	0.48935	0.3906	0.5	0.4	0.5163	0.41
0.99999	0.99745	0.99272	6.7E-05	-0.03106	-0.01996	0.73395	0.3904	0.75	0.4	0.7706	0.413
0.99988	0.99543	0.98669	0.00027	-0.05856	-0.03671	0.73598	0.4911	0.75	0.5	0.7811	0.509
Crack inclination (θ) 45°											
0.99963	0.99994	0.99971	0.00046	-0.00028	-0.00079	0.2447	0.0979	0.25	0.1	0.2574	0.103
0.99861	0.99996	0.99904	0.00278	-0.00078	-0.00316	0.24513	0.1952	0.25	0.2	0.2547	0.204
0.99893	0.99588	0.99978	0.00178	-0.00382	0.01317	0.48825	0.293	0.5	0.3	0.5179	0.308
0.9981	0.99191	0.99993	0.00375	-0.00763	0.01217	0.48935	0.3901	0.5	0.4	0.5128	0.411
0.99999	0.99714	0.99184	0.00013	-0.03492	-0.02265	0.73583	0.3915	0.75	0.4	0.7817	0.412
0.99992	0.99491	0.98492	0.00034	-0.06586	-0.04142	0.73508	0.4911	0.75	0.5	0.7676	0.52

5.5. Discussion

The results obtained from theoretical and FEA have been compared with the result obtained from experimental as shown in Fig. 5.2 to Fig. 5.6 and Table 5.1. Above Fig. 5.2, Fig. 5.4 and Fig. 5.6 represent the deviation of first three mode shapes for the presence of inclined crack in cantilever beam and Fig. 5.3, Fig. 5.5 and Fig. 5.7 represent the magnified view of the deviation of mode shapes at the respective crack locations.

CHAPTER 06

ANALYSIS OF FUZZY INFERENCE SYSTEM (FIS) FOR IDENTIFICATION OF CRACK

- 6.1 Introduction**
- 6.2 Fuzzy inference system (FIS)**
- 6.3 Analysis of fuzzy controller used for inclined crack identification**
 - 6.3.1 Fuzzy mechanism for inclined crack identification*
 - 6.3.2 Results of fuzzy model*
 - 6.3.3 Summary*

CHAPTER 06

ANALYSIS OF FUZZY INFERENCE SYSTEM (FIS) FOR INCLINED CRACK IDENTIFICATION

6.1. Introduction

In this chapter, an inclined edge crack identification algorithm using fuzzy inference system has been designed and the performance has been calculated. The fuzzy inference system for crack detection has been formulated with six inputs (first three relative natural frequencies and first three relative mode shape differences) and three outputs (relative crack location, relative crack depth and crack angle). A number of fuzzy linguistic terms and fuzzy membership functions (triangular, trapezoidal, Gaussian, bell shape and hybrid) have been taken to improve the proposed crack detection technique. The vibrating response obtained from the numerical, finite element and experimental analyses have been used to set up the rule base for designing of the fuzzy system. The performance of the proposed fuzzy based system for crack detection have been compared with the results obtained from FEA, numerical and experimental analysis and it is observed that, the current fuzzy model can be implemented successfully for structural health monitoring.

6.2. Fuzzy inference system

The fuzzy system generally consists of five steps. They are as follows,

Step 1: Inputs to fuzzy system: The fuzzy system at first is fed with the input parameters and then the system recognizes the degree of association of the data with the corresponding fuzzy set through the membership functions.

Step 2: Application of fuzzy operator: After the fuzzification of the inputs, the fuzzy model measures the degree to which each of the antecedents satisfies for each rule of the fuzzy rule data base. If the rule has a more than one part, the fuzzy operator is employed to obtain a single value for the given rule.

Step 3: Application of method for fulfillment of rules: Method is applied to reshape the output of the membership functions, which is represented by a fuzzy set. The reshaping of the output is done by a function related to the antecedent.

Step 4: Aggregation of results: The results obtained from each rule are unified to get a decision from the system. Aggregation process leads to a combined fuzzy set as output.

Step 5 : Defuzzification: In this process the defuzzification layer of the fuzzy system incorporate method like centroid, maxima etc. in order to convert the fuzzy set into crisp value, which will be easier to analyze.

6.3. Analysis of fuzzy controller used for inclined crack identification

The fuzzy controllers designed in the present analysis based on membership functions having six input parameters and three output parameters as shown in Fig. 6.1.

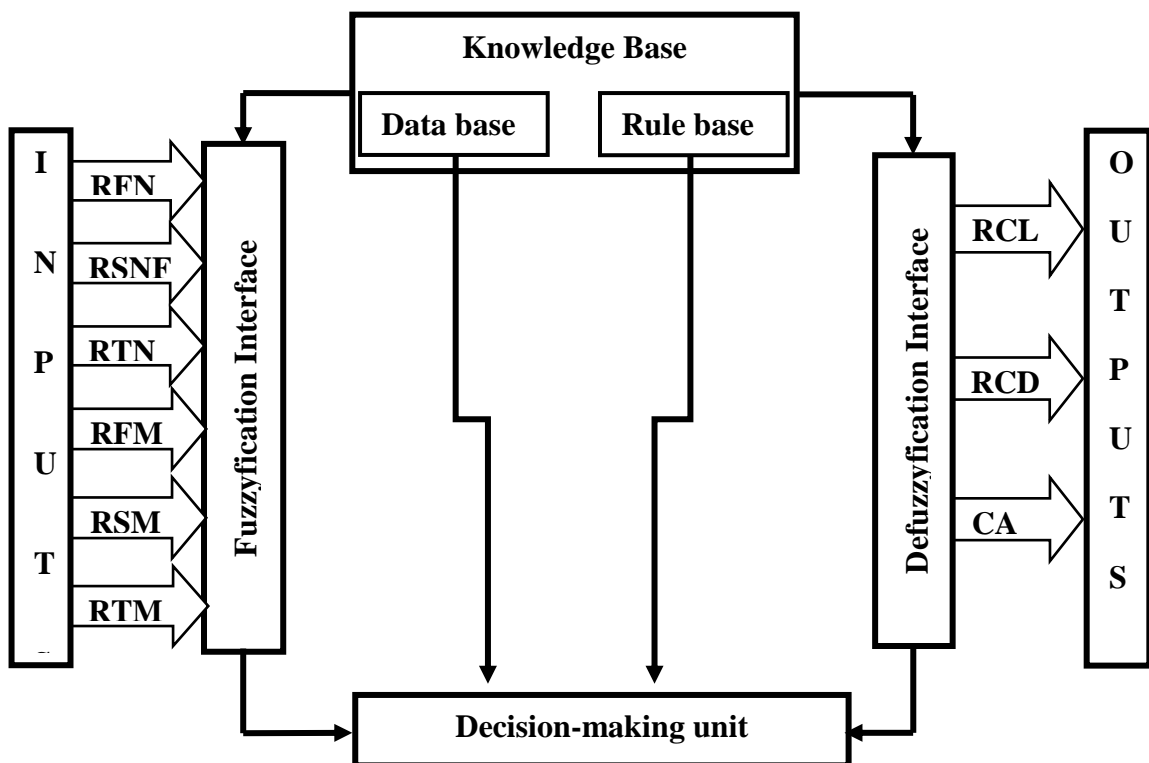


Fig.6.1. Fuzzy inference system

The linguistic term used for the inputs are as follows;

- Relative first natural frequency = “RFNF”;

- Relative second natural frequency = “RSNF”;
- Relative third natural frequency = “RTNF”;
- Average relative first mode shape difference = “RFMD”;
- Average relative second mode shape difference = “RSMD”;
- Average relative third mode shape difference = “RTMD”.

The linguistic term used for the outputs are as follows;

- Relative crack location = “RCL”;
- Relative crack depth = “RCD”;
- Crack inclination or angle = “CA”.

The pictorial representation of the triangular, Gaussian, trapezoidal, bell-shape and hybrid membership fuzzy controllers are shown in Fig. 6.2 to Fig. 6.6 respectively.

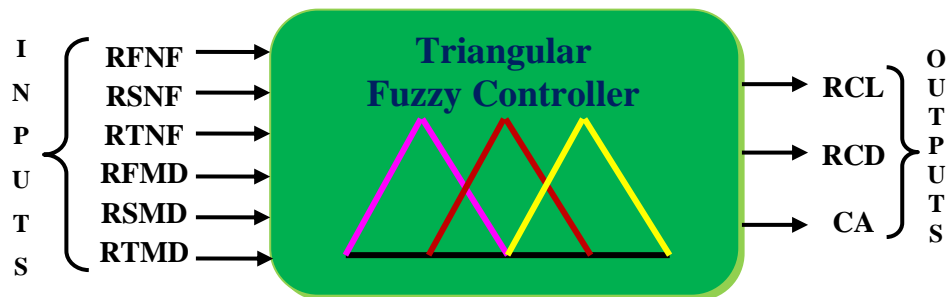


Fig. 6.2. Triangular Fuzzy Controller

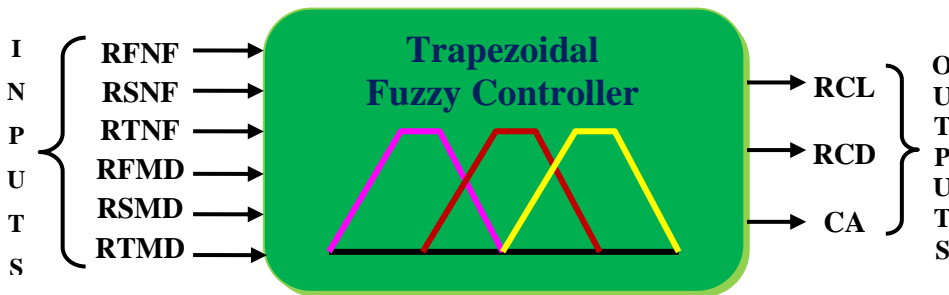


Fig. 6.3. Trapezoidal Fuzzy Controller

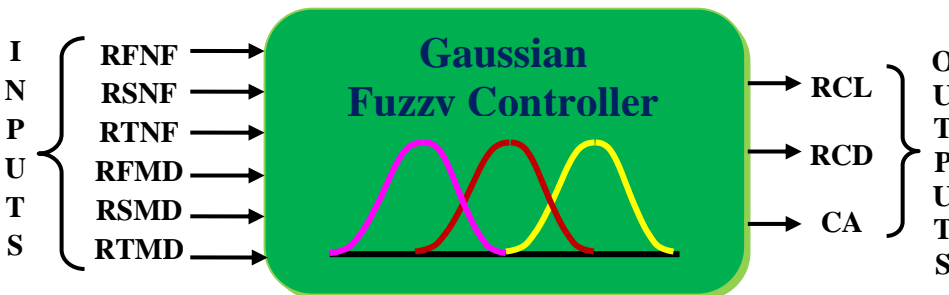


Fig. 6.4. Gaussian Fuzzy Controller

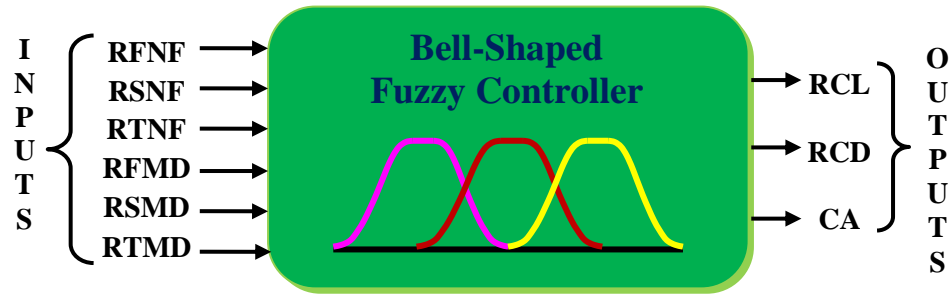


Fig. 6.5. Bell-Shaped Fuzzy Controller

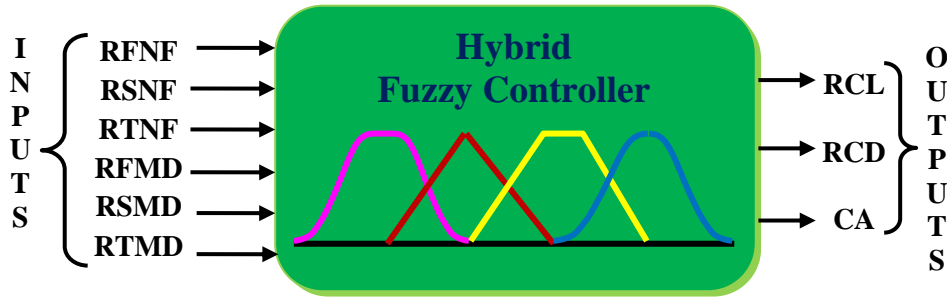


Fig. 6.6. Hybrid Fuzzy Controller

6.3.1. Fuzzy mechanism for inclined crack identification

Based on the above fuzzy subsets, the fuzzy control rules are defined in a general form as follows:

If (RFNF is $RFNF_i$ and RSNF is $RSNF_j$ and RTNF is $RTNF_k$ and RFMD is $RFMD_l$ and RSMD is $RSMD_m$ and RTMD is $RTMD_n$) then (RCL is RCL_{ijklmn} and RCD is RCD_{ijklmn} and CA is CA_{ijklmn})

$$(6.1)$$

where $i=1$ to 9 , $j=1$ to 9 , $k=1$ to 9 , $l=1$ to 9 , $m=1$ to 9 , $n=1$ to 9

As “RFNF”, “RSNF”, “RTNF”, “RFMD”, “RSMD” and “RTMD” have nine membership functions each. From the above equation (6.1), three sets of rules can be written

- i. If (RFNF is $RFNF_i$ and RSNF is $RSNF_j$ and RTNF is $RTNF_k$ and RFMD is $RFMD_l$ and RSMD is $RSMD_m$ and RTMD is $RTMD_n$) then (RCL is RCL_{ijklmn})
- ii. If (RFNF is $RFNF_i$ and RSNF is $RSNF_j$ and RTNF is $RTNF_k$ and RFMD is $RFMD_l$ and RSMD is $RSMD_m$ and RTMD is $RTMD_n$) then (RCD is RCD_{ijklmn})
- iii. If (RFNF is $RFNF_i$ and RSNF is $RSNF_j$ and RTNF is $RTNF_k$ and RFMD is $RFMD_l$ and RSMD is $RSMD_m$ and RTMD is $RTMD_n$) then (CA is CA_{ijklmn})

According to the usual fuzzy logic control method [64, 65], a factor is defined in the rules as follows:

$$W_{ijklmn} = \mu_{RFNF_i}(RF_i) \wedge \mu_{RSNF_j}(RF_j) \wedge \mu_{RTNF_k}(RF_k) \wedge \mu_{RFMD_l}(RM_l) \wedge \mu_{RSMD_m}(RM_m) \wedge \mu_{RTMD_n}(RM_n)$$

Where RF_i , RF_j and RF_k are the relative first, second and third mode natural frequencies of the inclined crack cantilever beam respectively; RM_l , RM_m and RM_n are the relative first, second and third mode shape differences of the inclined crack cantilever beam respectively. By applying the composition rule of inference [64, 65], the membership values of the relative crack location, relative crack depth and crack angle, $(location)_{RCL}$, $(depth)_{RCD}$ and $(angle)_{CA}$ can be computed as;

$$\left. \begin{aligned} \mu_{RCLijklmn}(\text{location}) &= W_{ijklmn} \wedge \mu_{RCLijklmn}(\text{location}) & \forall_{\text{length}} \in \text{RCL} \\ \mu_{RCDijklmn}(\text{depth}) &= W_{ijklmn} \wedge \mu_{RCDijklmn}(\text{depth}) & \forall_{\text{depth}} \in \text{RCD} \\ \mu_{CAijklmn}(\text{angle}) &= W_{ijklmn} \wedge \mu_{CAijklmn}(\text{angle}) & \forall_{\text{angle}} \in \text{CA} \end{aligned} \right\} (6.2)$$

The overall conclusion by combining the outputs of all the fuzzy rules can be written as follows:

$$\left. \begin{aligned} \mu_{RCL}(\text{location}) &= \mu_{RCL111111}(\text{location}) \vee \dots \vee \mu_{RCLijklmn}(\text{location}) \vee \dots \vee \mu_{RCL101010101010}(\text{location}) \\ \mu_{RCD}(\text{depth}) &= \mu_{RCD111111}(\text{depth}) \vee \dots \vee \mu_{RCDijklmn}(\text{depth}) \vee \dots \vee \mu_{RCD101010101010}(\text{depth}) \\ \mu_{CA}(\text{angle}) &= \mu_{CA111111}(\text{angle}) \vee \dots \vee \mu_{CAijklmn}(\text{angle}) \vee \dots \vee \mu_{CA101010101010}(\text{angle}) \end{aligned} \right\} (6.3)$$

The crisp values of the relative crack location, relative crack depth and crack angle are computed using the center of gravity method [64, 65] as:

$$\left. \begin{aligned} \text{Relative crack location} = RCL_{1,2} &= \frac{\int (\text{location}) \cdot \mu_{RCL1,2}(\text{location}) \cdot d(\text{location})}{\int (\mu_{RCL1,2}(\text{location}) \cdot d(\text{location}))} \\ \text{Relative crack depth} = RCD_{1,2} &= \frac{\int (\text{depth}) \cdot \mu_{RCD1,2}(\text{depth}) \cdot d(\text{depth})}{\int (\mu_{RCD1,2}(\text{depth}) \cdot d(\text{depth}))} \\ \text{Crack angle} = CA_{1,2} &= \frac{\int (\text{angle}) \cdot \mu_{CA1,2}(\text{angle}) \cdot d(\text{angle})}{\int (\mu_{CA1,2}(\text{angle}) \cdot d(\text{angle}))} \end{aligned} \right\} (6.4)$$

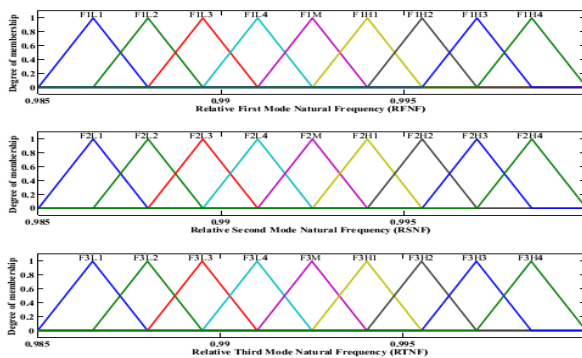


Fig.6.7. Triangular Membership functions for RFNF, RSNF and RTNF of vibration respectively

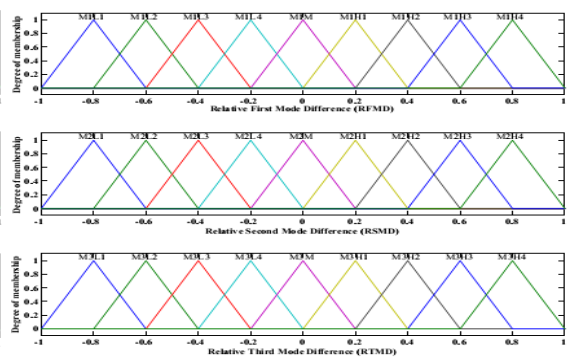


Fig.6.8. Triangular Membership functions for RFMD, RSMD and RTMD of vibration respectively

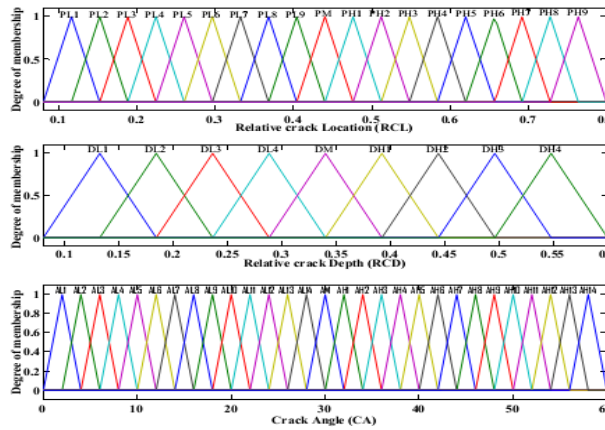


Fig.6.9. Triangular Membership functions for RCL, RCD and CA of vibration respectively

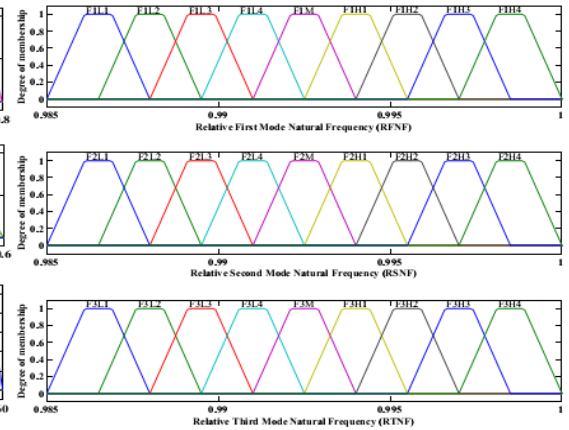


Fig.6.10. Trapezoidal Membership functions for RFNF, RSNF and RTNF of vibration respectively

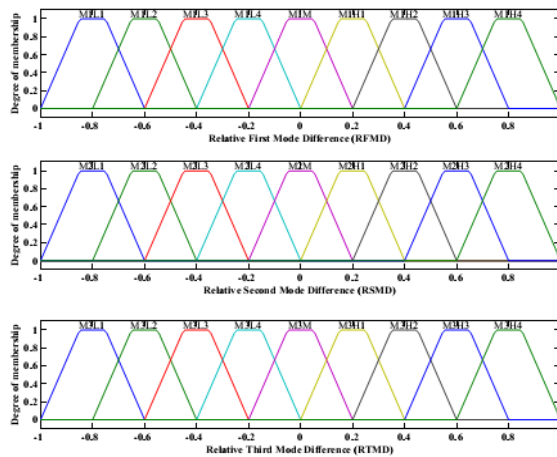


Fig.6.11. Trapezoidal Membership functions for RFMD, RSMD and RTMD of vibration respectively

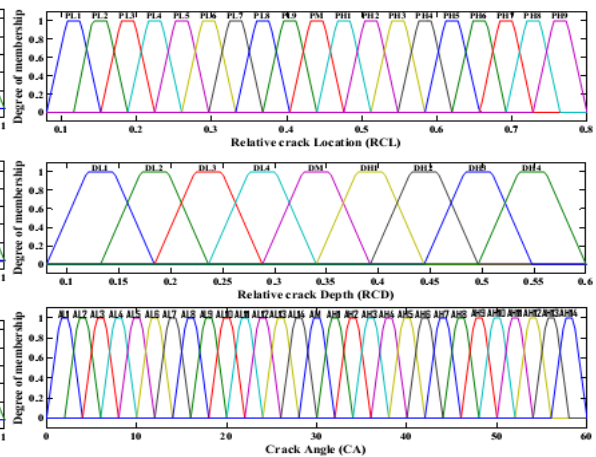


Fig.6.12. Trapezoidal Membership functions for RCL, RCD and CA of vibration respectively

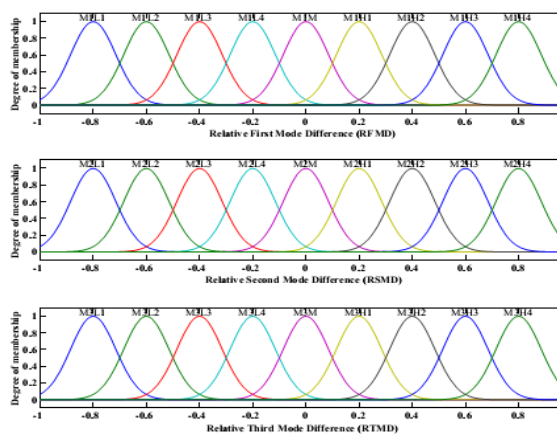


Fig.6.13. Gaussian Membership functions for RFNF, RSNF and RTNF of vibration respectively

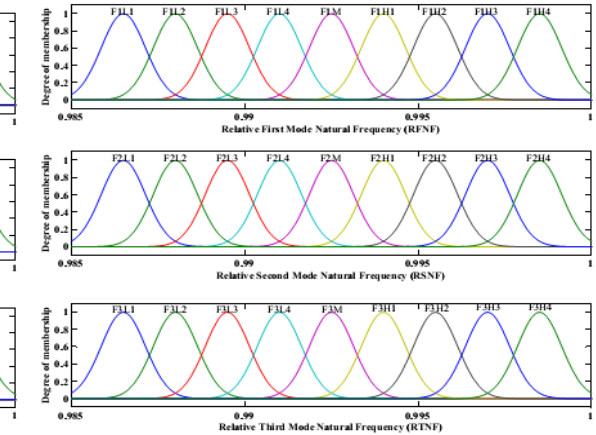


Fig.6.14. Gaussian Membership functions for RFMD, RSMD and RTMD of vibration respectively

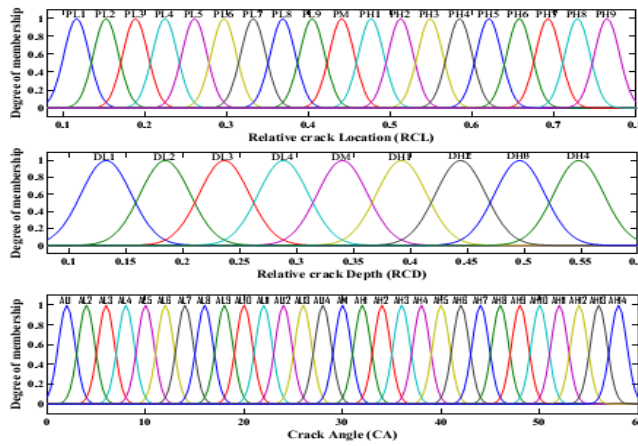


Fig.6.15. Gaussian Membership functions for RCL, RCD and CA of vibration respectively

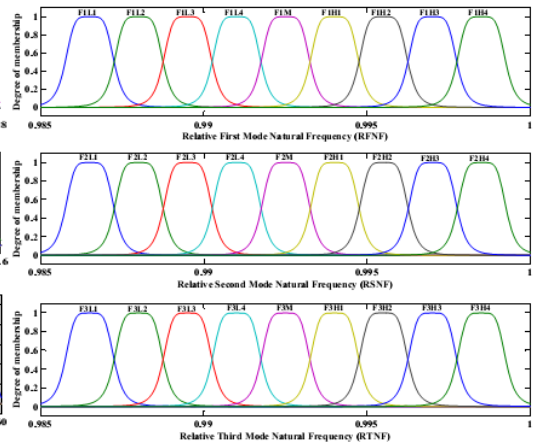


Fig.6.16. Bell-Shape Membership functions for RFNF, RSNF and RTNF of vibration respectively

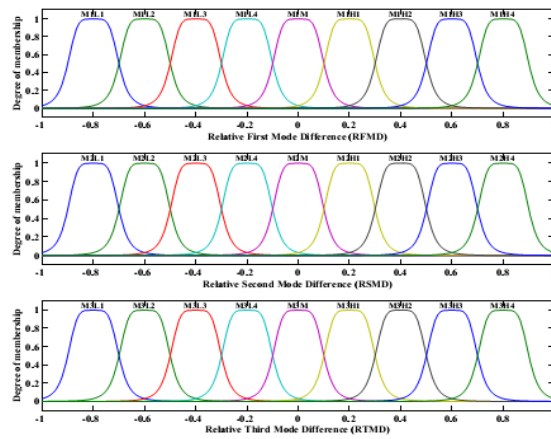


Fig.6.17. Bell-Shape Membership functions for RFMD, RSMD and RTMD of vibration respectively

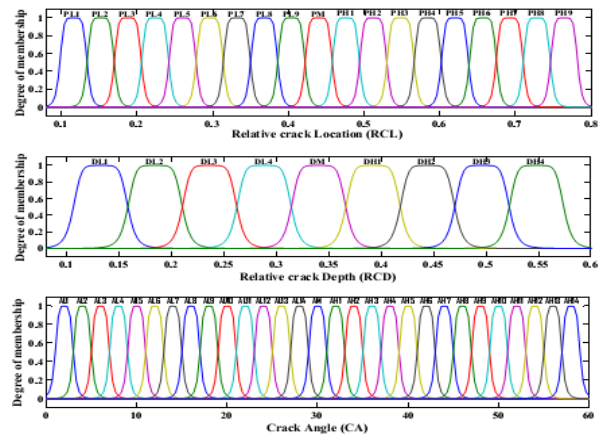


Fig.6.18. Bell-Shape Membership functions for RCL, RCD and CA of vibration respectively

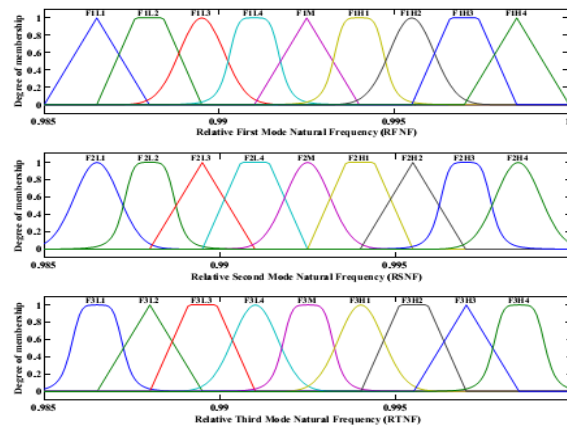


Fig.6.19. Hybrid Membership functions for RFNF, RSNF and RTNF of vibration respectively

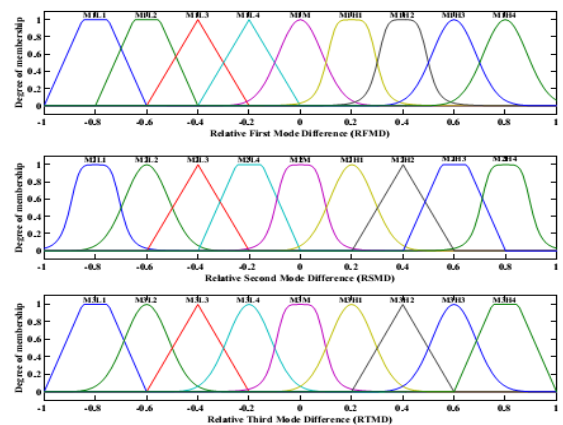


Fig.6.20. Hybrid Membership functions for RFMD, RSMD and RTMD of vibration respectively

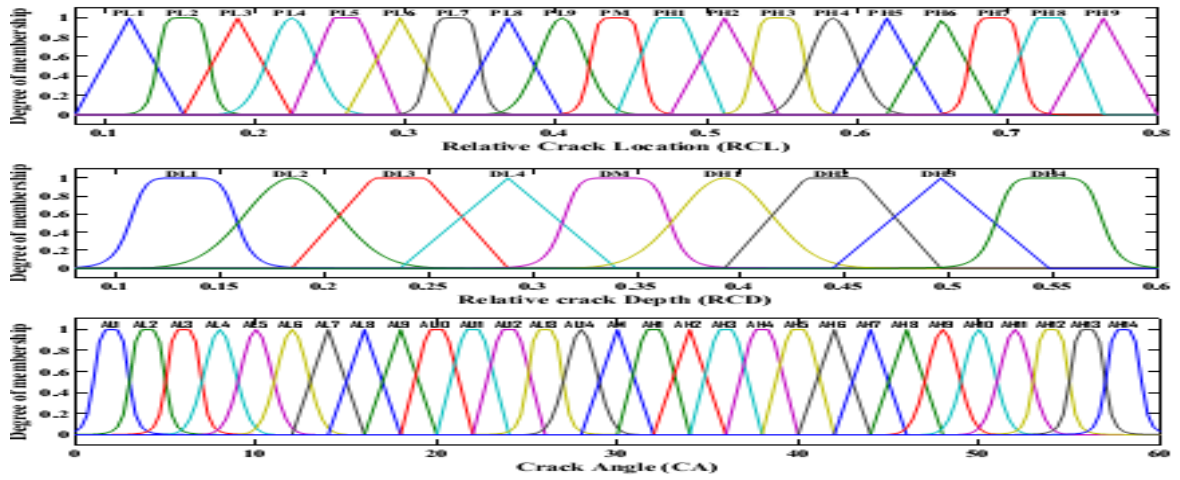


Fig.6.21. Hybrid Membership functions for RCL, RCD and CA of vibration respectively

Table 6.1. Description of Linguistic terms in fuzzy controllers

Membership Functions Name	Linguistic Terms	Definition of the Linguistic terms
F1L1, F1L2, F1L3	RFNF _{1 to 3}	Low ranges of relative first natural frequencies for the first mode of vibration
F1L4, F1M, F1H1	RFNF _{4 to 6}	Medium ranges of relative first natural frequencies for the first mode of vibration
F1H2, F1H3, F1H4	RFNF _{7 to 9}	Higher ranges of relative first natural frequencies of the first mode of vibration
F2L1, F2L2, F2L3	RSNF _{1 to 3}	Low ranges of relative second natural frequencies for the second mode of vibration
F2L4, F2M, F2H1	RSNF _{4 to 6}	Medium ranges of relative second natural frequencies for the second mode of vibration
F2H2, F2H3, F2H4	RSNF _{7 to 9}	Higher ranges of relative second natural frequencies for the second mode of vibration
F3L1, F3L2, F3L3	RTNF _{1 to 3}	Low ranges of relative third natural frequencies for the third mode of vibration
F3L4, F3M, F3H1	RTNF _{4 to 6}	Medium ranges of relative third natural frequencies for the third mode of vibration
F3H2, F3H3, F3H4	RTNF _{7 to 9}	Higher ranges of relative third natural frequencies for the third mode of vibration
M1L1, M1L2, M1L3	RFMD _{1 to 3}	Low ranges of relative first mode shape difference
M1L4, M1M, M1H1	RFMD _{4 to 6}	Medium ranges of relative first mode shape difference
M1H2, M1H3, M1H4	RFMD _{7 to 9}	Higher ranges of relative first mode shape difference
M2L1, M2L2, M2L3	RSMD _{1 to 3}	Small ranges of second relative mode shape difference
M2L4, M2M, M2H1	RSMD _{4 to 6}	Medium ranges of second relative mode shape difference
M2H2, M2H3, M2H4	RSMD _{7 to 9}	Higher ranges of second relative mode shape difference
M3L1, M3L2, M3L3	RTMD _{1 to 3}	Small ranges of third relative mode shape difference
M3L4, M3M, M3H1	RTMD _{4 to 6}	Medium ranges of third relative mode shape difference

M3H2, M3H3, M3H4	RTMD _{7 to 9}	Higher ranges of third relative mode shape difference
PL1, PL2, PL3, PL4	RCL _{1 to 4}	Very low ranges of relative crack locations
PL5, PL6, PL7, PL8	RCL _{5 to 8}	Low ranges of relative crack locations
PL9, PM, PH1	RCL _{9 to 11}	Medium ranges of relative crack locations
PH2, PH3, PH4, PH5	RCL _{12 to 15}	High ranges of relative crack locations
PH6, PH7, PH8, PH9	RCL _{16 to 19}	Very high ranges of relative crack locations
DL1, DL2, DL3	RCD _{1 to 3}	Low ranges of relative crack depths
DL4, DM, DH1	RCD _{4 to 6}	Medium ranges of relative crack depths
DH2, DH3, DH4	RCD _{7 to 9}	High ranges of relative crack depths
AL1, AL2, AL3, AL4	CA _{1 to 4}	Very very low crack angles
AL5, AL6, AL7, AL8	CA _{5 to 9}	Very low crack angles
AL9,AL10,AL11,AL12	CA _{9 to 12}	Low crack angles
AL13,AL14,AM,AH1,AH2	CA _{13 to 17}	Medium crack angles
AH3,AH4,AH5,AH6	CA _{18 to 21}	High crack angles
AH7,AH8,AH9,AH10	CA _{22 to 25}	Very high crack angles
AH11,AH12,AH13,AH14	CA _{26 to 29}	Very very high crack angles

6.3.2. Results of fuzzy model

The results calculated from the designed fuzzy inference system for inclined crack detection are shown in this section. The fuzzy inference model (Fig. 6.1) has been designed with six inputs (relative first three natural frequencies and relative first three mode shape differences) and three outputs (relative crack location, relative crack depth and crack angle). Five types of membership functions (triangular, Gaussian, trapezoidal, bell shape and hybrid) have been engaged to develop the fuzzy inference model (Fig.6.2 to Fig 6.21). The results obtained from numerical, finite element, fuzzy triangular, fuzzy trapezoidal, fuzzy Gaussian, fuzzy bell shape and hybrid model and experimental analysis are compared in Table 6.2 and Table 6.3.

Table 6.2. Comparison between Triangular, Trapezoidal, Gaussian, Bell Shape & Hybrid Fuzzy Controllers results of inclined edge crack in cantilever beams

Crack inclination (θ) 45°			Crack inclination (θ) 30°			Crack inclination (θ) 15°			Crack inclination (θ) 0°				
0.9999	0.9989	0.9996	0.9998	0.9990	0.9995	0.9998	0.9990	0.9996	0.9999	0.9989	0.9996	RFNF	
0.9949	0.9958	0.9999	0.9954	0.9963	0.9999	0.9948	0.9960	0.9999	0.9949	0.9958	0.9999		RSNF
0.9849	0.9997	0.9997	0.9866	0.9998	0.9997	0.9851	0.9999	0.9997	0.9852	0.9998	0.9997		
0.0003	0.0017	0.0004	0.0002	0.0016	0.0003	0.0003	0.0018	0.0006	0.0003	0.0018	0.0006	RFMD	
-0.0658	-0.0038	-0.0002	-0.0585	-0.0035	-0.0003	-0.0654	-0.0038	-0.0001	-0.0651	-0.0039	-0.0001		RSMD
-0.0414	0.0131	-0.0007	-0.0367	0.0075	-0.0007	-0.0411	0.0076	-0.0007	-0.0405	0.0122	-0.0007		
0.72	0.43	0.23	0.73	0.42	0.22	0.72	0.43	0.22	0.71	0.41	0.21	Triangular	
0.46	0.27	0.06	0.46	0.26	0.07	0.44	0.26	0.06	0.45	0.25	0.05		
0.732	0.437	0.234	0.737	0.431	0.232	0.729	0.435	0.230	0.731	0.423	0.221	Trapezoidal	
0.463	0.272	0.062	0.463	0.263	0.071	0.447	0.262	0.061	0.459	0.255	0.061		
0.735	0.443	0.245	0.746	0.447	0.246	0.737	0.441	0.241	0.742	0.435	0.239	Gaussian	
0.481	0.288	0.078	0.473	0.275	0.081	0.452	0.275	0.069	0.479	0.267	0.072		
0.745	0.467	0.248	0.749	0.465	0.249	0.741	0.450	0.249	0.748	0.456	0.242	Bell shape	
0.489	0.295	0.089	0.482	0.286	0.091	0.465	0.283	0.075	0.485	0.279	0.083		
0.758	0.502	0.254	0.756	0.482	0.252	0.752	0.498	0.253	0.752	0.501	0.251	Hybrid	
0.502	0.305	0.101	0.503	0.306	0.103	0.497	0.298	0.09	0.502	0.301	0.101		

Table 6.3. Comparison between Gaussian, Bell Shape & Hybrid Fuzzy Controllers with FEA & Experimental results of inclined edge crack in cantilever beams

Crack inclination (θ) 45°		Crack inclination (θ) 30°			Crack inclination (θ) 15°			Crack inclination (θ) 0°			
0.9999	0.9989	0.9996	0.9998	0.9990	0.9998	0.9990	0.9996	0.9999	0.9989	0.9996	RFNF
0.9949	0.9958	0.9999	0.9954	0.9963	0.9999	0.9948	0.9960	0.9999	0.9958	0.9999	RSNF
0.9849	0.9997	0.9997	0.9866	0.9998	0.9997	0.9851	0.9999	0.9997	0.9998	0.9997	RTNF
0.0003	0.0017	0.0004	0.0002	0.0016	0.0003	0.0003	0.0018	0.0006	0.0018	0.0006	RFMD
-0.0658	-0.0038	-0.0002	-0.0585	-0.0035	-0.0003	-0.0654	-0.0038	-0.0001	-0.0039	-0.0001	RSMD
-0.0414	0.0131	-0.0007	-0.0367	0.0075	-0.0007	-0.0411	0.0076	-0.0007	0.0122	-0.0007	RTMD
0.735	0.443	0.245	0.746	0.447	0.246	0.737	0.441	0.241	0.435	0.239	Gaussian
0.481	0.288	0.078	0.473	0.275	0.081	0.452	0.275	0.069	0.267	0.072	
0.745	0.467	0.248	0.749	0.465	0.249	0.741	0.450	0.249	0.456	0.242	Bell shape
0.489	0.295	0.089	0.482	0.286	0.091	0.465	0.283	0.075	0.279	0.083	
0.758	0.502	0.254	0.756	0.482	0.252	0.752	0.498	0.253	0.501	0.251	Hybrid
0.502	0.305	0.101	0.503	0.306	0.103	0.497	0.298	0.09	0.301	0.101	
0.75	0.5	0.25	0.75	0.5	0.25	0.75	0.5	0.25	0.5	0.25	FEA
0.5	0.3	0.1	0.5	0.3	0.1	0.5	0.3	0.1	0.3	0.1	
0.767	0.517	0.257	0.781	0.522	0.253	0.7743	0.521	0.258	0.512	0.257	Experiment
0.52	0.308	0.103	0.509	0.306	0.103	0.517	0.312	0.103	0.311	0.104	

6.3.3. Summary

The fuzzy method agreed in the current analysis has been studied and following conclusions are made. The presence of inclined crack in cantilever beam has considerable effect on the dynamic response of the dynamic structure. The first three relative natural frequencies and first three relative mode shape differences are taken as inputs to the fuzzy controller and relative crack location, relative crack depth and crack angle are the output parameters. The validity of the proposed method has been established by comparing the results from the fuzzy models (triangular, trapezoidal, Gaussian, bell shape and hybrid) with that of the numerical, finite element and experimental analysis. The results are found to be well in agreement. From the analysis of the results obtained from the fuzzy models using various membership functions, it is observed that the fuzzy system based on Gaussian, bell shape and hybrid membership function provides better results in comparison to numerical, finite element analysis, trapezoidal and triangular fuzzy models. Hence, the proposed Gaussian, bell shape and hybrid fuzzy model can be effectively used as inclined crack diagnostic tools in dynamically vibrating structures.

CHAPTER 07

ANALYSIS OF ARTIFICIAL NEURAL NETWORK FOR IDENTIFICATION OF CRACK

- 7.1 Introduction**
- 7.2 Development of an ANN Model**
- 7.3 Model Building**
- 7.4 Architecture of Neural Networks**
- 7.5 Back propagation Algorithm**
- 7.6 Analysis of Artificial Neural Network model for crack identification**
- 7.7 Results and discussion of neural controller**
- 7.8 Summary**

CHAPTER 07

ANALYSIS OF ARTIFICIAL NEURAL NETWORK FOR IDENTIFICATION OF CRACK

The presence of crack in the engineering structure increases the flexibility, decreases the stiffness or decreases the modal frequencies and changes the modal amplitude of vibration. Those variations of vibration parameters used to locate the crack position, crack depth and crack inclination. Hence, it is of importance to develop and design an Artificial Intelligent technique for inclined crack identification to avoid catastrophic failure of a structural element. In this chapter, an intelligent technique has been developed, called Artificial Neural Network (ANN) to identify the presence of inclined crack in vibrating structure. ANN is designed with required amount of trained data generated from back propagation technique. Finally, the results from this model have been compared with the experimental results for validate the proposed neural technique.

7.1. Introduction

Artificial Neural Networks (ANNs) are non-linear mapping structures based on the function of the human brain. They are powerful tools for modeling, especially when the underlying data relationship is unknown. ANNs can identify and learn correlated patterns between input data sets and corresponding target values. After training, ANNs can be used to predict the outcome of new independent input data. ANNs imitate the learning process of the human brain and can process problems involving non-linear and complex data even if the data are imprecise and noisy. An ANN is a computational structure that is inspired by observed process in natural networks of biological neurons in the brain. It consists of simple computational units called neurons, which are highly interconnected. A very important feature of these networks is their adaptive nature, where “learning by example” replaces “programming” in solving problems. This feature makes such computational models very appealing in application domains where one has little or incomplete understanding of the problem to be solved but where training data is readily available. The most widely used learning algorithm in an ANN is the Back propagation algorithm. There

are various types of ANNs like Multilayered Perceptron, Radial Basis Function and Kohonen networks.

7.2. Development of an ANN Model

Development of ANN model is discussed here briefly. ANNs are constructed with layers of units, and thus are termed multilayer ANNs. A layer of units in such an ANN is composed of units that perform similar tasks. First layer of a multilayer ANN consists of input units. These units are known as independent variables in statistical literature. Last layer contains output units. In statistical nomenclature, these units are known as dependent or response variables. All other units in the model are called hidden units and constitute hidden layers. There are two functions governing the behavior of a unit in a particular layer, which normally are the same for all units within the whole ANN, i.e.

- the input function, and
- the output/activation function.

Input into a node is a weighted sum of outputs from nodes connected to it. The input function is normally given by equation (1) as follows:

$$\text{net}_i = \sum_j w_{ij} x_j + \mu_i \quad (7.1)$$

where net_i describes the result of the net inputs x_i (weighted by the weights w_{ij}) impacting on unit i . Also, w_{ij} are weights connecting neuron j to neuron i , x_j is output from unit j and μ_i is a threshold for neuron i . Threshold term is baseline input to a node in absence of any other inputs. If a weight w_{ij} is negative, it is termed inhibitory because it decreases net input, otherwise it is called excitatory.

Each unit takes its net input and applies an activation function to it. For example, output of j^{th} unit, also called activation value of the unit, is $g(\sum w_{ij} x_i)$, where $g(\cdot)$ is activation function and x_i is output of i^{th} unit connected to unit j . A number of nonlinear functions have been used in the literature as activation functions. The threshold function is useful in situations where the inputs and outputs are binary encoded. However, most common choice is sigmoid functions, such as

$$g(\text{netinput}) = \left[1 + e^{-\text{netinput}} \right]^{-1}$$

Or, $g(\text{netinput}) = \tanh(\text{netinput})$

The activation function exhibits a great variety, and has the biggest impact on behavior and performance of the ANN. The main task of the activation function is to map the outlying values of the obtained neural input back to a bounded interval such as [0, 1] or [-1, 1]. The sigmoid function has some advantages, due to its differentiability within the context of finding a steepest descent gradient for the back propagation method and moreover maps a wide domain of values into the interval [0, 1].

The various steps in developing a neural network forecasting model are:

1. Variable Selection:

The input variables important for modeling/ forecasting variable(s) under study are selected by suitable variable selection procedures.

2. Formation of Training, Testing and Validation Sets:

The data set is divided into three distinct sets called training, testing and validation sets. The training set is the largest set and is used by neural network to learn patterns present in the data. The testing set is used to evaluate the generalization ability of a supposedly trained network. A final check on the performance of the trained network is made using validation set.

3. Neural Network Architecture:

Neural network architecture defines its structure including number of hidden layers, number of hidden nodes and number of output nodes etc.

(i) Number of hidden layers: The hidden layer(s) provide the network with its ability to generalize. In theory, a neural network with one hidden layer with a sufficient number of hidden neurons is capable of approximating any continuous function. In practice, neural network with one and occasionally two hidden layers are widely used and have to perform very well.

(ii) Number of hidden nodes: There is no magic formula for selecting the optimum number of hidden neurons. However, some thumb rules are available for calculating number of hidden neurons. A rough approximation can be obtained by the geometric pyramid rule proposed by Masters (1993). For a three layer network with an input and m output neurons, the hidden layer would have $\sqrt{n*m}$ neurons.

(iii) Number of output nodes: Neural networks with multiple outputs, especially if these outputs are widely spaced, will produce inferior results as compared to a network with a single output.

(iv) Activation function: Activation functions are mathematical formulae that determine the output of a processing node. Each unit takes its net input and applies an activation function to it. Nonlinear functions have been used as activation functions such as logistic, tanh etc. The purpose of the transfer function is to prevent output from reaching very large value which can ‘paralyze’ neural networks and thereby inhibit training. Transfer functions such as sigmoid are commonly used because they are nonlinear and continuously differentiable which are desirable for network learning.

7.3. Model Building

Multilayer feed forward neural network or multilayer perceptron (MLP) is very popular and is used more than other neural network type for a wide variety of tasks. Multilayer feed forward neural network learned by back propagation algorithm is based on supervised procedure, i.e., the network constructs a model based on examples of data with known output. The characteristics of Multilayer Perceptron are as follows:

(i) has any number of inputs

(ii) has one or more hidden layers with any number of nodes. The internal layers are called “hidden” because they only receive internal input (input from other processing units) and produce internal output (output to other processing units). Consequently, they are hidden from the output world.

(iii) uses linear combination function in the hidden and output layers

(iv) uses generally sigmoid activation function in the hidden layers

(v) has any number of outputs with any activation function.

(vi) has connections between the input layer and the first hidden layer, between the hidden layers, and between the last hidden layer and the output layer.

An MLP with just one hidden layer can learn to approximate virtually any function to any degree of accuracy. One hidden layer is always sufficient provided we have enough data. Schematic representation of neural network is given in Fig. 1 and mathematical representation of neural network is given in Fig. 2.

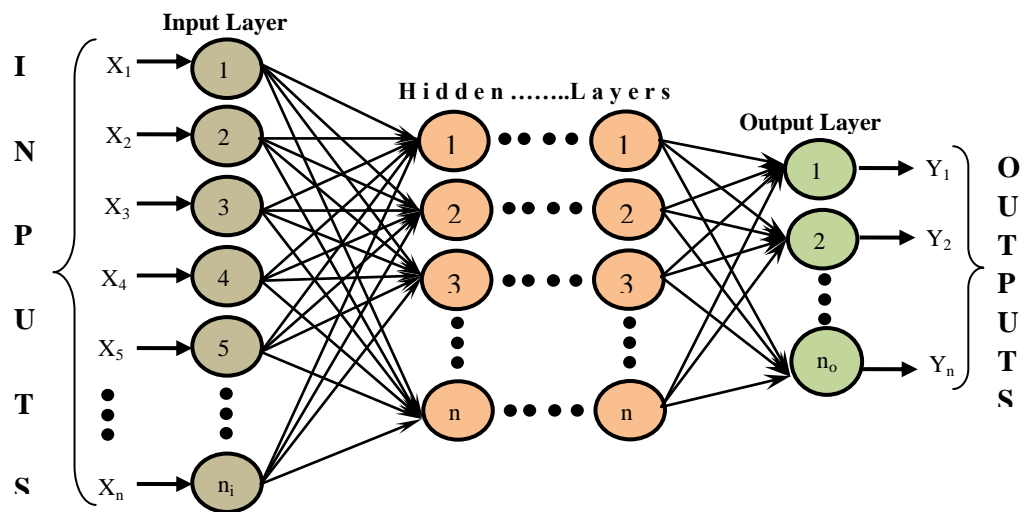


Fig.7.1: Schematic representation of neural network

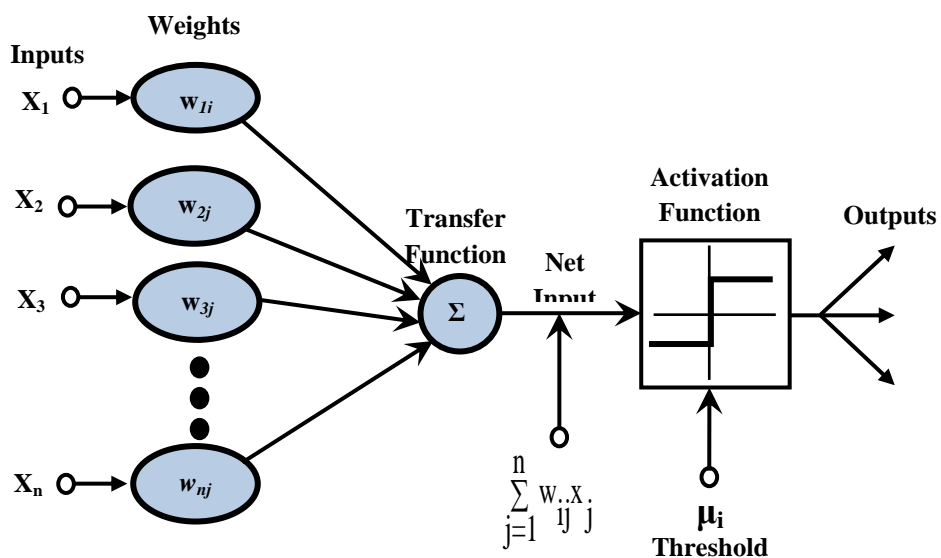


Fig.7.2: Mathematical representation of neural network

Each interconnection in an ANN has a strength that is expressed by a number referred to as weight. This is accomplished by adjusting the weights of given interconnection according to some learning algorithm. Learning methods in neural networks can be broadly classified into three basic types (i) supervised learning (ii) unsupervised learning and (iii) reinforced learning. In MLP, the supervised learning will be used for adjusting the weights. The graphic representation of this learning is given in Fig.7.3.

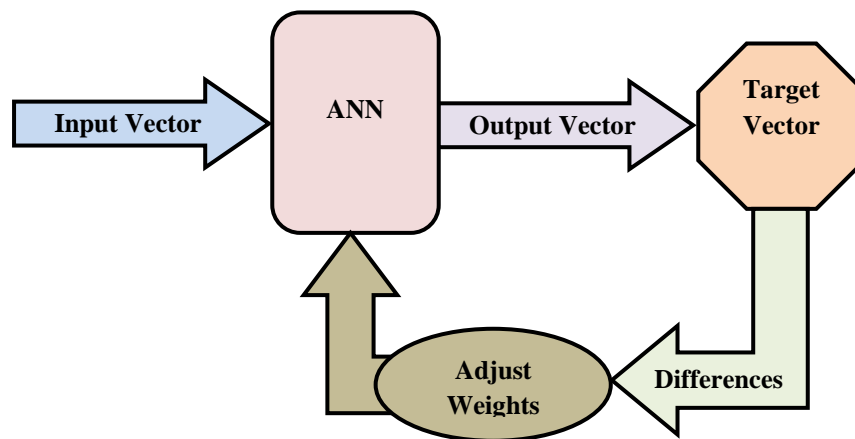


Fig.7.3: A learning cycle in the ANN model

7.4. Architecture of Neural Networks

There are several types of architecture of ANN. However, the two most widely used ANN are discussed below:

1. Feed forward Networks

Feed forward ANNs allow signals to travel one way only; from input to output. There is no feedback (loops) i.e. the output of any layer does not affect that same layer. They are extensively used in pattern recognition.

2. Feedback/Recurrent Networks

Feedback networks can have signals traveling in both directions by introducing loops in the network. Feedback networks are dynamic; their 'state' is changing continuously until they reach an equilibrium point. They remain at the equilibrium point until the input changes and a new equilibrium needs to be found.

7.5. Back propagation Algorithm

The MLP network is trained using one of the supervised learning algorithms of which the best known example is back propagation, which uses the data to adjust the network's weights and thresholds so as to minimize the error in its predictions on the training set.

We denote by W_{ij} the weight of the connection from unit u_i to unit u_j . It is then convenient to represent the pattern of connectivity in the network by a weight matrix W whose elements are the weights W_{ij} . The pattern of connectivity characterizes the architecture of the network. A unit in the output layer determines its activity by following a two-step procedure.

- First, it computes the total weighted input x_j , using the formula:

$$x_j = \sum_i y_i W_{ij} \quad (7.2)$$

where y_i is the activity level of the i^{th} unit in the previous layer and W_{ij} is the weight of the connection between the i^{th} and the j^{th} unit.

- Next, the unit calculates the activity y_j using some function of the total weighted input.

Typically we use the sigmoid function:

$$y_j = \left[1 + e^{-x_j} \right]^{-1} \quad (7.3)$$

Once the activities of all output units have been determined, the network computes the error E , which is defined by the expression:

$$E = \frac{1}{2} \sum_i (y_i - d_i)^2 \quad (7.4)$$

where y_j is the activity level of the j^{th} unit in the top layer and d_j is the desired output of the j^{th} unit.

The back propagation algorithm consists of four steps:

(i) Compute how fast the error changes as the activity of an output unit is changed.

This error derivative (EA) is the difference between the actual and the desired activity.

$$EA_j = \frac{\partial E}{\partial y_j} = y_j - d_j \quad (7.5)$$

(ii) Compute how fast the error changes as the total input received by an output unit is changed. This quantity (EI) is the answer from step (i) multiplied by the rate at which the output of a unit changes as its total input is changed.

$$EI_j = \frac{\partial E}{\partial X_j} = \frac{\partial E}{\partial y_j} \times \frac{\partial y_j}{\partial X_j} = EA_j y_j (1 - y_j) \quad (7.6)$$

(iii) Compute how fast the error changes as a weight on the connection into an output unit is changed. This quantity (EW) is the answer from step (ii) multiplied by the activity level of the unit from which the connection emanates.

$$EW_{ij} = \frac{\partial E}{\partial W_{ij}} = \frac{\partial E}{\partial X_j} \times \frac{\partial X_j}{\partial W_{ij}} = EI_j y_i \quad (7.7)$$

(iv) Compute how fast the error changes as the activity of a unit in the previous layer is changed. This crucial step allows back propagation to be applied to multilayer networks. When the activity of a unit in the previous layer changes, it affects the activities of all the output units to which it is connected. So to compute the overall effect on the error, we add together all these separate effects on output units. But each effect is simple to calculate. It is the answer in step (iii) multiplied by the weight on the connection to that output unit.

$$EA_i = \frac{\partial E}{\partial y_i} = \frac{\partial E}{\partial X_j} \times \frac{\partial X_j}{\partial y_i} = \sum_j EI_j W_{ij} \quad (7.8)$$

By using steps (ii) and (iv), we can convert the EAs of one layer of units into EAs for the previous layer. This procedure can be repeated to get the EAs for as many previous layers as desired. Once we know the EA of a unit, we can use steps (ii) and (iii) to

compute the EWs on its incoming connections.

7.6. Analysis of Artificial Neural Network model for crack identification

A back propagation artificial neural network model has been developed for detection of inclined crack (i.e. relative crack location, relative crack depth and crack angle) of a cantilever beam (Fig.7.4). The designed neural model has been developed with six input parameters and three output parameters. The input parameters to the neural network model are “RFNF”, “RSNF”, “RTNF”, “RFMD”, “RSMD” and “RTMD”. The output parameters from the neural network model are “RCL”, “RCD” and “CA”. The back propagation neural network has been designed with one input layer, one output layer and five hidden layers. The input layer contains six neurons, whereas the output layer contains three neurons. The number of neurons in each hidden layers i.e. 1st, 2nd, 3rd, 4th and 5th layer are 9, 11, 13, 11 and 9 neurons respectively in order to give the neural network a diamond shape and for better convergence of results (Fig.5).

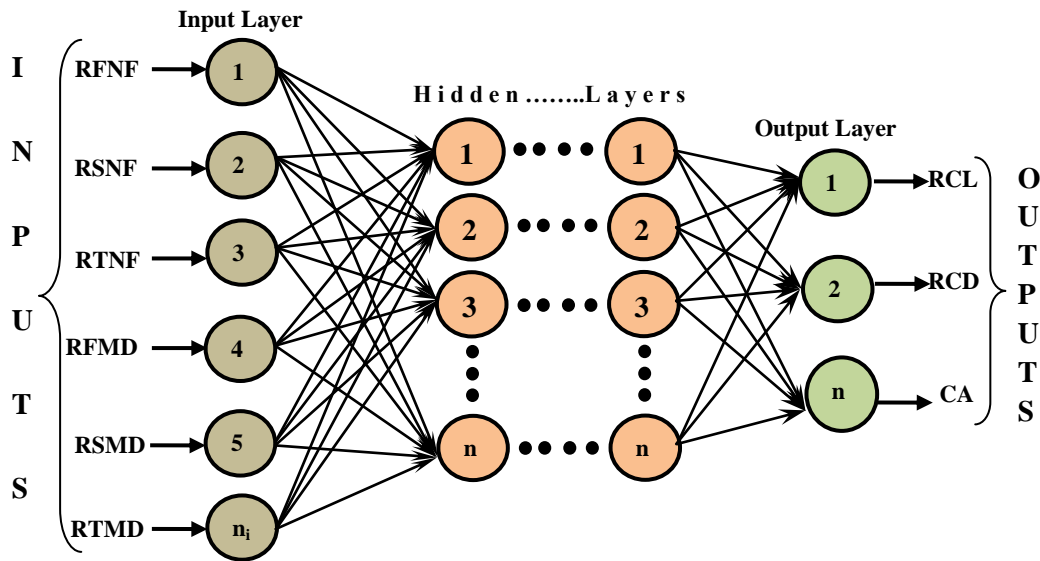


Fig.7.4. Schematic Representation of Neural Model

The neural network model used in the present analysis is a seven-layered feed forward neural network model trained with back propagation technique. The chosen number of layers was found empirically to facilitate training.

The designed artificial neural network model for inclined crack detection has been trained with 800 patterns of data featuring various conditions of the structural element. During the

training, the model is fed with six input parameters i.e. first three relative natural frequencies and first three mode shape differences. The outputs are relative crack location, relative crack depth and crack angle.

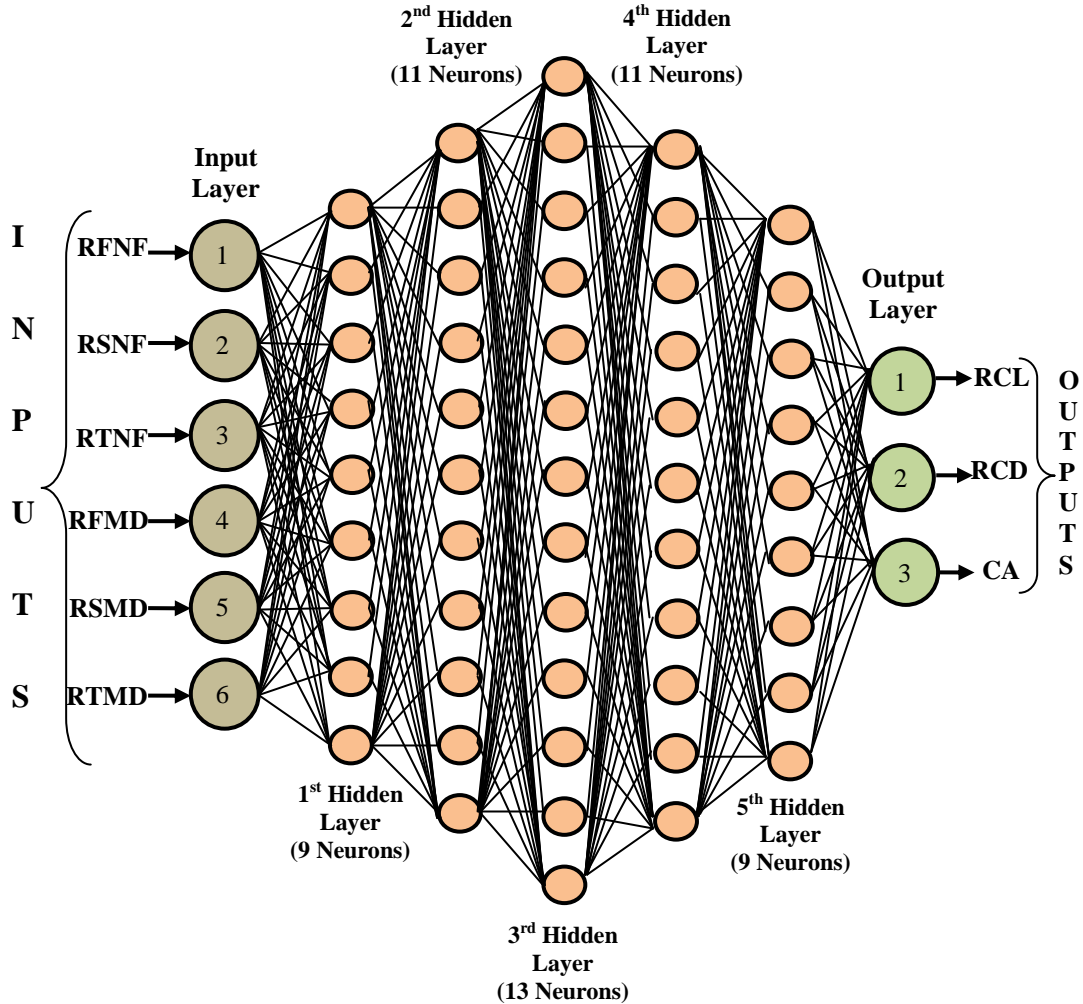


Fig.7.5. Schematic Representation of Neural Model

During training and during normal operation, the input patterns fed to the neural network comprise the following components:

$$y_1^{\{1\}} = \text{relative deviation of first natural frequency} \quad (7.9(a))$$

$$y_2^{\{1\}} = \text{relative deviation of second natural frequency} \quad (7.9 (b))$$

$$y_3^{\{1\}} = \text{relative deviation of third natural frequency} \quad (7.9 (c))$$

$$y_4^{\{1\}} = \text{relative deviation of first mode shape difference} \quad (7.9 \text{ (d)})$$

$$y_5^{\{1\}} = \text{relative deviation of second mode shape difference} \quad (7.9 \text{ (e)})$$

$$y_6^{\{1\}} = \text{relative deviation of third mode shape difference} \quad (7.9 \text{ (f)})$$

The outputs generated due to the distribution of the input to the hidden neurons are given by [66]:

$$f(V_j^{\{\text{lay}\}}) = y_j^{\{\text{lay}\}} \quad (7.10)$$

Where,

$$\sum_i W_{ji}^{\{\text{lay}\}} \cdot y_i^{\{\text{lay}-1\}} = V_j^{\{\text{lay}\}} \quad (7.11)$$

layer number (2 or 6) = lay

label for j^{th} neuron in hidden layer 'lay' = j

label for i^{th} neuron in hidden layer 'lay-1' = i

Weight of the connection from neuron i in layer 'lay-1' to neuron j in layer 'lay' = $W_{ji}^{\{\text{lay}\}}$

Activation function, chosen in this work as the hyperbolic tangent function = $f(\cdot)$, where,

$$\frac{e^x - e^{-x}}{e^x + e^{-x}} = f(x) \quad (7.12)$$

In the process of training, the network output $\theta_{\text{actual}, n}$ ($i=1$ to 2) may differ from the desired output $\theta_{\text{desired}, n}$ ($n=1$ to 2) as specified in the training pattern presented to the network. The measure of performance of the network is the instantaneous sum-squared difference between $\theta_{\text{desired}, n}$ and $\theta_{\text{actual}, n}$ for the set of presented training patterns:

$$Err = \frac{1}{2} \sum_{\substack{\text{all training} \\ \text{patterns}}} (\theta_{\text{desired}, n} - \theta_{\text{actual}, n})^2 \quad (7.13)$$

Where $\theta_{actual, n}$ (n=1) represents the relative crack location (“RCL”)

$\theta_{actual, n}$ (n=2) represents the relative crack depth (“RCD”)

$\theta_{actual, n}$ (n=3) represents crack angle (“CA”)

During the development of the neural model, the error back propagation method is employed to train the network [66]. This method requires the computation of local error gradients in order to determine appropriate weight corrections to reduce error. For the output layer, the error gradient $\delta^{\{5\}}$ is:

$$\delta^{\{5\}} = f'(V_1^{\{5\}}) (\theta_{desired, n} - \theta_{actual, n}) \quad (7.14)$$

Hence, the local gradient for neurons in hidden layer {lay} is given by:

$$\delta_j^{\{lay\}} = f'(V_j^{\{lay\}}) \left(\sum_k \delta_k^{\{lay+1\}} W_{kj}^{\{lay+1\}} \right) \quad (7.15)$$

Synaptic weights are updated according to the following expressions:

$$W_{ji}(t+1) = W_{ji}(t) + \Delta W_{ji}(t+1) \quad (7.16)$$

$$\text{and } \Delta W_{ji}(t+1) = \alpha \Delta W_{ji}(t) + \eta \delta_j^{\{lay\}} y_i^{\{lay-1\}} \quad (7.17)$$

Where Momentum coefficient (chosen statistically as 0.2 in this work) = α , Learning rate (chosen statistically as 0.35 in this work) = η , Iteration number, each iteration consisting of the presentation of a training pattern and correction of the weights = t, Following expression shows, the final output from the neural network as;

$$\theta_{actual, n} = f(V_n^{\{5\}}) \quad (7.18)$$

$$\text{Where } V_n^{\{5\}} = \sum_i W_{ni}^{\{5\}} y_i^{\{4\}} \quad (7.19)$$

η = learning rate (chosen empirically as 0.35 in this work)

t = iteration number, each iteration consisting of the presentation of a training pattern and correction of the weights.

7.7. Results and discussion of neural controller

Table 7.1. The results of modal analysis obtained from ANN Controller

Input to the ANN Controller						Output from the ANN Controller	
RFNF	RSNF	RTNF	RFMD	RSMD	RTMD	RCL (β)	RCD (α)
Crack inclination (θ) 0°							
0.99968	0.99998	0.99978	0.0006	-0.00017	-0.00073	0.257	0.103
0.99846	0.99988	0.9989	0.00259	-0.00093	-0.00328	0.2575	0.2068
0.99893	0.99582	0.99985	0.00187	-0.00394	0.01222	0.5122	0.309
0.99809	0.99182	0.99993	0.00391	-0.00788	0.00928	0.518	0.4
0.99999	0.99703	0.9914	0.00013	-0.03827	-0.02445	0.775	0.408
0.99992	0.99491	0.98529	0.00034	-0.06516	-0.04052	0.781	0.509
Crack inclination (θ) 15°							
0.99966	0.99998	0.99978	0.0006	-0.00019	-0.00073	0.251	0.101
0.99852	0.99992	0.99897	0.00269	-0.00088	-0.00328	0.256	0.201
0.99908	0.99609	0.99993	0.00186	-0.00382	0.00767	0.518	0.309
0.99817	0.99215	0.99993	0.00375	-0.00757	0.01086	0.513	0.408
0.99999	0.99714	0.99162	0.00013	-0.0371	-0.02377	0.781	0.435
0.99981	0.99483	0.98514	0.00034	-0.06545	-0.04119	0.772	0.511
Crack inclination (θ) 30°							
0.99959	0.9999	0.99971	0.00032	-0.00036	-0.00079	0.252	0.102
0.99855	0.99988	0.99897	0.00245	-0.0009	-0.0031	0.254	0.202
0.99908	0.99633	0.99985	0.00165	-0.00357	0.00753	0.521	0.302
0.99832	0.99294	0.99993	0.00327	-0.00671	0.01007	0.514	0.406
0.99999	0.99745	0.99272	6.7E-05	-0.03106	-0.01996	0.7699	0.41
0.99988	0.99543	0.98669	0.00027	-0.05856	-0.03671	0.779	0.503
Crack inclination (θ) 45°							
0.99963	0.99994	0.99971	0.00046	-0.00028	-0.00079	0.2568	0.101
0.99861	0.99996	0.99904	0.00278	-0.00078	-0.00316	0.25398	0.202
0.99893	0.99588	0.99978	0.00178	-0.00382	0.01317	0.516	0.303
0.9981	0.99191	0.99993	0.00375	-0.00763	0.01217	0.519	0.408
0.99999	0.99714	0.99184	0.00013	-0.03492	-0.02265	0.779	0.409
0.99992	0.99491	0.98492	0.00034	-0.06586	-0.04142	0.761	0.515

Table 7.2. Comparing the results of modal analysis between numerical, FEA, ANN and Experimental

Crack inclination (θ) 15°										Crack inclination (θ) 0°																																																																																																																																																																																																																																																																																																																																																																																																																																																																																																																																																																																																													
0.99981	0.99999	0.99817	0.99908	0.99852	0.99966	0.99992	0.99999	0.99809	0.99893	0.99846	0.99968	0.99483	0.99714	0.99215	0.99609	0.99992	0.99998	0.99491	0.99703	0.99182	0.99582	0.99988	0.99998	0.98514	0.99162	0.99993	0.99993	0.99897	0.99978	0.98529	0.9914	0.99993	0.99985	0.9989	0.99978	0.00034	0.00013	0.00375	0.00186	0.00269	0.0006	0.00034	0.00013	0.00391	0.00187	0.00259	0.0006	-0.06545	-0.0371	-0.00757	-0.00382	-0.00088	-0.00019	-0.06516	-0.03827	-0.00788	-0.00394	-0.00093	-0.00017	-0.04119	-0.02377	0.01086	0.00767	-0.00328	-0.00073	-0.04052	-0.02445	0.00928	0.01222	-0.00328	-0.00073	0.73688	0.73313	0.49	0.49375	0.24563	0.24625	0.73125	0.72938	0.4875	0.49125	0.24625	0.245	0.4894	0.3906	0.3898	0.2933	0.1963	0.0988	0.4875	0.392	0.389	0.294	0.195	0.0985	0.75	0.75	0.5	0.5	0.25	0.25	0.75	0.75	0.5	0.5	0.25	0.25	0.5	0.4	0.4	0.3	0.2	0.1	0.5	0.4	0.4	0.3	0.2	0.1	0.772	0.781	0.513	0.518	0.256	0.251	0.781	0.775	0.518	0.5122	0.2575	0.257	0.511	0.435	0.408	0.309	0.201	0.101	0.509	0.408	0.4	0.309	0.2068	0.103	0.7743	0.7826	0.5138	0.521	0.2594	0.258	0.7838	0.7799	0.52	0.5125	0.2588	0.2575	0.517	0.441	0.41	0.312	0.207	0.103	0.515	0.411	0.41	0.311	0.207	0.104	Crack inclination (θ) 30°												0.99992	0.99999	0.9981	0.99893	0.99861	0.99963	0.99988	0.99999	0.99832	0.99908	0.99855	0.99959	0.99491	0.99714	0.99191	0.99588	0.99996	0.99994	0.99543	0.99745	0.99294	0.99633	0.99988	0.9999	0.98492	0.99184	0.99993	0.99978	0.99904	0.99971	0.98669	0.99272	0.99993	0.99985	0.99897	0.99971	0.00034	0.00013	0.00375	0.00178	0.00278	0.00046	0.00027	6.7E-05	0.00327	0.00165	0.00245	0.00032	-0.06586	-0.03492	-0.00763	-0.00382	-0.00078	-0.00028	-0.05856	-0.03106	-0.00671	-0.00357	-0.0009	-0.00036	-0.04142	-0.02265	0.01217	0.01317	-0.00316	-0.00079	-0.03671	-0.01996	0.01007	0.00753	-0.0031	-0.00079	0.73508	0.73583	0.48935	0.48825	0.24513	0.2447	0.73598	0.73395	0.48935	0.4925	0.2455	0.24638	0.4911	0.3915	0.3901	0.293	0.1952	0.0979	0.4911	0.3904	0.3906	0.2929	0.1957	0.0987	0.75	0.75	0.5	0.5	0.25	0.25	0.75	0.75	0.5	0.5	0.25	0.25	0.5	0.4	0.4	0.3	0.2	0.1	0.5	0.4	0.4	0.3	0.2	0.1	0.761	0.779	0.519	0.516	0.25398	0.2568	0.779	0.7699	0.514	0.521	0.254	0.252	0.515	0.409	0.408	0.303	0.202	0.101	0.503	0.41	0.406	0.302	0.202	0.102	0.7676	0.7817	0.5128	0.5179	0.2547	0.2574	0.7811	0.7706	0.5163	0.5225	0.2563	0.2538	0.52	0.412	0.411	0.308	0.204	0.103	0.509	0.413	0.41	0.306	0.207	0.103	Crack inclination (θ) 45°												0.99992	0.99999	0.9981	0.99893	0.99861	0.99963	0.99988	0.99999	0.99832	0.99908	0.99855	0.99959	0.99491	0.99714	0.99191	0.99588	0.99996	0.99994	0.99543	0.99745	0.99294	0.99633	0.99988	0.9999	0.98492	0.99184	0.99993	0.99978	0.99904	0.99971	0.98669	0.99272	0.99993	0.99985	0.99897	0.99971	0.00034	0.00013	0.00375	0.00178	0.00278	0.00046	0.00027	6.7E-05	0.00327	0.00165	0.00245	0.00032	-0.06586	-0.03492	-0.00763	-0.00382	-0.00078	-0.00028	-0.05856	-0.03106	-0.00671	-0.00357	-0.0009	-0.00036	-0.04142	-0.02265	0.01217	0.01317	-0.00316	-0.00079	-0.03671	-0.01996	0.01007	0.00753	-0.0031	-0.00079	0.73508	0.73583	0.48935	0.48825	0.24513	0.2447	0.73598	0.73395	0.48935	0.4925	0.2455	0.24638	0.4911	0.3915	0.3901	0.293	0.1952	0.0979	0.4911	0.3904	0.3906	0.2929	0.1957	0.0987	0.75	0.75	0.5	0.5	0.25	0.25	0.75	0.75	0.5	0.5	0.25	0.25	0.5	0.4	0.4	0.3	0.2	0.1	0.5	0.4	0.4	0.3	0.2	0.1	0.761	0.779	0.519	0.516	0.25398	0.2568	0.779	0.7699	0.514	0.521	0.254	0.252	0.515	0.409	0.408	0.303	0.202	0.101	0.503	0.41	0.406	0.302	0.202	0.102	0.7676	0.7817	0.5128	0.5179	0.2547	0.2574	0.7811	0.7706	0.5163	0.5225	0.2563	0.2538	0.52	0.412	0.411	0.308	0.204	0.103	0.509	0.413	0.41	0.306	0.207	0.103	Numerical												FEA												ANN												Experiment												β												α											
0.99483	0.99714	0.99215	0.99609	0.99992	0.99998	0.99491	0.99703	0.99182	0.99582	0.99988	0.99998	0.98514	0.99162	0.99993	0.99993	0.99897	0.99978	0.98529	0.9914	0.99993	0.99985	0.9989	0.99978	0.00034	0.00013	0.00375	0.00186	0.00269	0.0006	0.00034	0.00013	0.00391	0.00187	0.00259	0.0006	-0.06545	-0.0371	-0.00757	-0.00382	-0.00088	-0.00019	-0.06516	-0.03827	-0.00788	-0.00394	-0.00093	-0.00017	-0.04119	-0.02377	0.01086	0.00767	-0.00328	-0.00073	-0.04052	-0.02445	0.00928	0.01222	-0.00328	-0.00073	0.73688	0.73313	0.49	0.49375	0.24563	0.24625	0.73125	0.72938	0.4875	0.49125	0.24625	0.245	0.4894	0.3906	0.3898	0.2933	0.1963	0.0988	0.4875	0.392	0.389	0.294	0.195	0.0985	0.75	0.75	0.5	0.5	0.25	0.25	0.75	0.75	0.5	0.5	0.25	0.25	0.5	0.4	0.4	0.3	0.2	0.1	0.5	0.4	0.4	0.3	0.2	0.1	0.772	0.781	0.513	0.518	0.256	0.251	0.781	0.775	0.518	0.5122	0.2575	0.257	0.511	0.435	0.408	0.309	0.201	0.101	0.509	0.408	0.4	0.309	0.2068	0.103	0.7743	0.7826	0.5138	0.521	0.2594	0.258	0.7838	0.7799	0.52	0.5125	0.2588	0.2575	0.517	0.441	0.41	0.312	0.207	0.103	0.515	0.411	0.41	0.311	0.207	0.104	Crack inclination (θ) 30°												0.99992	0.99999	0.9981	0.99893	0.99861	0.99963	0.99988	0.99999	0.99832	0.99908	0.99855	0.99959	0.99491	0.99714	0.99191	0.99588	0.99996	0.99994	0.99543	0.99745	0.99294	0.99633	0.99988	0.9999	0.98492	0.99184	0.99993	0.99978	0.99904	0.99971	0.98669	0.99272	0.99993	0.99985	0.99897	0.99971	0.00034	0.00013	0.00375	0.00178	0.00278	0.00046	0.00027	6.7E-05	0.00327	0.00165	0.00245	0.00032	-0.06586	-0.03492	-0.00763	-0.00382	-0.00078	-0.00028	-0.05856	-0.03106	-0.00671	-0.00357	-0.0009	-0.00036	-0.04142	-0.02265	0.01217	0.01317	-0.00316	-0.00079	-0.03671	-0.01996	0.01007	0.00753	-0.0031	-0.00079	0.73508	0.73583	0.48935	0.48825	0.24513	0.2447	0.73598	0.73395	0.48935	0.4925	0.2455	0.24638	0.4911	0.3915	0.3901	0.293	0.1952	0.0979	0.4911	0.3904	0.3906	0.2929	0.1957	0.0987	0.75	0.75	0.5	0.5	0.25	0.25	0.75	0.75	0.5	0.5	0.25	0.25	0.5	0.4	0.4	0.3	0.2	0.1	0.5	0.4	0.4	0.3	0.2	0.1	0.761	0.779	0.519	0.516	0.25398	0.2568	0.779	0.7699	0.514	0.521	0.254	0.252	0.515	0.409	0.408	0.303	0.202	0.101	0.503	0.41	0.406	0.302	0.202	0.102	0.7676	0.7817	0.5128	0.5179	0.2547	0.2574	0.7811	0.7706	0.5163	0.5225	0.2563	0.2538	0.52	0.412	0.411	0.308	0.204	0.103	0.509	0.413	0.41	0.306	0.207	0.103	Crack inclination (θ) 45°												0.99992	0.99999	0.9981	0.99893	0.99861	0.99963	0.99988	0.99999	0.99832	0.99908	0.99855	0.99959	0.99491	0.99714	0.99191	0.99588	0.99996	0.99994	0.99543	0.99745	0.99294	0.99633	0.99988	0.9999	0.98492	0.99184	0.99993	0.99978	0.99904	0.99971	0.98669	0.99272	0.99993	0.99985	0.99897	0.99971	0.00034	0.00013	0.00375	0.00178	0.00278	0.00046	0.00027	6.7E-05	0.00327	0.00165	0.00245	0.00032	-0.06586	-0.03492	-0.00763	-0.00382	-0.00078	-0.00028	-0.05856	-0.03106	-0.00671	-0.00357	-0.0009	-0.00036	-0.04142	-0.02265	0.01217	0.01317	-0.00316	-0.00079	-0.03671	-0.01996	0.01007	0.00753	-0.0031	-0.00079	0.73508	0.73583	0.48935	0.48825	0.24513	0.2447	0.73598	0.73395	0.48935	0.4925	0.2455	0.24638	0.4911	0.3915	0.3901	0.293	0.1952	0.0979	0.4911	0.3904	0.3906	0.2929	0.1957	0.0987	0.75	0.75	0.5	0.5	0.25	0.25	0.75	0.75	0.5	0.5	0.25	0.25	0.5	0.4	0.4	0.3	0.2	0.1	0.5	0.4	0.4	0.3	0.2	0.1	0.761	0.779	0.519	0.516	0.25398	0.2568	0.779	0.7699	0.514	0.521	0.254	0.252	0.515	0.409	0.408	0.303	0.202	0.101	0.503	0.41	0.406	0.302	0.202	0.102	0.7676	0.7817	0.5128	0.5179	0.2547	0.2574	0.7811	0.7706	0.5163	0.5225	0.2563	0.2538	0.52	0.412	0.411	0.308	0.204	0.103	0.509	0.413	0.41	0.306	0.207	0.103	Numerical												FEA												ANN												Experiment												β												α																							
0.98514	0.99162	0.99993	0.99993	0.99897	0.99978	0.98529	0.9914	0.99993	0.99985	0.9989	0.99978	0.00034	0.00013	0.00375	0.00186	0.00269	0.0006	0.00034	0.00013	0.00391	0.00187	0.00259	0.0006	-0.06545	-0.0371	-0.00757	-0.00382	-0.00088	-0.00019	-0.06516	-0.03827	-0.00788	-0.00394	-0.00093	-0.00017	-0.04119	-0.02377	0.01086	0.00767	-0.00328	-0.00073	-0.04052	-0.02445	0.00928	0.01222	-0.00328	-0.00073	0.73688	0.73313	0.49	0.49375	0.24563	0.24625	0.73125	0.72938	0.4875	0.49125	0.24625	0.245	0.4894	0.3906	0.3898	0.2933	0.1963	0.0988	0.4875	0.392	0.389	0.294	0.195	0.0985	0.75	0.75	0.5	0.5	0.25	0.25	0.75	0.75	0.5	0.5	0.25	0.25	0.5	0.4	0.4	0.3	0.2	0.1	0.5	0.4	0.4	0.3	0.2	0.1	0.772	0.781	0.513	0.518	0.256	0.251	0.781	0.775	0.518	0.5122	0.2575	0.257	0.511	0.435	0.408	0.309	0.201	0.101	0.509	0.408	0.4	0.309	0.2068	0.103	0.7743	0.7826	0.5138	0.521	0.2594	0.258	0.7838	0.7799	0.52	0.5125	0.2588	0.2575	0.517	0.441	0.41	0.312	0.207	0.103	0.515	0.411	0.41	0.311	0.207	0.104	Crack inclination (θ) 30°												0.99992	0.99999	0.9981	0.99893	0.99861	0.99963	0.99988	0.99999	0.99832	0.99908	0.99855	0.99959	0.99491	0.99714	0.99191	0.99588	0.99996	0.99994	0.99543	0.99745	0.99294	0.99633	0.99988	0.9999	0.98492	0.99184	0.99993	0.99978	0.99904	0.99971	0.98669	0.99272	0.99993	0.99985	0.99897	0.99971	0.00034	0.00013	0.00375	0.00178	0.00278	0.00046	0.00027	6.7E-05	0.00327	0.00165	0.00245	0.00032	-0.06586	-0.03492	-0.00763	-0.00382	-0.00078	-0.00028	-0.05856	-0.03106	-0.00671	-0.00357	-0.0009	-0.00036	-0.04142	-0.02265	0.01217	0.01317	-0.00316	-0.00079	-0.03671	-0.01996	0.01007	0.00753	-0.0031	-0.00079	0.73508	0.73583	0.48935	0.48825	0.24513	0.2447	0.73598	0.73395	0.48935	0.4925	0.2455	0.24638	0.4911	0.3915	0.3901	0.293	0.1952	0.0979	0.4911	0.3904	0.3906	0.2929	0.1957	0.0987	0.75	0.75	0.5	0.5	0.25	0.25	0.75	0.75	0.5	0.5	0.25	0.25	0.5	0.4	0.4	0.3	0.2	0.1	0.5	0.4	0.4	0.3	0.2	0.1	0.761	0.779	0.519	0.516	0.25398	0.2568	0.779	0.7699	0.514	0.521	0.254	0.252	0.515	0.409	0.408	0.303	0.202	0.101	0.503	0.41	0.406	0.302	0.202	0.102	0.7676	0.7817	0.5128	0.5179	0.2547	0.2574	0.7811	0.7706	0.5163	0.5225	0.2563	0.2538	0.52	0.412	0.411	0.308	0.204	0.103	0.509	0.413	0.41	0.306	0.207	0.103	Crack inclination (θ) 45°												0.99992	0.99999	0.9981	0.99893	0.99861	0.99963	0.99988	0.99999	0.99832	0.99908	0.99855	0.99959	0.99491	0.99714	0.99191	0.99588	0.99996	0.99994	0.99543	0.99745	0.99294	0.99633	0.99988	0.9999	0.98492	0.99184	0.99993	0.99978	0.99904	0.99971	0.98669	0.99272	0.99993	0.99985	0.99897	0.99971	0.00034	0.00013	0.00375	0.00178	0.00278	0.00046	0.00027	6.7E-05	0.00327	0.00165	0.00245	0.00032	-0.06586	-0.03492	-0.00763	-0.00382	-0.00078	-0.00028	-0.05856	-0.03106	-0.00671	-0.00357	-0.0009	-0.00036	-0.04142	-0.02265	0.01217	0.01317	-0.00316	-0.00079	-0.03671	-0.01996	0.01007	0.00753	-0.0031	-0.00079	0.73508	0.73583	0.48935	0.48825	0.24513	0.2447	0.73598	0.73395	0.48935	0.4925	0.2455	0.24638	0.4911	0.3915	0.3901	0.293	0.1952	0.0979	0.4911	0.3904	0.3906	0.2929	0.1957	0.0987	0.75	0.75	0.5	0.5	0.25	0.25	0.75	0.75	0.5	0.5	0.25	0.25	0.5	0.4	0.4	0.3	0.2	0.1	0.5	0.4	0.4	0.3	0.2	0.1	0.761	0.779	0.519	0.516	0.25398	0.2568	0.779	0.7699	0.514	0.521	0.254	0.252	0.515	0.409	0.408	0.303	0.202	0.101	0.503	0.41	0.406	0.302	0.202	0.102	0.7676	0.7817	0.5128	0.5179	0.2547	0.2574	0.7811	0.7706	0.5163	0.5225	0.2563	0.2538	0.52	0.412	0.411	0.308	0.204	0.103	0.509	0.413	0.41	0.306	0.207	0.103	Numerical												FEA												ANN												Experiment												β												α																																			
0.00034	0.00013	0.00375	0.00186	0.00269	0.0006	0.00034	0.00013	0.00391	0.00187	0.00259	0.0006	-0.06545	-0.0371	-0.00757	-0.00382	-0.00088	-0.00019	-0.06516	-0.03827	-0.00788	-0.00394	-0.00093	-0.00017	-0.04119	-0.02377	0.01086	0.00767	-0.00328	-0.00073	-0.04052	-0.02445	0.00928	0.01222	-0.00328	-0.00073	0.73688	0.73313	0.49	0.49375	0.24563	0.24625	0.73125	0.72938	0.4875	0.49125	0.24625	0.245	0.4894	0.3906	0.3898	0.2933	0.1963	0.0988	0.4875	0.392	0.389	0.294	0.195	0.0985	0.75	0.75	0.5	0.5	0.25	0.25	0.75	0.75	0.5	0.5	0.25	0.25	0.5	0.4	0.4	0.3	0.2	0.1	0.5	0.4	0.4	0.3	0.2	0.1	0.772	0.781	0.513	0.518	0.256	0.251	0.781	0.775	0.518	0.5122	0.2575	0.257	0.511	0.435	0.408	0.309	0.201	0.101	0.509	0.408	0.4	0.309	0.2068	0.103	0.7743	0.7826	0.5138	0.521	0.2594	0.258	0.7838	0.7799	0.52	0.5125	0.2588	0.2575	0.517	0.441	0.41	0.312	0.207	0.103	0.515	0.411	0.41	0.311	0.207	0.104	Crack inclination (θ) 30°												0.99992	0.99999	0.9981	0.99893	0.99861	0.99963	0.99988	0.99999	0.99832	0.99908	0.99855	0.99959	0.99491	0.99714	0.99191	0.99588	0.99996	0.99994	0.99543	0.99745	0.99294	0.99633	0.99988	0.9999	0.98492	0.99184	0.99993	0.99978	0.99904	0.99971	0.98669	0.99272	0.99993	0.99985	0.99897	0.99971	0.00034	0.00013	0.00375	0.00178	0.00278	0.00046	0.00027	6.7E-05	0.00327	0.00165	0.00245	0.00032	-0.06586	-0.03492	-0.00763	-0.00382	-0.00078	-0.00028	-0.05856	-0.03106	-0.00671	-0.00357	-0.0009	-0.00036	-0.04142	-0.02265	0.01217	0.01317	-0.00316	-0.00079	-0.03671	-0.01996	0.01007	0.00753	-0.0031	-0.00079	0.73508	0.73583	0.48935	0.48825	0.24513	0.2447	0.73598	0.73395	0.48935	0.4925	0.2455	0.24638	0.4911	0.3915	0.3901	0.293	0.1952	0.0979	0.4911	0.3904	0.3906	0.2929	0.1957	0.0987	0.75	0.75	0.5	0.5	0.25	0.25	0.75	0.75	0.5	0.5	0.25	0.25	0.5	0.4	0.4	0.3	0.2	0.1	0.5	0.4	0.4	0.3	0.2	0.1	0.761	0.779	0.519	0.516	0.25398	0.2568	0.779	0.7699	0.514	0.521	0.254	0.252	0.515	0.409	0.408	0.303	0.202	0.101	0.503	0.41	0.406	0.302	0.202	0.102	0.7676	0.7817	0.5128	0.5179	0.2547	0.2574	0.7811	0.7706	0.5163	0.5225	0.2563	0.2538	0.52	0.412	0.411	0.308	0.204	0.103	0.509	0.413	0.41	0.306	0.207	0.103	Crack inclination (θ) 45°												0.99992	0.99999	0.9981	0.99893	0.99861	0.99963	0.99988	0.99999	0.99832	0.99908	0.99855	0.99959	0.99491	0.99714	0.99191	0.99588	0.99996	0.99994	0.99543	0.99745	0.99294	0.99633	0.99988	0.9999	0.98492	0.99184	0.99993	0.99978	0.99904	0.99971	0.98669	0.99272	0.99993	0.99985	0.99897	0.99971	0.00034	0.00013	0.00375	0.00178	0.00278	0.00046	0.00027	6.7E-05	0.00327	0.00165	0.00245	0.00032	-0.06586	-0.03492	-0.00763	-0.00382	-0.00078	-0.00028	-0.05856	-0.03106	-0.00671	-0.00357	-0.0009	-0.00036	-0.04142	-0.02265	0.01217	0.01317	-0.00316	-0.00079	-0.03671	-0.01996	0.01007	0.00753	-0.0031	-0.00079	0.73508	0.73583	0.48935	0.48825	0.24513	0.2447	0.73598	0.73395	0.48935	0.4925	0.2455	0.24638	0.4911	0.3915	0.3901	0.293	0.1952	0.0979	0.4911	0.3904	0.3906	0.2929	0.1957	0.0987	0.75	0.75	0.5	0.5	0.25	0.25	0.75	0.75	0.5	0.5	0.25	0.25	0.5	0.4	0.4	0.3	0.2	0.1	0.5	0.4	0.4	0.3	0.2	0.1	0.761	0.779	0.519	0.516	0.25398	0.2568	0.779	0.7699	0.514	0.521	0.254	0.252	0.515	0.409	0.408	0.303	0.202	0.101	0.503	0.41	0.406	0.302	0.202	0.102	0.7676	0.7817	0.5128	0.5179	0.2547	0.2574	0.7811	0.7706	0.5163	0.5225	0.2563	0.2538	0.52	0.412	0.411	0.308	0.204	0.103	0.509	0.413	0.41	0.306	0.207	0.103	Numerical												FEA												ANN												Experiment												β												α																																															
-0.06545	-0.0371	-0.00757	-0.00382	-0.00088	-0.00019	-0.06516	-0.03827	-0.00788	-0.00394	-0.00093	-0.00017	-0.04119	-0.02377	0.01086	0.00767	-0.00328	-0.00073	-0.04052	-0.02445	0.00928	0.01222	-0.00328	-0.00073	0.73688	0.73313	0.49	0.49375	0.24563	0.24625	0.73125	0.72938	0.4875	0.49125	0.24625	0.245	0.4894	0.3906	0.3898	0.2933	0.1963	0.0988	0.4875	0.392	0.389	0.294	0.195	0.0985	0.75	0.75	0.5	0.5	0.25	0.25	0.75	0.75	0.5	0.5	0.25	0.25	0.5	0.4	0.4	0.3	0.2	0.1	0.5	0.4	0.4	0.3	0.2	0.1	0.772	0.781	0.513	0.518	0.256	0.251	0.781	0.775	0.518	0.5122	0.2575	0.257	0.511	0.435	0.408	0.309	0.201	0.101	0.509	0.408	0.4	0.309	0.2068	0.103	0.7743	0.7826	0.5138	0.521	0.2594	0.258	0.7838	0.7799	0.52	0.5125	0.2588	0.2575	0.517	0.441	0.41	0.312	0.207	0.103	0.515	0.411	0.41	0.311	0.207	0.104	Crack inclination (θ) 30°												0.99992	0.99999	0.9981	0.99893	0.99861	0.99963	0.99988	0.99999	0.99832	0.99908	0.99855	0.99959	0.99491	0.99714	0.99191	0.99588	0.99996	0.99994	0.99543	0.99745	0.99294	0.99633	0.99988	0.9999	0.98492	0.99184	0.99993	0.99978	0.99904	0.99971	0.98669	0.99272	0.99993	0.99985	0.99897	0.99971	0.00034	0.00013	0.00375	0.00178	0.00278	0.00046	0.00027	6.7E-05	0.00327	0.00165	0.00245	0.00032	-0.06586	-0.03492	-0.00763	-0.00382	-0.00078	-0.00028	-0.05856	-0.03106	-0.00671	-0.00357	-0.0009	-0.00036	-0.04142	-0.02265	0.01217	0.01317	-0.00316	-0.00079	-0.03671	-0.01996	0.01007	0.00753	-0.0031	-0.00079	0.73508	0.73583	0.48935	0.48825	0.24513	0.2447	0.73598	0.73395	0.48935	0.4925	0.2455	0.24638	0.4911	0.3915	0.3901	0.293	0.1952	0.0979	0.4911	0.3904	0.3906	0.2929	0.1957	0.0987	0.75	0.75	0.5	0.5	0.25	0.25	0.75	0.75	0.5	0.5	0.25	0.25	0.5	0.4	0.4	0.3	0.2	0.1	0.5	0.4	0.4	0.3	0.2	0.1	0.761	0.779	0.519	0.516	0.25398	0.2568	0.779	0.7699	0.514	0.521	0.254	0.252	0.515	0.409	0.408	0.303	0.202	0.101	0.503	0.41	0.406	0.302	0.202	0.102	0.7676	0.7817	0.5128	0.5179	0.2547	0.2574	0.7811	0.7706	0.5163	0.5225	0.2563	0.2538	0.52	0.412	0.411	0.308	0.204	0.103	0.509	0.413	0.41	0.306	0.207	0.103	Crack inclination (θ) 45°												0.99992	0.99999	0.9981	0.99893	0.99861	0.99963	0.99988	0.99999	0.99832	0.99908	0.99855	0.99959	0.99491	0.99714	0.99191	0.99588	0.99996	0.99994	0.99543	0.99745	0.99294	0.99633	0.99988	0.9999	0.98492	0.99184	0.99993	0.99978	0.99904	0.99971	0.98669	0.99272	0.99993	0.99985	0.99897	0.99971	0.00034	0.00013	0.00375	0.00178	0.00278	0.00046	0.00027	6.7E-05	0.00327	0.00165	0.00245	0.00032	-0.06586	-0.03492	-0.00763	-0.00382	-0.00078	-0.00028	-0.05856	-0.03106	-0.00671	-0.00357	-0.0009	-0.00036	-0.04142	-0.02265	0.01217	0.01317	-0.00316	-0.00079	-0.03671	-0.01996	0.01007	0.00753	-0.0031	-0.00079	0.73508	0.73583	0.48935	0.48825	0.24513	0.2447	0.73598	0.73395	0.48935	0.4925	0.2455	0.24638	0.4911	0.3915	0.3901	0.293	0.1952	0.0979	0.4911	0.3904	0.3906	0.2929	0.1957	0.0987	0.75	0.75	0.5	0.5	0.25	0.25	0.75	0.75	0.5	0.5	0.25	0.25	0.5	0.4	0.4	0.3	0.2	0.1	0.5	0.4	0.4	0.3	0.2	0.1	0.761	0.779	0.519	0.516	0.25398	0.2568	0.779	0.7699	0.514	0.521	0.254	0.252	0.515	0.409	0.408	0.303	0.202	0.101	0.503	0.41	0.406	0.302	0.202	0.102	0.7676	0.7817	0.5128	0.5179	0.2547	0.2574	0.7811	0.7706	0.5163	0.5225	0.2563	0.2538	0.52	0.412	0.411	0.308	0.204	0.103	0.509	0.413	0.41	0.306	0.207	0.103	Numerical												FEA												ANN												Experiment												β												α																																																											
-0.04119	-0.02377	0.01086	0.00767	-0.00328	-0.00073	-0.04052	-0.02445	0.00928	0.01222	-0.00328	-0.00073	0.73688	0.73313	0.49	0.49375	0.24563	0.24625	0.73125	0.72938	0.4875	0.49125	0.24625	0.245	0.4894	0.3906	0.3898	0.2933	0.1963	0.0988	0.4875	0.392	0.389	0.294	0.195	0.0985	0.75	0.75	0.5	0.5	0.25	0.25	0.75	0.75	0.5	0.5	0.25	0.25	0.5	0.4	0.4	0.3	0.2	0.1	0.5	0.4	0.4	0.3	0.2	0.1	0.772	0.781	0.513	0.518	0.256	0.251	0.781	0.775	0.518	0.5122	0.2575	0.257	0.511	0.435	0.408	0.309	0.201	0.101	0.509	0.408	0.4	0.309	0.2068	0.103	0.7743	0.7826	0.5138	0.521	0.2594	0.258	0.7838	0.7799	0.52	0.5125	0.2588	0.2575	0.517	0.441	0.41	0.312	0.207	0.103	0.515	0.411	0.41	0.311	0.207	0.104	Crack inclination (θ) 30°												0.99992	0.99999	0.9981	0.99893	0.99861	0.99963	0.99988	0.99999	0.99832	0.99908	0.99855	0.99959	0.99491	0.99714	0.99191	0.99588	0.99996	0.99994	0.99543	0.99745	0.99294	0.99633	0.99988	0.9999	0.98492	0.99184	0.99993	0.99978	0.99904	0.99971	0.98669	0.99272	0.99993	0.99985	0.99897	0.99971	0.00034	0.00013	0.00375	0.00178	0.00278	0.00046	0.00027	6.7E-05	0.00327	0.00165	0.00245	0.00032	-0.06586	-0.03492	-0.00763	-0.00382	-0.00078	-0.00028	-0.05856	-0.03106	-0.00671	-0.00357	-0.0009	-0.00036	-0.04142	-0.02265	0.01217	0.01317	-0.00316	-0.00079	-0.03671	-0.01996	0.01007	0.00753	-0.0031	-0.00079	0.73508	0.73583	0.48935	0.48825	0.24513	0.2447	0.73598	0.73395	0.48935	0.4925	0.2455	0.24638	0.4911	0.3915	0.3901	0.293	0.1952	0.0979	0.4911	0.3904	0.3906	0.2929	0.1957	0.0987	0.75	0.75	0.5	0.5	0.25	0.25	0.75	0.75	0.5	0.5	0.25	0.25	0.5	0.4	0.4	0.3	0.2	0.1	0.5	0.4	0.4	0.3	0.2	0.1	0.761	0.779	0.519	0.516	0.25398	0.2568	0.779	0.7699	0.514	0.521	0.254	0.252	0.515	0.409	0.408	0.303	0.202	0.101	0.503	0.41	0.406	0.302	0.202	0.102	0.7676	0.7817	0.5128	0.5179	0.2547	0.2574	0.7811	0.7706	0.5163	0.5225	0.2563	0.2538	0.52	0.412	0.411	0.308	0.204	0.103	0.509	0.413	0.41	0.306	0.207	0.103	Crack inclination (θ) 45°												0.99992	0.99999	0.9981	0.99893	0.99861	0.99963	0.99988	0.99999	0.99832	0.99908	0.99855	0.99959	0.99491	0.99714	0.99191	0.99588	0.99996	0.99994	0.99543	0.99745	0.99294	0.99633	0.99988	0.9999	0.98492	0.99184	0.99993	0.99978	0.99904	0.99971	0.98669	0.99272	0.99993	0.99985	0.99897	0.99971	0.00034	0.00013	0.00375	0.00178	0.00278	0.00046	0.00027	6.7E-05	0.00327	0.00165	0.00245	0.00032	-0.06586	-0.03492	-0.00763	-0.00382	-0.00078	-0.00028	-0.05856	-0.03106	-0.00671	-0.00357	-0.0009	-0.00036	-0.04142	-0.02265	0.01217	0.01317	-0.00316	-0.00079	-0.03671	-0.01996	0.01007	0.00753	-0.0031	-0.00079	0.73508	0.73583	0.48935	0.48825	0.24513	0.2447	0.73598	0.73395	0.48935	0.4925	0.2455	0.24638	0.4911	0.3915	0.3901	0.293	0.1952	0.0979	0.4911	0.3904	0.3906	0.2929	0.1957	0.0987	0.75	0.75	0.5	0.5	0.25	0.25	0.75	0.75	0.5	0.5	0.25	0.25	0.5	0.4	0.4	0.3	0.2	0.1	0.5	0.4	0.4	0.3	0.2	0.1	0.761	0.779	0.519	0.516	0.25398	0.2568	0.779	0.7699	0.514	0.521	0.254	0.252	0.515	0.409	0.408	0.303	0.202	0.101	0.503	0.41	0.406	0.302	0.202	0.102	0.7676	0.7817	0.5128	0.5179	0.2547	0.2574	0.7811	0.7706	0.5163	0.5225	0.2563	0.2538	0.52	0.412	0.411	0.308	0.204	0.103	0.509	0.413	0.41	0.306	0.207	0.103	Numerical												FEA												ANN												Experiment												β												α																																																																							
0.73688	0.73313	0.49	0.49375	0.24563	0.24625	0.73125	0.72938	0.4875	0.49125	0.24625	0.245	0.4894	0.3906	0.3898	0.2933	0.1963	0.0988	0.4875	0.392	0.389	0.294	0.195	0.0985	0.75	0.75	0.5	0.5	0.25	0.25	0.75	0.75	0.5	0.5	0.25	0.25	0.5	0.4	0.4	0.3	0.2	0.1	0.5	0.4	0.4	0.3	0.2	0.1	0.772	0.781	0.513	0.518	0.256	0.251	0.781	0.775	0.518	0.5122	0.2575	0.257	0.511	0.435	0.408	0.309	0.201	0.101	0.509	0.408	0.4	0.309	0.2068	0.103	0.7743	0.7826	0.5138	0.521	0.2594	0.258	0.7838	0.7799	0.52	0.5125	0.2588	0.2575	0.517	0.441	0.41	0.312	0.207	0.103	0.515	0.411	0.41	0.311	0.207	0.104	Crack inclination (θ) 30°												0.99992	0.99999	0.9981	0.99893	0.99861	0.99963	0.99988	0.99999	0.99832	0.99908	0.99855	0.99959	0.99491	0.99714	0.99191	0.99588	0.99996	0.99994	0.99543	0.99745	0.99294	0.99633	0.99988	0.9999	0.98492	0.99184	0.99993	0.99978	0.99904	0.99971	0.98669	0.99272	0.99993	0.99985	0.99897	0.99971	0.00034	0.00013	0.00375	0.00178	0.00278	0.00046	0.00027	6.7E-05	0.00327	0.00165	0.00245	0.00032	-0.06586	-0.03492	-0.00763	-0.00382	-0.00078	-0.00028	-0.05856	-0.03106	-0.00671	-0.00357	-0.0009	-0.00036	-0.04142	-0.02265	0.01217	0.01317	-0.00316	-0.00079	-0.03671	-0.01996	0.01007	0.00753	-0.0031	-0.00079	0.73508	0.73583	0.48935	0.48825	0.24513	0.2447	0.73598	0.73395	0.48935	0.4925	0.2455	0.24638	0.4911	0.3915	0.3901	0.293	0.1952	0.0979	0.4911	0.3904	0.3906	0.2929	0.1957	0.0987	0.75	0.75	0.5	0.5	0.25	0.25	0.75	0.75	0.5	0.5	0.25	0.25	0.5	0.4	0.4	0.3	0.2	0.1	0.5	0.4	0.4	0.3	0.2	0.1	0.761	0.779	0.519	0.516	0.25398	0.2568	0.779	0.7699	0.514	0.521	0.254	0.252	0.515	0.409	0.408	0.303	0.202	0.101	0.503	0.41	0.406	0.302	0.202	0.102	0.7676	0.7817	0.5128	0.5179	0.2547	0.2574	0.7811	0.7706	0.5163	0.5225	0.2563	0.2538	0.52	0.412	0.411	0.308	0.204	0.103	0.509	0.413	0.41	0.306	0.207	0.103	Crack inclination (θ) 45°												0.99992	0.99999	0.9981	0.99893	0.99861	0.99963	0.99988	0.99999	0.99832	0.99908	0.99855	0.99959	0.99491	0.99714	0.99191	0.99588	0.99996	0.99994	0.99543	0.99745	0.99294	0.99633	0.99988	0.9999	0.98492	0.99184	0.99993	0.99978	0.99904	0.99971	0.98669	0.99272	0.99993	0.99985	0.99897	0.99971	0.00034	0.00013	0.00375	0.00178	0.00278	0.00046	0.00027	6.7E-05	0.00327	0.00165	0.00245	0.00032	-0.06586	-0.03492	-0.00763	-0.00382	-0.00078	-0.00028	-0.05856	-0.03106	-0.00671	-0.00357	-0.0009	-0.00036	-0.04142	-0.02265	0.01217	0.01317	-0.00316	-0.00079	-0.03671	-0.01996	0.01007	0.00753	-0.0031	-0.00079	0.73508	0.73583	0.48935	0.48825	0.24513	0.2447	0.73598	0.73395	0.48935	0.4925	0.2455	0.24638	0.4911	0.3915	0.3901	0.293	0.1952	0.0979	0.4911	0.3904	0.3906	0.2929	0.1957	0.0987	0.75	0.75	0.5	0.5	0.25	0.25	0.75	0.75	0.5	0.5	0.25	0.25	0.5	0.4	0.4	0.3	0.2	0.1	0.5	0.4	0.4	0.3	0.2	0.1	0.761	0.779	0.519	0.516	0.25398	0.2568	0.779	0.7699	0.514	0.521	0.254	0.252	0.515	0.409	0.408	0.303	0.202	0.101	0.503	0.41	0.406	0.302	0.202	0.102	0.7676	0.7817	0.5128	0.5179	0.2547	0.2574	0.7811	0.7706	0.5163	0.5225	0.2563	0.2538	0.52	0.412	0.411	0.308	0.204	0.103	0.509	0.413	0.41	0.306	0.207	0.103	Numerical												FEA												ANN												Experiment												β												α																																																																																			
0.4894	0.3906	0.3898	0.2933	0.1963	0.0988	0.4875	0.392	0.389	0.294	0.195	0.0985	0.75	0.75	0.5	0.5	0.25	0.25	0.75	0.75	0.5	0.5	0.25	0.25	0.5	0.4	0.4	0.3	0.2	0.1	0.5	0.4	0.4	0.3	0.2	0.1	0.772	0.781	0.513	0.518	0.256	0.251	0.781	0.775	0.518	0.5122	0.2575	0.257	0.511	0.435	0.408	0.309	0.201	0.101	0.509	0.408	0.4	0.309	0.2068	0.103	0.7743	0.7826	0.5138	0.521	0.2594	0.258	0.7838	0.7799	0.52	0.5125	0.2588	0.2575	0.517	0.441	0.41	0.312	0.207	0.103	0.515	0.411	0.41	0.311	0.207	0.104	Crack inclination (θ) 30°												0.99992	0.99999	0.9981	0.99893	0.99861	0.99963	0.99988	0.99999	0.99832	0.99908	0.99855	0.99959	0.99491	0.99714	0.99191	0.99588	0.99996	0.99994	0.99543	0.99745	0.99294	0.99633	0.99988	0.9999	0.98492	0.99184	0.99993	0.99978	0.99904	0.99971	0.98669	0.99272	0.99993	0.99985	0.99897	0.99971	0.00034	0.00013	0.00375	0.00178	0.00278	0.00046	0.00027	6.7E-05	0.00327	0.00165	0.00245	0.00032	-0.06586	-0.03492	-0.00763	-0.00382	-0.00078	-0.00028	-0.05856	-0.03106	-0.00671	-0.00357	-0.0009	-0.00036	-0.04142	-0.02265	0.01217	0.01317	-0.00316	-0.00079	-0.03671	-0.01996	0.01007	0.00753	-0.0031	-0.00079	0.73508	0.73583	0.48935	0.48825	0.24513	0.2447	0.73598	0.73395	0.48935	0.4925	0.2455	0.24638	0.4911	0.3915	0.3901	0.293	0.1952	0.0979	0.4911	0.3904	0.3906	0.2929	0.1957	0.0987	0.75	0.75	0.5	0.5	0.25	0.25	0.75	0.75	0.5	0.5	0.25	0.25	0.5	0.4	0.4	0.3	0.2	0.1	0.5	0.4	0.4	0.3	0.2	0.1	0.761	0.779	0.519	0.516	0.25398	0.2568	0.779	0.7699	0.514	0.521	0.254	0.252	0.515	0.409	0.408	0.303	0.202	0.101	0.503	0.41	0.406	0.302	0.202	0.102	0.7676	0.7817	0.5128	0.5179	0.2547	0.2574	0.7811	0.7706	0.5163	0.5225	0.2563	0.2538	0.52	0.412	0.411	0.308	0.204	0.103	0.509	0.413	0.41	0.306	0.207	0.103	Crack inclination (θ) 45°												0.99992	0.99999	0.9981	0.99893	0.99861	0.99963	0.99988	0.99999	0.99832	0.99908	0.99855	0.99959	0.99491	0.99714	0.99191	0.99588	0.99996	0.99994	0.99543	0.99745	0.99294	0.99633	0.99988	0.9999	0.98492	0.99184	0.99993	0.99978	0.99904	0.99971	0.98669	0.99272	0.99993	0.99985	0.99897	0.99971	0.00034	0.00013	0.00375	0.00178	0.00278	0.00046	0.00027	6.7E-05	0.00327	0.00165	0.00245	0.00032	-0.06586	-0.03492	-0.00763	-0.00382	-0.00078	-0.00028	-0.05856	-0.03106	-0.00671	-0.00357	-0.0009	-0.00036	-0.04142	-0.02265	0.01217	0.01317	-0.00316	-0.00079	-0.03671	-0.01996	0.01007	0.00753	-0.0031	-0.00079	0.73508	0.73583	0.48935	0.48825	0.24513	0.2447	0.73598	0.73395	0.48935	0.4925	0.2455	0.24638	0.4911	0.3915	0.3901	0.293	0.1952	0.0979	0.4911	0.3904	0.3906	0.2929	0.1957	0.0987	0.75	0.75	0.5	0.5	0.25	0.25	0.75	0.75	0.5	0.5	0.25	0.25	0.5	0.4	0.4	0.3	0.2	0.1	0.5	0.4	0.4	0.3	0.2	0.1	0.761	0.779	0.519	0.516	0.25398	0.2568	0.779	0.7699	0.514	0.521	0.254	0.252	0.515	0.409	0.408	0.303	0.202	0.101	0.503	0.41	0.406	0.302	0.202	0.102	0.7676	0.7817	0.5128	0.5179	0.2547	0.2574	0.7811	0.7706	0.5163	0.5225	0.2563	0.2538	0.52	0.412	0.411	0.308	0.204	0.103	0.509	0.413	0.41	0.306	0.207	0.103	Numerical												FEA												ANN												Experiment												β												α																																																																																															
0.75	0.75	0.5	0.5	0.25	0.25	0.75	0.75	0.5	0.5	0.25	0.25	0.5	0.4	0.4	0.3	0.2	0.1	0.5	0.4	0.4	0.3	0.2	0.1	0.772	0.781	0.513	0.518	0.256	0.251	0.781	0.775	0.518	0.5122	0.2575	0.257	0.511	0.435	0.408	0.309	0.201	0.101	0.509	0.408	0.4	0.309	0.2068	0.103	0.7743	0.7826	0.5138	0.521	0.2594	0.258	0.7838	0.7799	0.52	0.5125	0.2588	0.2575	0.517	0.441	0.41	0.312	0.207	0.103	0.515	0.411	0.41	0.311	0.207	0.104	Crack inclination (θ) 30°												0.99992	0.99999	0.9981	0.99893	0.99861	0.99963	0.99988	0.99999	0.99832	0.99908	0.99855	0.99959	0.99491	0.99714	0.99191	0.99588	0.99996	0.99994	0.99543	0.99745	0.99294	0.99633	0.99988	0.9999	0.98492	0.99184	0.99993	0.99978	0.99904	0.99971	0.98669	0.99272	0.99993	0.99985	0.99897	0.99971	0.00034	0.00013	0.00375	0.00178	0.00278	0.00046	0.00027	6.7E-05	0.00327	0.00165	0.00245	0.00032	-0.06586	-0.03492	-0.00763	-0.00382	-0.00078	-0.00028	-0.05856	-0.03106	-0.00671	-0.00357	-0.0009	-0.00036	-0.04142	-0.02265	0.01217	0.01317	-0.00316	-0.00079	-0.03671	-0.01996	0.01007	0.00753	-0.0031	-0.00079	0.73508	0.73583	0.48935	0.48825	0.24513	0.2447	0.73598	0.73395	0.48935	0.4925	0.2455	0.24638	0.4911	0.3915	0.3901	0.293	0.1952	0.0979	0.4911	0.3904	0.3906	0.2929	0.1957	0.0987	0.75	0.75	0.5	0.5	0.25	0.25	0.75	0.75	0.5	0.5	0.25	0.25	0.5	0.4	0.4	0.3	0.2	0.1	0.5	0.4	0.4	0.3	0.2	0.1	0.761	0.779	0.519	0.516	0.25398	0.2568	0.779	0.7699	0.514	0.521	0.254	0.252	0.515	0.409	0.408	0.303	0.202	0.101	0.503	0.41	0.406	0.302	0.202	0.102	0.7676	0.7817	0.5128	0.5179	0.2547	0.2574	0.7811	0.7706	0.5163	0.5225	0.2563	0.2538	0.52	0.412	0.411	0.308	0.204	0.103	0.509	0.413	0.41	0.306	0.207	0.103	Crack inclination (θ) 45°												0.99992	0.99999	0.9981	0.99893	0.99861	0.99963	0.99988	0.99999	0.99832	0.99908	0.99855	0.99959	0.99491	0.99714	0.99191	0.99588	0.99996	0.99994	0.99543	0.99745	0.99294	0.99633	0.99988	0.9999	0.98492	0.99184	0.99993	0.99978	0.99904	0.99971	0.98669	0.99272	0.99993	0.99985	0.99897	0.99971	0.00034	0.00013	0.00375	0.00178	0.00278	0.00046	0.00027	6.7E-05	0.00327	0.00165	0.00245	0.00032	-0.06586	-0.03492	-0.00763	-0.00382	-0.00078	-0.00028	-0.05856	-0.03106	-0.00671	-0.00357	-0.0009	-0.00036	-0.04142	-0.02265	0.01217	0.01317	-0.00316	-0.00079	-0.03671	-0.01996	0.01007	0.00753	-0.0031	-0.00079	0.73508	0.73583	0.48935	0.48825	0.24513	0.2447	0.73598	0.73395	0.48935	0.4925	0.2455	0.24638	0.4911	0.3915	0.3901	0.293	0.1952	0.0979	0.4911	0.3904	0.3906	0.2929	0.1957	0.0987	0.75	0.75	0.5	0.5	0.25	0.25	0.75	0.75	0.5	0.5	0.25	0.25	0.5	0.4	0.4	0.3	0.2	0.1	0.5	0.4	0.4	0.3	0.2	0.1	0.761	0.779	0.519	0.516	0.25398	0.2568	0.779	0.7699	0.514	0.521	0.254	0.252	0.515	0.409	0.408	0.303	0.202	0.101	0.503	0.41	0.406	0.302	0.202	0.102	0.7676	0.7817	0.5128	0.5179	0.2547	0.2574	0.7811	0.7706	0.5163	0.5225	0.2563	0.2538	0.52	0.412	0.411	0.308	0.204	0.103	0.509	0.413	0.41	0.306	0.207	0.103	Numerical												FEA												ANN												Experiment												β												α																																																																																																											
0.5	0.4	0.4	0.3	0.2	0.1	0.5	0.4	0.4	0.3	0.2	0.1	0.772	0.781	0.513	0.518	0.256	0.251	0.781	0.775	0.518	0.5122	0.2575	0.257	0.511	0.435	0.408	0.309	0.201	0.101	0.509	0.408	0.4	0.309	0.2068	0.103	0.7743	0.7826	0.5138	0.521	0.2594	0.258	0.7838	0.7799	0.52	0.5125	0.2588	0.2575	0.517	0.441	0.41	0.312	0.207	0.103	0.515	0.411	0.41	0.311	0.207	0.104	Crack inclination (θ) 30°												0.99992	0.99999	0.9981	0.99893	0.99861	0.99963	0.99988	0.99999	0.99832	0.99908	0.99855	0.99959	0.99491	0.99714	0.99191	0.99588	0.99996	0.99994	0.99543	0.99745	0.99294	0.99633	0.99988	0.9999	0.98492	0.99184	0.99993	0.99978	0.99904	0.99971	0.98669	0.99272	0.99993	0.99985	0.99897	0.99971	0.00034	0.00013	0.00375	0.00178	0.00278	0.00046	0.00027	6.7E-05	0.00327	0.00165	0.00245	0.00032	-0.06586	-0.03492	-0.00763	-0.00382	-0.00078	-0.00028	-0.05856	-0.03106	-0.00671	-0.00357	-0.0009	-0.00036	-0.04142	-0.02265	0.01217	0.01317	-0.00316	-0.00079	-0.03671	-0.01996	0.01007	0.00753	-0.0031	-0.00079	0.73508	0.73583	0.48935	0.48825	0.24513	0.2447	0.73598	0.73395	0.48935	0.4925	0.2455	0.24638	0.4911	0.3915	0.3901	0.293	0.1952	0.0979	0.4911	0.3904	0.3906	0.2929	0.1957	0.0987	0.75	0.75	0.5	0.5	0.25	0.25	0.75	0.75	0.5	0.5	0.25	0.25	0.5	0.4	0.4	0.3	0.2	0.1	0.5	0.4	0.4	0.3	0.2	0.1	0.761	0.779	0.519	0.516	0.25398	0.2568	0.779	0.7699	0.514	0.521	0.254	0.252	0.515	0.409	0.408	0.303	0.202	0.101	0.503	0.41	0.406	0.302	0.202	0.102	0.7676	0.7817	0.5128	0.5179	0.2547	0.2574	0.7811	0.7706	0.5163	0.5225	0.2563	0.2538	0.52	0.412	0.411	0.308	0.204	0.103	0.509	0.413	0.41	0.306	0.207	0.103	Crack inclination (θ) 45°												0.99992	0.99999	0.9981	0.99893	0.99861	0.99963	0.99988	0.99999	0.99832	0.99908	0.99855	0.99959	0.99491	0.99714	0.99191	0.99588	0.99996	0.99994	0.99543	0.99745	0.99294	0.99633	0.99988	0.9999	0.98492	0.99184	0.99993	0.99978	0.99904	0.99971	0.98669	0.99272	0.99993	0.99985	0.99897	0.99971	0.00034	0.00013	0.00375	0.00178	0.00278	0.00046	0.00027	6.7E-05	0.00327	0.00165	0.00245	0.00032	-0.06586	-0.03492	-0.00763	-0.00382	-0.00078	-0.00028	-0.05856	-0.03106	-0.00671	-0.00357	-0.0009	-0.00036	-0.04142	-0.02265	0.01217	0.01317	-0.00316	-0.00079	-0.03671	-0.01996	0.01007	0.00753	-0.0031	-0.00079	0.73508	0.73583	0.48935	0.48825	0.24513	0.2447	0.73598	0.73395	0.48935	0.4925	0.2455	0.24638	0.4911	0.3915	0.3901	0.293	0.1952	0.0979	0.4911	0.3904	0.3906	0.2929	0.1957	0.0987	0.75	0.75	0.5	0.5	0.25	0.25	0.75	0.75	0.5	0.5	0.25	0.25	0.5	0.4	0.4	0.3	0.2	0.1	0.5	0.4	0.4	0.3	0.2	0.1	0.761	0.779	0.519	0.516	0.25398	0.2568	0.779	0.7699	0.514	0.521	0.254	0.252	0.515	0.409	0.408	0.303	0.202	0.101	0.503	0.41	0.406	0.302	0.202	0.102	0.7676	0.7817	0.5128	0.5179	0.2547	0.2574	0.7811	0.7706	0.5163	0.5225	0.2563	0.2538	0.52	0.412	0.411	0.308	0.204	0.103	0.509	0.413	0.41	0.306	0.207	0.103	Numerical												FEA												ANN												Experiment												β												α																																																																																																																							
0.772	0.781	0.513	0.518	0.256	0.251	0.781	0.775	0.518	0.5122	0.2575	0.257	0.511	0.435	0.408	0.309	0.201	0.101	0.509	0.408	0.4	0.309	0.2068	0.103	0.7743	0.7826	0.5138	0.521	0.2594	0.258	0.7838	0.7799	0.52	0.5125	0.2588	0.2575	0.517	0.441	0.41	0.312	0.207	0.103	0.515	0.411	0.41	0.311	0.207	0.104	Crack inclination (θ) 30°												0.99992	0.99999	0.9981	0.99893	0.99861	0.99963	0.99988	0.99999	0.99832	0.99908	0.99855	0.99959	0.99491	0.99714	0.99191	0.99588	0.99996	0.99994	0.99543	0.99745	0.99294	0.99633	0.99988	0.9999	0.98492	0.99184	0.99993	0.99978	0.99904	0.99971	0.98669	0.99272	0.99993	0.99985	0.99897	0.99971	0.00034	0.00013	0.00375	0.00178	0.00278	0.00046	0.00027	6.7E-05	0.00327	0.00165	0.00245	0.00032	-0.06586	-0.03492	-0.00763	-0.00382	-0.00078	-0.00028	-0.05856	-0.03106	-0.00671	-0.00357	-0.0009	-0.00036	-0.04142	-0.02265	0.01217	0.01317	-0.00316	-0.00079	-0.03671	-0.01996	0.01007	0.00753	-0.0031	-0.00079	0.73508	0.73583	0.48935	0.48825	0.24513	0.2447	0.73598	0.73395	0.48935	0.4925	0.2455	0.24638	0.4911	0.3915	0.3901	0.293	0.1952	0.0979	0.4911	0.3904	0.3906	0.2929	0.1957	0.0987	0.75	0.75	0.5	0.5	0.25	0.25	0.75	0.75	0.5	0.5	0.25	0.25	0.5	0.4	0.4	0.3	0.2	0.1	0.5	0.4	0.4	0.3	0.2	0.1	0.761	0.779	0.519	0.516	0.25398	0.2568	0.779	0.7699	0.514	0.521	0.254	0.252	0.515	0.409	0.408	0.303	0.202	0.101	0.503	0.41	0.406	0.302	0.202	0.102	0.7676	0.7817	0.5128	0.5179	0.2547	0.2574	0.7811	0.7706	0.5163	0.5225	0.2563	0.2538	0.52	0.412	0.411	0.308	0.204	0.103	0.509	0.413	0.41	0.306	0.207	0.103	Crack inclination (θ) 45°												0.99992	0.99999	0.9981	0.99893	0.99861	0.99963	0.99988	0.99999	0.99832	0.99908	0.99855	0.99959	0.99491	0.99714	0.99191	0.99588	0.99996	0.99994	0.99543	0.99745	0.99294	0.99633	0.99988	0.9999	0.98492	0.99184	0.99993	0.99978	0.99904	0.99971	0.98669	0.99272	0.99993	0.99985	0.99897	0.99971	0.00034	0.00013	0.00375	0.00178	0.00278	0.00046	0.00027	6.7E-05	0.00327	0.00165	0.00245	0.00032	-0.06586	-0.03492	-0.00763	-0.00382	-0.00078	-0.00028	-0.05856	-0.03106	-0.00671	-0.00357	-0.0009	-0.00036	-0.04142	-0.02265	0.01217	0.01317	-0.00316	-0.00079	-0.03671	-0.01996	0.01007	0.00753	-0.0031	-0.00079	0.73508	0.73583	0.48935	0.48825	0.24513	0.2447	0.73598	0.73395	0.48935	0.4925	0.2455	0.24638	0.4911	0.3915	0.3901	0.293	0.1952	0.0979	0.4911	0.3904	0.3906	0.2929	0.1957	0.0987	0.75	0.75	0.5	0.5	0.25	0.25	0.75	0.75	0.5	0.5	0.25	0.25	0.5	0.4	0.4	0.3	0.2	0.1	0.5	0.4	0.4	0.3	0.2	0.1	0.761	0.779	0.519	0.516	0.25398	0.2568	0.779	0.7699	0.514	0.521	0.254	0.252	0.515	0.409	0.408	0.303	0.202	0.101	0.503	0.41	0.406	0.302	0.202	0.102	0.7676	0.7817	0.5128	0.5179	0.2547	0.2574	0.7811	0.7706	0.5163	0.5225	0.2563	0.2538	0.52	0.412	0.411	0.308	0.204	0.103	0.509	0.413	0.41	0.306	0.207	0.103	Numerical												FEA												ANN												Experiment												β												α																																																																																																																																			
0.511	0.435	0.408	0.309	0.201	0.101	0.509	0.408	0.4	0.309	0.2068	0.103	0.7743	0.7826	0.5138	0.521	0.2594	0.258	0.7838	0.7799	0.52	0.5125	0.2588	0.2575	0.517	0.441	0.41	0.312	0.207	0.103	0.515	0.411	0.41	0.311	0.207	0.104	Crack inclination (θ) 30°												0.99992	0.99999	0.9981	0.99893	0.99861	0.99963	0.99988	0.99999	0.99832	0.99908	0.99855	0.99959	0.99491	0.99714	0.99191	0.99588	0.99996	0.99994	0.99543	0.99745	0.99294	0.99633	0.99988	0.9999	0.98492	0.99184	0.99993	0.99978	0.99904	0.99971	0.98669	0.99272	0.99993	0.99985	0.99897	0.99971	0.00034	0.00013	0.00375	0.00178	0.00278	0.00046	0.00027	6.7E-05	0.00327	0.00165	0.00245	0.00032	-0.06586	-0.03492	-0.00763	-0.00382	-0.00078	-0.00028	-0.05856	-0.03106	-0.00671	-0.00357	-0.0009	-0.00036	-0.04142	-0.02265	0.01217	0.01317	-0.00316	-0.00079	-0.03671	-0.01996	0.01007	0.00753	-0.0031	-0.00079	0.73508	0.73583	0.48935	0.48825	0.24513	0.2447	0.73598	0.73395	0.48935	0.4925	0.2455	0.24638	0.4911	0.3915	0.3901	0.293	0.1952	0.0979	0.4911	0.3904	0.3906	0.2929	0.1957	0.0987	0.75	0.75	0.5	0.5	0.25	0.25	0.75	0.75	0.5	0.5	0.25	0.25	0.5	0.4	0.4	0.3	0.2	0.1	0.5	0.4	0.4	0.3	0.2	0.1	0.761	0.779	0.519	0.516	0.25398	0.2568	0.779	0.7699	0.514	0.521	0.254	0.252	0.515	0.409	0.408	0.303	0.202	0.101	0.503	0.41	0.406	0.302	0.202	0.102	0.7676	0.7817	0.5128	0.5179	0.2547	0.2574	0.7811	0.7706	0.5163	0.5225	0.2563	0.2538	0.52	0.412	0.411	0.308	0.204	0.103	0.509	0.413	0.41	0.306	0.207	0.103	Crack inclination (θ) 45°												0.99992	0.99999	0.9981	0.99893	0.99861	0.99963	0.99988	0.99999	0.99832	0.99908	0.99855	0.99959	0.99491	0.99714	0.99191	0.99588	0.99996	0.99994	0.99543	0.99745	0.99294	0.99633	0.99988	0.9999	0.98492	0.99184	0.99993	0.99978	0.99904	0.99971	0.98669	0.99272	0.99993	0.99985	0.99897	0.99971	0.00034	0.00013	0.00375	0.00178	0.00278	0.00046	0.00027	6.7E-05	0.00327	0.00165	0.00245	0.00032	-0.06586	-0.03492	-0.00763	-0.00382	-0.00078	-0.00028	-0.05856	-0.03106	-0.00671	-0.00357	-0.0009	-0.00036	-0.04142	-0.02265	0.01217	0.01317	-0.00316	-0.00079	-0.03671	-0.01996	0.01007	0.00753	-0.0031	-0.00079	0.73508	0.73583	0.48935	0.48825	0.24513	0.2447	0.73598	0.73395	0.48935	0.4925	0.2455	0.24638	0.4911	0.3915	0.3901	0.293	0.1952	0.0979	0.4911	0.3904	0.3906	0.2929	0.1957	0.0987	0.75	0.75	0.5	0.5	0.25	0.25	0.75	0.75	0.5	0.5	0.25	0.25	0.5	0.4	0.4	0.3	0.2	0.1	0.5	0.4	0.4	0.3	0.2	0.1	0.761	0.779	0.519	0.516	0.25398	0.2568	0.779	0.7699	0.514	0.521	0.254	0.252	0.515	0.409	0.408	0.303	0.202	0.101	0.503	0.41	0.406	0.302	0.202	0.102	0.7676	0.7817	0.5128	0.5179	0.2547	0.2574	0.7811	0.7706	0.5163	0.5225	0.2563	0.2538	0.52	0.412	0.411	0.308	0.204	0.103	0.509	0.413	0.41	0.306	0.207	0.103	Numerical												FEA												ANN												Experiment												β												α																																																																																																																																															
0.7743	0.7826	0.5138	0.521	0.2594	0.258	0.7838	0.7799	0.52	0.5125	0.2588	0.2575	0.517	0.441	0.41	0.312	0.207	0.103	0.515	0.411	0.41	0.311	0.207	0.104	Crack inclination (θ) 30°												0.99992	0.99999	0.9981	0.99893	0.99861	0.99963	0.99988	0.99999	0.99832	0.99908	0.99855	0.99959	0.99491	0.99714	0.99191	0.99588	0.99996	0.99994	0.99543	0.99745	0.99294	0.99633	0.99988	0.9999	0.98492	0.99184	0.99993	0.99978	0.99904	0.99971	0.98669	0.99272	0.99993	0.99985	0.99897	0.99971	0.00034	0.00013	0.00375	0.00178	0.00278	0.00046	0.00027	6.7E-05	0.00327	0.00165	0.00245	0.00032	-0.06586	-0.03492	-0.00763	-0.00382	-0.00078	-0.00028	-0.05856	-0.03106	-0.00671	-0.00357	-0.0009	-0.00036	-0.04142	-0.02265	0.01217	0.01317	-0.00316	-0.00079	-0.03671	-0.01996	0.01007	0.00753	-0.0031	-0.00079	0.73508	0.73583	0.48935	0.48825	0.24513	0.2447	0.73598	0.73395	0.48935	0.4925	0.2455	0.24638	0.4911	0.3915	0.3901	0.293	0.1952	0.0979	0.4911	0.3904	0.3906	0.2929	0.1957	0.0987	0.75	0.75	0.5	0.5	0.25	0.25	0.75	0.75	0.5	0.5	0.25	0.25	0.5	0.4	0.4	0.3	0.2	0.1	0.5	0.4	0.4	0.3	0.2	0.1	0.761	0.779	0.519	0.516	0.25398	0.2568	0.779	0.7699	0.514	0.521	0.254	0.252	0.515	0.409	0.408	0.303	0.202	0.101	0.503	0.41	0.406	0.302	0.202	0.102	0.7676	0.7817	0.5128	0.5179	0.2547	0.2574	0.7811	0.7706	0.5163	0.5225	0.2563	0.2538	0.52	0.412	0.411	0.308	0.204	0.103	0.509	0.413	0.41	0.306	0.207	0.103	Crack inclination (θ) 45°												0.99992	0.99999	0.9981	0.99893	0.99861	0.99963	0.99988	0.99999	0.99832	0.99908	0.99855	0.99959	0.99491	0.99714	0.99191	0.99588	0.99996	0.99994	0.99543	0.99745	0.99294	0.99633	0.99988	0.9999	0.98492	0.99184	0.99993	0.99978	0.99904	0.99971	0.98669	0.99272	0.99993	0.99985	0.99897	0.99971	0.00034	0.00013	0.00375	0.00178	0.00278	0.00046	0.00027	6.7E-05	0.00327	0.00165	0.00245	0.00032	-0.06586	-0.03492	-0.00763	-0.00382	-0.00078	-0.00028	-0.05856	-0.03106	-0.00671	-0.00357	-0.0009	-0.00036	-0.04142	-0.02265	0.01217	0.01317	-0.00316	-0.00079	-0.03671	-0.01996	0.01007	0.00753	-0.0031	-0.00079	0.73508	0.73583	0.48935	0.48825	0.24513	0.2447	0.73598	0.73395	0.48935	0.4925	0.2455	0.24638	0.4911	0.3915	0.3901	0.293	0.1952	0.0979	0.4911	0.3904	0.3906	0.2929	0.1957	0.0987	0.75	0.75	0.5	0.5	0.25	0.25	0.75	0.75	0.5	0.5	0.25	0.25	0.5	0.4	0.4	0.3	0.2	0.1	0.5	0.4	0.4	0.3	0.2	0.1	0.761	0.779	0.519	0.516	0.25398	0.2568	0.779	0.7699	0.514	0.521	0.254	0.252	0.515	0.409	0.408	0.303	0.202	0.101	0.503	0.41	0.406	0.302	0.202	0.102	0.7676	0.7817	0.5128	0.5179	0.2547	0.2574	0.7811	0.7706	0.5163	0.5225	0.2563	0.2538	0.52	0.412	0.411	0.308	0.204	0.103	0.509	0.413	0.41	0.306	0.207	0.103	Numerical												FEA												ANN												Experiment												β												α																																																																																																																																																											
0.517	0.441	0.41	0.312	0.207	0.103	0.515	0.411	0.41	0.311	0.207	0.104																																																																																																																																																																																																																																																																																																																																																																																																																																																																																																																																																																																																												
Crack inclination (θ) 30°																																																																																																																																																																																																																																																																																																																																																																																																																																																																																																																																																																																																																							
0.99992	0.99999	0.9981	0.99893	0.99861	0.99963	0.99988	0.99999	0.99832	0.99908	0.99855	0.99959	0.99491	0.99714	0.99191	0.99588	0.99996	0.99994	0.99543	0.99745	0.99294	0.99633	0.99988	0.9999	0.98492	0.99184	0.99993	0.99978	0.99904	0.99971	0.98669	0.99272	0.99993	0.99985	0.99897	0.99971	0.00034	0.00013	0.00375	0.00178	0.00278	0.00046	0.00027	6.7E-05	0.00327	0.00165	0.00245	0.00032	-0.06586	-0.03492	-0.00763	-0.00382	-0.00078	-0.00028	-0.05856	-0.03106	-0.00671	-0.00357	-0.0009	-0.00036	-0.04142	-0.02265	0.01217	0.01317	-0.00316	-0.00079	-0.03671	-0.01996	0.01007	0.00753	-0.0031	-0.00079	0.73508	0.73583	0.48935	0.48825	0.24513	0.2447	0.73598	0.73395	0.48935	0.4925	0.2455	0.24638	0.4911	0.3915	0.3901	0.293	0.1952	0.0979	0.4911	0.3904	0.3906	0.2929	0.1957	0.0987	0.75	0.75	0.5	0.5	0.25	0.25	0.75	0.75	0.5	0.5	0.25	0.25	0.5	0.4	0.4	0.3	0.2	0.1	0.5	0.4	0.4	0.3	0.2	0.1	0.761	0.779	0.519	0.516	0.25398	0.2568	0.779	0.7699	0.514	0.521	0.254	0.252	0.515	0.409	0.408	0.303	0.202	0.101	0.503	0.41	0.406	0.302	0.202	0.102	0.7676	0.7817	0.5128	0.5179	0.2547	0.2574	0.7811	0.7706	0.5163	0.5225	0.2563	0.2538	0.52	0.412	0.411	0.308	0.204	0.103	0.509	0.413	0.41	0.306	0.207	0.103	Crack inclination (θ) 45°												0.99992	0.99999	0.9981	0.99893	0.99861	0.99963	0.99988	0.99999	0.99832	0.99908	0.99855	0.99959	0.99491	0.99714	0.99191	0.99588	0.99996	0.99994	0.99543	0.99745	0.99294	0.99633	0.99988	0.9999	0.98492	0.99184	0.99993	0.99978	0.99904	0.99971	0.98669	0.99272	0.99993	0.99985	0.99897	0.99971	0.00034	0.00013	0.00375	0.00178	0.00278	0.00046	0.00027	6.7E-05	0.00327	0.00165	0.00245	0.00032	-0.06586	-0.03492	-0.00763	-0.00382	-0.00078	-0.00028	-0.05856	-0.03106	-0.00671	-0.00357	-0.0009	-0.00036	-0.04142	-0.02265	0.01217	0.01317	-0.00316	-0.00079	-0.03671	-0.01996	0.01007	0.00753	-0.0031	-0.00079	0.73508	0.73583	0.48935	0.48825	0.24513	0.2447	0.73598	0.73395	0.48935	0.4925	0.2455	0.24638	0.4911	0.3915	0.3901	0.293	0.1952	0.0979	0.4911	0.3904	0.3906	0.2929	0.1957	0.0987	0.75	0.75	0.5	0.5	0.25	0.25	0.75	0.75	0.5	0.5	0.25	0.25	0.5	0.4	0.4	0.3	0.2	0.1	0.5	0.4	0.4	0.3	0.2	0.1	0.761	0.779	0.519	0.516	0.25398	0.2568	0.779	0.7699	0.514	0.521	0.254	0.252	0.515	0.409	0.408	0.303	0.202	0.101	0.503	0.41	0.406	0.302	0.202	0.102	0.7676	0.7817	0.5128	0.5179	0.2547	0.2574	0.7811	0.7706	0.5163	0.5225	0.2563	0.2538	0.52	0.412	0.411	0.308	0.204	0.103	0.509	0.413	0.41	0.306	0.207	0.103	Numerical												FEA												ANN												Experiment												β												α																																																																																																																																																																																															
0.99491	0.99714	0.99191	0.99588	0.99996	0.99994	0.99543	0.99745	0.99294	0.99633	0.99988	0.9999	0.98492	0.99184	0.99993	0.99978	0.99904	0.99971	0.98669	0.99272	0.99993	0.99985	0.99897	0.99971	0.00034	0.00013	0.00375	0.00178	0.00278	0.00046	0.00027	6.7E-05	0.00327	0.00165	0.00245	0.00032	-0.06586	-0.03492	-0.00763	-0.00382	-0.00078	-0.00028	-0.05856	-0.03106	-0.00671	-0.00357	-0.0009	-0.00036	-0.04142	-0.02265	0.01217	0.01317	-0.00316	-0.00079	-0.03671	-0.01996	0.01007	0.00753	-0.0031	-0.00079	0.73508	0.73583	0.48935	0.48825	0.24513	0.2447	0.73598	0.73395	0.48935	0.4925	0.2455	0.24638	0.4911	0.3915	0.3901	0.293	0.1952	0.0979	0.4911	0.3904	0.3906	0.2929	0.1957	0.0987	0.75	0.75	0.5	0.5	0.25	0.25	0.75	0.75	0.5	0.5	0.25	0.25	0.5	0.4	0.4	0.3	0.2	0.1	0.5	0.4	0.4	0.3	0.2	0.1	0.761	0.779	0.519	0.516	0.25398	0.2568	0.779	0.7699	0.514	0.521	0.254	0.252	0.515	0.409	0.408	0.303	0.202	0.101	0.503	0.41	0.406	0.302	0.202	0.102	0.7676	0.7817	0.5128	0.5179	0.2547	0.2574	0.7811	0.7706	0.5163	0.5225	0.2563	0.2538	0.52	0.412	0.411	0.308	0.204	0.103	0.509	0.413	0.41	0.306	0.207	0.103	Crack inclination (θ) 45°												0.99992	0.99999	0.9981	0.99893	0.99861	0.99963	0.99988	0.99999	0.99832	0.99908	0.99855	0.99959	0.99491	0.99714	0.99191	0.99588	0.99996	0.99994	0.99543	0.99745	0.99294	0.99633	0.99988	0.9999	0.98492	0.99184	0.99993	0.99978	0.99904	0.99971	0.98669	0.99272	0.99993	0.99985	0.99897	0.99971	0.00034	0.00013	0.00375	0.00178	0.00278	0.00046	0.00027	6.7E-05	0.00327	0.00165	0.00245	0.00032	-0.06586	-0.03492	-0.00763	-0.00382	-0.00078	-0.00028	-0.05856	-0.03106	-0.00671	-0.00357	-0.0009	-0.00036	-0.04142	-0.02265	0.01217	0.01317	-0.00316	-0.00079	-0.03671	-0.01996	0.01007	0.00753	-0.0031	-0.00079	0.73508	0.73583	0.48935	0.48825	0.24513	0.2447	0.73598	0.73395	0.48935	0.4925	0.2455	0.24638	0.4911	0.3915	0.3901	0.293	0.1952	0.0979	0.4911	0.3904	0.3906	0.2929	0.1957	0.0987	0.75	0.75	0.5	0.5	0.25	0.25	0.75	0.75	0.5	0.5	0.25	0.25	0.5	0.4	0.4	0.3	0.2	0.1	0.5	0.4	0.4	0.3	0.2	0.1	0.761	0.779	0.519	0.516	0.25398	0.2568	0.779	0.7699	0.514	0.521	0.254	0.252	0.515	0.409	0.408	0.303	0.202	0.101	0.503	0.41	0.406	0.302	0.202	0.102	0.7676	0.7817	0.5128	0.5179	0.2547	0.2574	0.7811	0.7706	0.5163	0.5225	0.2563	0.2538	0.52	0.412	0.411	0.308	0.204	0.103	0.509	0.413	0.41	0.306	0.207	0.103	Numerical												FEA												ANN												Experiment												β												α																																																																																																																																																																																																											
0.98492	0.99184	0.99993	0.99978	0.99904	0.99971	0.98669	0.99272	0.99993	0.99985	0.99897	0.99971	0.00034	0.00013	0.00375	0.00178	0.00278	0.00046	0.00027	6.7E-05	0.00327	0.00165	0.00245	0.00032	-0.06586	-0.03492	-0.00763	-0.00382	-0.00078	-0.00028	-0.05856	-0.03106	-0.00671	-0.00357	-0.0009	-0.00036	-0.04142	-0.02265	0.01217	0.01317	-0.00316	-0.00079	-0.03671	-0.01996	0.01007	0.00753	-0.0031	-0.00079	0.73508	0.73583	0.48935	0.48825	0.24513	0.2447	0.73598	0.73395	0.48935	0.4925	0.2455	0.24638	0.4911	0.3915	0.3901	0.293	0.1952	0.0979	0.4911	0.3904	0.3906	0.2929	0.1957	0.0987	0.75	0.75	0.5	0.5	0.25	0.25	0.75	0.75	0.5	0.5	0.25	0.25	0.5	0.4	0.4	0.3	0.2	0.1	0.5	0.4	0.4	0.3	0.2	0.1	0.761	0.779	0.519	0.516	0.25398	0.2568	0.779	0.7699	0.514	0.521	0.254	0.252	0.515	0.409	0.408	0.303	0.202	0.101	0.503	0.41	0.406	0.302	0.202	0.102	0.7676	0.7817	0.5128	0.5179	0.2547	0.2574	0.7811	0.7706	0.5163	0.5225	0.2563	0.2538	0.52	0.412	0.411	0.308	0.204	0.103	0.509	0.413	0.41	0.306	0.207	0.103	Crack inclination (θ) 45°												0.99992	0.99999	0.9981	0.99893	0.99861	0.99963	0.99988	0.99999	0.99832	0.99908	0.99855	0.99959	0.99491	0.99714	0.99191	0.99588	0.99996	0.99994	0.99543	0.99745	0.99294	0.99633	0.99988	0.9999	0.98492	0.99184	0.99993	0.99978	0.99904	0.99971	0.98669	0.99272	0.99993	0.99985	0.99897	0.99971	0.00034	0.00013	0.00375	0.00178	0.00278	0.00046	0.00027	6.7E-05	0.00327	0.00165	0.00245	0.00032	-0.06586	-0.03492	-0.00763	-0.00382	-0.00078	-0.00028	-0.05856	-0.03106	-0.00671	-0.00357	-0.0009	-0.00036	-0.04142	-0.02265	0.01217	0.01317	-0.00316	-0.00079	-0.03671	-0.01996	0.01007	0.00753	-0.0031	-0.00079	0.73508	0.73583	0.48935	0.48825	0.24513	0.2447	0.73598	0.73395	0.48935	0.4925	0.2455	0.24638	0.4911	0.3915	0.3901	0.293	0.1952	0.0979	0.4911	0.3904	0.3906	0.2929	0.1957	0.0987	0.75	0.75	0.5	0.5	0.25	0.25	0.75	0.75	0.5	0.5	0.25	0.25	0.5	0.4	0.4	0.3	0.2	0.1	0.5	0.4	0.4	0.3	0.2	0.1	0.761	0.779	0.519	0.516	0.25398	0.2568	0.779	0.7699	0.514	0.521	0.254	0.252	0.515	0.409	0.408	0.303	0.202	0.101	0.503	0.41	0.406	0.302	0.202	0.102	0.7676	0.7817	0.5128	0.5179	0.2547	0.2574	0.7811	0.7706	0.5163	0.5225	0.2563	0.2538	0.52	0.412	0.411	0.308	0.204	0.103	0.509	0.413	0.41	0.306	0.207	0.103	Numerical												FEA												ANN												Experiment												β												α																																																																																																																																																																																																																							
0.00034	0.00013	0.00375	0.00178	0.00278	0.00046	0.00027	6.7E-05	0.00327	0.00165	0.00245	0.00032	-0.06586	-0.03492	-0.00763	-0.00382	-0.00078	-0.00028	-0.05856	-0.03106	-0.00671	-0.00357	-0.0009	-0.00036	-0.04142	-0.02265	0.01217	0.01317	-0.00316	-0.00079	-0.03671	-0.01996	0.01007	0.00753	-0.0031	-0.00079	0.73508	0.73583	0.48935	0.48825	0.24513	0.2447	0.73598	0.73395	0.48935	0.4925	0.2455	0.24638	0.4911	0.3915	0.3901	0.293	0.1952	0.0979	0.4911	0.3904	0.3906	0.2929	0.1957	0.0987	0.75	0.75	0.5	0.5	0.25	0.25	0.75	0.75	0.5	0.5	0.25	0.25	0.5	0.4	0.4	0.3	0.2	0.1	0.5	0.4	0.4	0.3	0.2	0.1	0.761	0.779	0.519	0.516	0.25398	0.2568	0.779	0.7699	0.514	0.521	0.254	0.252	0.515	0.409	0.408	0.303	0.202	0.101	0.503	0.41	0.406	0.302	0.202	0.102	0.7676	0.7817	0.5128	0.5179	0.2547	0.2574	0.7811	0.7706	0.5163	0.5225	0.2563	0.2538	0.52	0.412	0.411	0.308	0.204	0.103	0.509	0.413	0.41	0.306	0.207	0.103	Crack inclination (θ) 45°												0.99992	0.99999	0.9981	0.99893	0.99861	0.99963	0.99988	0.99999	0.99832	0.99908	0.99855	0.99959	0.99491	0.99714	0.99191	0.99588	0.99996	0.99994	0.99543	0.99745	0.99294	0.99633	0.99988	0.9999	0.98492	0.99184	0.99993	0.99978	0.99904	0.99971	0.98669	0.99272	0.99993	0.99985	0.99897	0.99971	0.00034	0.00013	0.00375	0.00178	0.00278	0.00046	0.00027	6.7E-05	0.00327	0.00165	0.00245	0.00032	-0.06586	-0.03492	-0.00763	-0.00382	-0.00078	-0.00028	-0.05856	-0.03106	-0.00671	-0.00357	-0.0009	-0.00036	-0.04142	-0.02265	0.01217	0.01317	-0.00316	-0.00079	-0.03671	-0.01996	0.01007	0.00753	-0.0031	-0.00079	0.73508	0.73583	0.48935	0.48825	0.24513	0.2447	0.73598	0.73395	0.48935	0.4925	0.2455	0.24638	0.4911	0.3915	0.3901	0.293	0.1952	0.0979	0.4911	0.3904	0.3906	0.2929	0.1957	0.0987	0.75	0.75	0.5	0.5	0.25	0.25	0.75	0.75	0.5	0.5	0.25	0.25	0.5	0.4	0.4	0.3	0.2	0.1	0.5	0.4	0.4	0.3	0.2	0.1	0.761	0.779	0.519	0.516	0.25398	0.2568	0.779	0.7699	0.514	0.521	0.254	0.252	0.515	0.409	0.408	0.303	0.202	0.101	0.503	0.41	0.406	0.302	0.202	0.102	0.7676	0.7817	0.5128	0.5179	0.2547	0.2574	0.7811	0.7706	0.5163	0.5225	0.2563	0.2538	0.52	0.412	0.411	0.308	0.204	0.103	0.509	0.413	0.41	0.306	0.207	0.103	Numerical												FEA												ANN												Experiment												β												α																																																																																																																																																																																																																																			
-0.06586	-0.03492	-0.00763	-0.00382	-0.00078	-0.00028	-0.05856	-0.03106	-0.00671	-0.00357	-0.0009	-0.00036	-0.04142	-0.02265	0.01217	0.01317	-0.00316	-0.00079	-0.03671	-0.01996	0.01007	0.00753	-0.0031	-0.00079	0.73508	0.73583	0.48935	0.48825	0.24513	0.2447	0.73598	0.73395	0.48935	0.4925	0.2455	0.24638	0.4911	0.3915	0.3901	0.293	0.1952	0.0979	0.4911	0.3904	0.3906	0.2929	0.1957	0.0987	0.75	0.75	0.5	0.5	0.25	0.25	0.75	0.75	0.5	0.5	0.25	0.25	0.5	0.4	0.4	0.3	0.2	0.1	0.5	0.4	0.4	0.3	0.2	0.1	0.761	0.779	0.519	0.516	0.25398	0.2568	0.779	0.7699	0.514	0.521	0.254	0.252	0.515	0.409	0.408	0.303	0.202	0.101	0.503	0.41	0.406	0.302	0.202	0.102	0.7676	0.7817	0.5128	0.5179	0.2547	0.2574	0.7811	0.7706	0.5163	0.5225	0.2563	0.2538	0.52	0.412	0.411	0.308	0.204	0.103	0.509	0.413	0.41	0.306	0.207	0.103	Crack inclination (θ) 45°												0.99992	0.99999	0.9981	0.99893	0.99861	0.99963	0.99988	0.99999	0.99832	0.99908	0.99855	0.99959	0.99491	0.99714	0.99191	0.99588	0.99996	0.99994	0.99543	0.99745	0.99294	0.99633	0.99988	0.9999	0.98492	0.99184	0.99993	0.99978	0.99904	0.99971	0.98669	0.99272	0.99993	0.99985	0.99897	0.99971	0.00034	0.00013	0.00375	0.00178	0.00278	0.00046	0.00027	6.7E-05	0.00327	0.00165	0.00245	0.00032	-0.06586	-0.03492	-0.00763	-0.00382	-0.00078	-0.00028	-0.05856	-0.03106	-0.00671	-0.00357	-0.0009	-0.00036	-0.04142	-0.02265	0.01217	0.01317	-0.00316	-0.00079	-0.03671	-0.01996	0.01007	0.00753	-0.0031	-0.00079	0.73508	0.73583	0.48935	0.48825	0.24513	0.2447	0.73598	0.73395	0.48935	0.4925	0.2455	0.24638	0.4911	0.3915	0.3901	0.293	0.1952	0.0979	0.4911	0.3904	0.3906	0.2929	0.1957	0.0987	0.75	0.75	0.5	0.5	0.25	0.25	0.75	0.75	0.5	0.5	0.25	0.25	0.5	0.4	0.4	0.3	0.2	0.1	0.5	0.4	0.4	0.3	0.2	0.1	0.761	0.779	0.519	0.516	0.25398	0.2568	0.779	0.7699	0.514	0.521	0.254	0.252	0.515	0.409	0.408	0.303	0.202	0.101	0.503	0.41	0.406	0.302	0.202	0.102	0.7676	0.7817	0.5128	0.5179	0.2547	0.2574	0.7811	0.7706	0.5163	0.5225	0.2563	0.2538	0.52	0.412	0.411	0.308	0.204	0.103	0.509	0.413	0.41	0.306	0.207	0.103	Numerical												FEA												ANN												Experiment												β												α																																																																																																																																																																																																																																															
-0.04142	-0.02265	0.01217	0.01317	-0.00316	-0.00079	-0.03671	-0.01996	0.01007	0.00753	-0.0031	-0.00079	0.73508	0.73583	0.48935	0.48825	0.24513	0.2447	0.73598	0.73395	0.48935	0.4925	0.2455	0.24638	0.4911	0.3915	0.3901	0.293	0.1952	0.0979	0.4911	0.3904	0.3906	0.2929	0.1957	0.0987	0.75	0.75	0.5	0.5	0.25	0.25	0.75	0.75	0.5	0.5	0.25	0.25	0.5	0.4	0.4	0.3	0.2	0.1	0.5	0.4	0.4	0.3	0.2	0.1	0.761	0.779	0.519	0.516	0.25398	0.2568	0.779	0.7699	0.514	0.521	0.254	0.252	0.515	0.409	0.408	0.303	0.202	0.101	0.503	0.41	0.406	0.302	0.202	0.102	0.7676	0.7817	0.5128	0.5179	0.2547	0.2574	0.7811	0.7706	0.5163	0.5225	0.2563	0.2538	0.52	0.412	0.411	0.308	0.204	0.103	0.509	0.413	0.41	0.306	0.207	0.103	Crack inclination (θ) 45°												0.99992	0.99999	0.9981	0.99893	0.99861	0.99963	0.99988	0.99999	0.99832	0.99908	0.99855	0.99959	0.99491	0.99714	0.99191	0.99588	0.99996	0.99994	0.99543	0.99745	0.99294	0.99633	0.99988	0.9999	0.98492	0.99184	0.99993	0.99978	0.99904	0.99971	0.98669	0.99272	0.99993	0.99985	0.99897	0.99971	0.00034	0.00013	0.00375	0.00178	0.00278	0.00046	0.00027	6.7E-05	0.00327	0.00165	0.00245	0.00032	-0.06586	-0.03492	-0.00763	-0.00382	-0.00078	-0.00028	-0.05856	-0.03106	-0.00671	-0.00357	-0.0009	-0.00036	-0.04142	-0.02265	0.01217	0.01317	-0.00316	-0.00079	-0.03671	-0.01996	0.01007	0.00753	-0.0031	-0.00079	0.73508	0.73583	0.48935	0.48825	0.24513	0.2447	0.73598	0.73395	0.48935	0.4925	0.2455	0.24638	0.4911	0.3915	0.3901	0.293	0.1952	0.0979	0.4911	0.3904	0.3906	0.2929	0.1957	0.0987	0.75	0.75	0.5	0.5	0.25	0.25	0.75	0.75	0.5	0.5	0.25	0.25	0.5	0.4	0.4	0.3	0.2	0.1	0.5	0.4	0.4	0.3	0.2	0.1	0.761	0.779	0.519	0.516	0.25398	0.2568	0.779	0.7699	0.514	0.521	0.254	0.252	0.515	0.409	0.408	0.303	0.202	0.101	0.503	0.41	0.406	0.302	0.202	0.102	0.7676	0.7817	0.5128	0.5179	0.2547	0.2574	0.7811	0.7706	0.5163	0.5225	0.2563	0.2538	0.52	0.412	0.411	0.308	0.204	0.103	0.509	0.413	0.41	0.306	0.207	0.103	Numerical												FEA												ANN												Experiment												β												α																																																																																																																																																																																																																																																											
0.73508	0.73583	0.48935	0.48825	0.24513	0.2447	0.73598	0.73395	0.48935	0.4925	0.2455	0.24638	0.4911	0.3915	0.3901	0.293	0.1952	0.0979	0.4911	0.3904	0.3906	0.2929	0.1957	0.0987	0.75	0.75	0.5	0.5	0.25	0.25	0.75	0.75	0.5	0.5	0.25	0.25	0.5	0.4	0.4	0.3	0.2	0.1	0.5	0.4	0.4	0.3	0.2	0.1	0.761	0.779	0.519	0.516	0.25398	0.2568	0.779	0.7699	0.514	0.521	0.254	0.252	0.515	0.409	0.408	0.303	0.202	0.101	0.503	0.41	0.406	0.302	0.202	0.102	0.7676	0.7817	0.5128	0.5179	0.2547	0.2574	0.7811	0.7706	0.5163	0.5225	0.2563	0.2538	0.52	0.412	0.411	0.308	0.204	0.103	0.509	0.413	0.41	0.306	0.207	0.103	Crack inclination (θ) 45°												0.99992	0.99999	0.9981	0.99893	0.99861	0.99963	0.99988	0.99999	0.99832	0.99908	0.99855	0.99959	0.99491	0.99714	0.99191	0.99588	0.99996	0.99994	0.99543	0.99745	0.99294	0.99633	0.99988	0.9999	0.98492	0.99184	0.99993	0.99978	0.99904	0.99971	0.98669	0.99272	0.99993	0.99985	0.99897	0.99971	0.00034	0.00013	0.00375	0.00178	0.00278	0.00046	0.00027	6.7E-05	0.00327	0.00165	0.00245	0.00032	-0.06586	-0.03492	-0.00763	-0.00382	-0.00078	-0.00028	-0.05856	-0.03106	-0.00671	-0.00357	-0.0009	-0.00036	-0.04142	-0.02265	0.01217	0.01317	-0.00316	-0.00079	-0.03671	-0.01996	0.01007	0.00753	-0.0031	-0.00079	0.73508	0.73583	0.48935	0.48825	0.24513	0.2447	0.73598	0.73395	0.48935	0.4925	0.2455	0.24638	0.4911	0.3915	0.3901	0.293	0.1952	0.0979	0.4911	0.3904	0.3906	0.2929	0.1957	0.0987	0.75	0.75	0.5	0.5	0.25	0.25	0.75	0.75	0.5	0.5	0.25	0.25	0.5	0.4	0.4	0.3	0.2	0.1	0.5	0.4	0.4	0.3	0.2	0.1	0.761	0.779	0.519	0.516	0.25398	0.2568	0.779	0.7699	0.514	0.521	0.254	0.252	0.515	0.409	0.408	0.303	0.202	0.101	0.503	0.41	0.406	0.302	0.202	0.102	0.7676	0.7817	0.5128	0.5179	0.2547	0.2574	0.7811	0.7706	0.5163	0.5225	0.2563	0.2538	0.52	0.412	0.411	0.308	0.204	0.103	0.509	0.413	0.41	0.306	0.207	0.103	Numerical												FEA												ANN												Experiment												β												α																																																																																																																																																																																																																																																																							
0.4911	0.3915	0.3901	0.293	0.1952	0.0979	0.4911	0.3904	0.3906	0.2929	0.1957	0.0987	0.75	0.75	0.5	0.5	0.25	0.25	0.75	0.75	0.5	0.5	0.25	0.25	0.5	0.4	0.4	0.3	0.2	0.1	0.5	0.4	0.4	0.3	0.2	0.1	0.761	0.779	0.519	0.516	0.25398	0.2568	0.779	0.7699	0.514	0.521	0.254	0.252	0.515	0.409	0.408	0.303	0.202	0.101	0.503	0.41	0.406	0.302	0.202	0.102	0.7676	0.7817	0.5128	0.5179	0.2547	0.2574	0.7811	0.7706	0.5163	0.5225	0.2563	0.2538	0.52	0.412	0.411	0.308	0.204	0.103	0.509	0.413	0.41	0.306	0.207	0.103	Crack inclination (θ) 45°												0.99992	0.99999	0.9981	0.99893	0.99861	0.99963	0.99988	0.99999	0.99832	0.99908	0.99855	0.99959	0.99491	0.99714	0.99191	0.99588	0.99996	0.99994	0.99543	0.99745	0.99294	0.99633	0.99988	0.9999	0.98492	0.99184	0.99993	0.99978	0.99904	0.99971	0.98669	0.99272	0.99993	0.99985	0.99897	0.99971	0.00034	0.00013	0.00375	0.00178	0.00278	0.00046	0.00027	6.7E-05	0.00327	0.00165	0.00245	0.00032	-0.06586	-0.03492	-0.00763	-0.00382	-0.00078	-0.00028	-0.05856	-0.03106	-0.00671	-0.00357	-0.0009	-0.00036	-0.04142	-0.02265	0.01217	0.01317	-0.00316	-0.00079	-0.03671	-0.01996	0.01007	0.00753	-0.0031	-0.00079	0.73508	0.73583	0.48935	0.48825	0.24513	0.2447	0.73598	0.73395	0.48935	0.4925	0.2455	0.24638	0.4911	0.3915	0.3901	0.293	0.1952	0.0979	0.4911	0.3904	0.3906	0.2929	0.1957	0.0987	0.75	0.75	0.5	0.5	0.25	0.25	0.75	0.75	0.5	0.5	0.25	0.25	0.5	0.4	0.4	0.3	0.2	0.1	0.5	0.4	0.4	0.3	0.2	0.1	0.761	0.779	0.519	0.516	0.25398	0.2568	0.779	0.7699	0.514	0.521	0.254	0.252	0.515	0.409	0.408	0.303	0.202	0.101	0.503	0.41	0.406	0.302	0.202	0.102	0.7676	0.7817	0.5128	0.5179	0.2547	0.2574	0.7811	0.7706	0.5163	0.5225	0.2563	0.2538	0.52	0.412	0.411	0.308	0.204	0.103	0.509	0.413	0.41	0.306	0.207	0.103	Numerical												FEA												ANN												Experiment												β												α																																																																																																																																																																																																																																																																																			
0.75	0.75	0.5	0.5	0.25	0.25	0.75	0.75	0.5	0.5	0.25	0.25	0.5	0.4	0.4	0.3	0.2	0.1	0.5	0.4	0.4	0.3	0.2	0.1	0.761	0.779	0.519	0.516	0.25398	0.2568	0.779	0.7699	0.514	0.521	0.254	0.252	0.515	0.409	0.408	0.303	0.202	0.101	0.503	0.41	0.406	0.302	0.202	0.102	0.7676	0.7817	0.5128	0.5179	0.2547	0.2574	0.7811	0.7706	0.5163	0.5225	0.2563	0.2538	0.52	0.412	0.411	0.308	0.204	0.103	0.509	0.413	0.41	0.306	0.207	0.103	Crack inclination (θ) 45°												0.99992	0.99999	0.9981	0.99893	0.99861	0.99963	0.99988	0.99999	0.99832	0.99908	0.99855	0.99959	0.99491	0.99714	0.99191	0.99588	0.99996	0.99994	0.99543	0.99745	0.99294	0.99633	0.99988	0.9999	0.98492	0.99184	0.99993	0.99978	0.99904	0.99971	0.98669	0.99272	0.99993	0.99985	0.99897	0.99971	0.00034	0.00013	0.00375	0.00178	0.00278	0.00046	0.00027	6.7E-05	0.00327	0.00165	0.00245	0.00032	-0.06586	-0.03492	-0.00763	-0.00382	-0.00078	-0.00028	-0.05856	-0.03106	-0.00671	-0.00357	-0.0009	-0.00036	-0.04142	-0.02265	0.01217	0.01317	-0.00316	-0.00079	-0.03671	-0.01996	0.01007	0.00753	-0.0031	-0.00079	0.73508	0.73583	0.48935	0.48825	0.24513	0.2447	0.73598	0.73395	0.48935	0.4925	0.2455	0.24638	0.4911	0.3915	0.3901	0.293	0.1952	0.0979	0.4911	0.3904	0.3906	0.2929	0.1957	0.0987	0.75	0.75	0.5	0.5	0.25	0.25	0.75	0.75	0.5	0.5	0.25	0.25	0.5	0.4	0.4	0.3	0.2	0.1	0.5	0.4	0.4	0.3	0.2	0.1	0.761	0.779	0.519	0.516	0.25398	0.2568	0.779	0.7699	0.514	0.521	0.254	0.252	0.515	0.409	0.408	0.303	0.202	0.101	0.503	0.41	0.406	0.302	0.202	0.102	0.7676	0.7817	0.5128	0.5179	0.2547	0.2574	0.7811	0.7706	0.5163	0.5225	0.2563	0.2538	0.52	0.412	0.411	0.308	0.204	0.103	0.509	0.413	0.41	0.306	0.207	0.103	Numerical												FEA												ANN												Experiment												β												α																																																																																																																																																																																																																																																																																															
0.5	0.4	0.4	0.3	0.2	0.1	0.5	0.4	0.4	0.3	0.2	0.1	0.761	0.779	0.519	0.516	0.25398	0.2568	0.779	0.7699	0.514	0.521	0.254	0.252	0.515	0.409	0.408	0.303	0.202	0.101	0.503	0.41	0.406	0.302	0.202	0.102	0.7676	0.7817	0.5128	0.5179	0.2547	0.2574	0.7811	0.7706	0.5163	0.5225	0.2563	0.2538	0.52	0.412	0.411	0.308	0.204	0.103	0.509	0.413	0.41	0.306	0.207	0.103	Crack inclination (θ) 45°												0.99992	0.99999	0.9981	0.99893	0.99861	0.99963	0.99988	0.99999	0.99832	0.99908	0.99855	0.99959	0.99491	0.99714	0.99191	0.99588	0.99996	0.99994	0.99543	0.99745	0.99294	0.99633	0.99988	0.9999	0.98492	0.99184	0.99993	0.99978	0.99904	0.99971	0.98669	0.99272	0.99993	0.99985	0.99897	0.99971	0.00034	0.00013	0.00375	0.00178	0.00278	0.00046	0.00027	6.7E-05	0.00327	0.00165	0.00245	0.00032	-0.06586	-0.03492	-0.00763	-0.00382	-0.00078	-0.00028	-0.05856	-0.03106	-0.00671	-0.00357	-0.0009	-0.00036	-0.04142	-0.02265	0.01217	0.01317	-0.00316	-0.00079	-0.03671	-0.01996	0.01007	0.00753	-0.0031	-0.00079	0.73508	0.73583	0.48935	0.48825	0.24513	0.2447	0.73598	0.73395	0.48935	0.4925	0.2455	0.24638	0.4911	0.3915	0.3901	0.293	0.1952	0.0979	0.4911	0.3904	0.3906	0.2929	0.1957	0.0987	0.75	0.75	0.5	0.5	0.25	0.25	0.75	0.75	0.5	0.5	0.25	0.25	0.5	0.4	0.4	0.3	0.2	0.1	0.5	0.4	0.4	0.3	0.2	0.1	0.761	0.779	0.519	0.516	0.25398	0.2568	0.779	0.7699	0.514	0.521	0.254	0.252	0.515	0.409	0.408	0.303	0.202	0.101	0.503	0.41	0.406	0.302	0.202	0.102	0.7676	0.7817	0.5128	0.5179	0.2547	0.2574	0.7811	0.7706	0.5163	0.5225	0.2563	0.2538	0.52	0.412	0.411	0.308	0.204	0.103	0.509	0.413	0.41	0.306	0.207	0.103	Numerical												FEA												ANN												Experiment												β												α																																																																																																																																																																																																																																																																																																											
0.761	0.779	0.519	0.516	0.25398	0.2568	0.779	0.7699	0.514	0.521	0.254	0.252	0.515	0.409	0.408	0.303	0.202	0.101	0.503	0.41	0.406	0.302	0.202	0.102	0.7676	0.7817	0.5128	0.5179	0.2547	0.2574	0.7811	0.7706	0.5163	0.5225	0.2563	0.2538	0.52	0.412	0.411	0.308	0.204	0.103	0.509	0.413	0.41	0.306	0.207	0.103	Crack inclination (θ) 45°												0.99992	0.99999	0.9981	0.99893	0.99861	0.99963	0.99988	0.99999	0.99832	0.99908	0.99855	0.99959	0.99491	0.99714	0.99191	0.99588	0.99996	0.99994	0.99543	0.99745	0.99294	0.99633	0.99988	0.9999	0.98492	0.99184	0.99993	0.99978	0.99904	0.99971	0.98669	0.99272	0.99993	0.99985	0.99897	0.99971	0.00034	0.00013	0.00375	0.00178	0.00278	0.00046	0.00027	6.7E-05	0.00327	0.00165	0.00245	0.00032	-0.06586	-0.03492	-0.00763	-0.00382	-0.00078	-0.00028	-0.05856	-0.03106	-0.00671	-0.00357	-0.0009	-0.00036	-0.04142	-0.02265	0.01217	0.01317	-0.00316	-0.00079	-0.03671	-0.01996	0.01007	0.00753	-0.0031	-0.00079	0.73508	0.73583	0.48935	0.48825	0.24513	0.2447	0.73598	0.73395	0.48935	0.4925	0.2455	0.24638	0.4911	0.3915	0.3901	0.293	0.1952	0.0979	0.4911	0.3904	0.3906	0.2929	0.1957	0.0987	0.75	0.75	0.5	0.5	0.25	0.25	0.75	0.75	0.5	0.5	0.25	0.25	0.5	0.4	0.4	0.3	0.2	0.1	0.5	0.4	0.4	0.3	0.2	0.1	0.761	0.779	0.519	0.516	0.25398	0.2568	0.779	0.7699	0.514	0.521	0.254	0.252	0.515	0.409	0.408	0.303	0.202	0.101	0.503	0.41	0.406	0.302	0.202	0.102	0.7676	0.7817	0.5128	0.5179	0.2547	0.2574	0.7811	0.7706	0.5163	0.5225	0.2563	0.2538	0.52	0.412	0.411	0.308	0.204	0.103	0.509	0.413	0.41	0.306	0.207	0.103	Numerical												FEA												ANN												Experiment												β												α																																																																																																																																																																																																																																																																																																																							
0.515	0.409	0.408	0.303	0.202	0.101	0.503	0.41	0.406	0.302	0.202	0.102	0.7676	0.7817	0.5128	0.5179	0.2547	0.2574	0.7811	0.7706	0.5163	0.5225	0.2563	0.2538	0.52	0.412	0.411	0.308	0.204	0.103	0.509	0.413	0.41	0.306	0.207	0.103	Crack inclination (θ) 45°												0.99992	0.99999	0.9981	0.99893	0.99861	0.99963	0.99988	0.99999	0.99832	0.99908	0.99855	0.99959	0.99491	0.99714	0.99191	0.99588	0.99996	0.99994	0.99543	0.99745	0.99294	0.99633	0.99988	0.9999	0.98492	0.99184	0.99993	0.99978	0.99904	0.99971	0.98669	0.99272	0.99993	0.99985	0.99897	0.99971	0.00034	0.00013	0.00375	0.00178	0.00278	0.00046	0.00027	6.7E-05	0.00327	0.00165	0.00245	0.00032	-0.06586	-0.03492	-0.00763	-0.00382	-0.00078	-0.00028	-0.05856	-0.03106	-0.00671	-0.00357	-0.0009	-0.00036	-0.04142	-0.02265	0.01217	0.01317	-0.00316	-0.00079	-0.03671	-0.01996	0.01007	0.00753	-0.0031	-0.00079	0.73508	0.73583	0.48935	0.48825	0.24513	0.2447	0.73598	0.73395	0.48935	0.4925	0.2455	0.24638	0.4911	0.3915	0.3901	0.293	0.1952	0.0979	0.4911	0.3904	0.3906	0.2929	0.1957	0.0987	0.75	0.75	0.5	0.5	0.25	0.25	0.75	0.75	0.5	0.5	0.25	0.25	0.5	0.4	0.4	0.3	0.2	0.1	0.5	0.4	0.4	0.3	0.2	0.1	0.761	0.779	0.519	0.516	0.25398	0.2568	0.779	0.7699	0.514	0.521	0.254	0.252	0.515	0.409	0.408	0.303	0.202	0.101	0.503	0.41	0.406	0.302	0.202	0.102	0.7676	0.7817	0.5128	0.5179	0.2547	0.2574	0.7811	0.7706	0.5163	0.5225	0.2563	0.2538	0.52	0.412	0.411	0.308	0.204	0.103	0.509	0.413	0.41	0.306	0.207	0.103	Numerical												FEA												ANN												Experiment												β												α																																																																																																																																																																																																																																																																																																																																			
0.7676	0.7817	0.5128	0.5179	0.2547	0.2574	0.7811	0.7706	0.5163	0.5225	0.2563	0.2538	0.52	0.412	0.411	0.308	0.204	0.103	0.509	0.413	0.41	0.306	0.207	0.103	Crack inclination (θ) 45°												0.99992	0.99999	0.9981	0.99893	0.99861	0.99963	0.99988	0.99999	0.99832	0.99908	0.99855	0.99959	0.99491	0.99714	0.99191	0.99588	0.99996	0.99994	0.99543	0.99745	0.99294	0.99633	0.99988	0.9999	0.98492	0.99184	0.99993	0.99978	0.99904	0.99971	0.98669	0.99272	0.99993	0.99985	0.99897	0.99971	0.00034	0.00013	0.00375	0.00178	0.00278	0.00046	0.00027	6.7E-05	0.00327	0.00165	0.00245	0.00032	-0.06586	-0.03492	-0.00763	-0.00382	-0.00078	-0.00028	-0.05856	-0.03106	-0.00671	-0.00357	-0.0009	-0.00036	-0.04142	-0.02265	0.01217	0.01317	-0.00316	-0.00079	-0.03671	-0.01996	0.01007	0.00753	-0.0031	-0.00079	0.73508	0.73583	0.48935	0.48825	0.24513	0.2447	0.73598	0.73395	0.48935	0.4925	0.2455	0.24638	0.4911	0.3915	0.3901	0.293	0.1952	0.0979	0.4911	0.3904	0.3906	0.2929	0.1957	0.0987	0.75	0.75	0.5	0.5	0.25	0.25	0.75	0.75	0.5	0.5	0.25	0.25	0.5	0.4	0.4	0.3	0.2	0.1	0.5	0.4	0.4	0.3	0.2	0.1	0.761	0.779	0.519	0.516	0.25398	0.2568	0.779	0.7699	0.514	0.521	0.254	0.252	0.515	0.409	0.408	0.303	0.202	0.101	0.503	0.41	0.406	0.302	0.202	0.102	0.7676	0.7817	0.5128	0.5179	0.2547	0.2574	0.7811	0.7706	0.5163	0.5225	0.2563	0.2538	0.52	0.412	0.411	0.308	0.204	0.103	0.509	0.413	0.41	0.306	0.207	0.103	Numerical												FEA												ANN												Experiment												β												α																																																																																																																																																																																																																																																																																																																																															
0.52	0.412	0.411	0.308	0.204	0.103	0.509	0.413	0.41	0.306	0.207	0.103																																																																																																																																																																																																																																																																																																																																																																																																																																																																																																																																																																																																												
Crack inclination (θ) 45°																																																																																																																																																																																																																																																																																																																																																																																																																																																																																																																																																																																																																							
0.99992	0.99999	0.9981	0.99893	0.99861	0.99963	0.99988	0.99999	0.99832	0.99908	0.99855	0.99959	0.99491	0.99714	0.99191	0.99588	0.99996	0.99994	0.99543	0.99745	0.99294	0.99633	0.99988	0.9999	0.98492	0.99184	0.99993	0.99978	0.99904	0.99971	0.98669	0.99272	0.99993	0.99985	0.99897	0.99971	0.00034	0.00013	0.00375	0.00178	0.00278	0.00046	0.00027	6.7E-05	0.00327	0.00165	0.00245	0.00032	-0.06586	-0.03492	-0.00763	-0.00382	-0.00078	-0.00028	-0.05856	-0.03106	-0.00671	-0.00357	-0.0009	-0.00036	-0.04142	-0.02265	0.01217	0.01317	-0.00316	-0.00079	-0.03671	-0.01996	0.01007	0.00753	-0.0031	-0.00079	0.73508	0.73583	0.48935	0.48825	0.24513	0.2447	0.73598	0.73395	0.48935	0.4925	0.2455	0.24638	0.4911	0.3915	0.3901	0.293	0.1952	0.0979	0.4911	0.3904	0.3906	0.2929	0.1957	0.0987	0.75	0.75	0.5	0.5	0.25	0.25	0.75	0.75	0.5	0.5	0.25	0.25	0.5	0.4	0.4	0.3	0.2	0.1	0.5	0.4	0.4	0.3	0.2	0.1	0.761	0.779	0.519	0.516	0.25398	0.2568	0.779	0.7699	0.514	0.521	0.254	0.252	0.515	0.409	0.408	0.303	0.202	0.101	0.503	0.41	0.406	0.302	0.202	0.102	0.7676	0.7817	0.5128	0.5179	0.2547	0.2574	0.7811	0.7706	0.5163	0.5225	0.2563	0.2538	0.52	0.412	0.411	0.308	0.204	0.103	0.509	0.413	0.41	0.306	0.207	0.103	Numerical												FEA												ANN												Experiment												β												α																																																																																																																																																																																																																																																																																																																																																																																			
0.99491	0.99714	0.99191	0.99588	0.99996	0.99994	0.99543	0.99745	0.99294	0.99633	0.99988	0.9999	0.98492	0.99184	0.99993	0.99978	0.99904	0.99971	0.98669	0.99272	0.99993	0.99985	0.99897	0.99971	0.00034	0.00013	0.00375	0.00178	0.00278	0.00046	0.00027	6.7E-05	0.00327	0.00165	0.00245	0.00032	-0.06586	-0.03492	-0.00763	-0.00382	-0.00078	-0.00028	-0.05856	-0.03106	-0.00671	-0.00357	-0.0009	-0.00036	-0.04142	-0.02265	0.01217	0.01317	-0.00316	-0.00079	-0.03671	-0.01996	0.01007	0.00753	-0.0031	-0.00079	0.73508	0.73583	0.48935	0.48825	0.24513	0.2447	0.73598	0.73395	0.48935	0.4925	0.2455	0.24638	0.4911	0.3915	0.3901	0.293	0.1952	0.0979	0.4911	0.3904	0.3906	0.2929	0.1957	0.0987	0.75	0.75	0.5	0.5	0.25	0.25	0.75	0.75	0.5	0.5	0.25	0.25	0.5	0.4	0.4	0.3	0.2	0.1	0.5	0.4	0.4	0.3	0.2	0.1	0.761	0.779	0.519	0.516	0.25398	0.2568	0.779	0.7699	0.514	0.521	0.254	0.252	0.515	0.409	0.408	0.303	0.202	0.101	0.503	0.41	0.406	0.302	0.202	0.102	0.7676	0.7817	0.5128	0.5179	0.2547	0.2574	0.7811	0.7706	0.5163	0.5225	0.2563	0.2538	0.52	0.412	0.411	0.308	0.204	0.103	0.509	0.413	0.41	0.306	0.207	0.103	Numerical												FEA												ANN												Experiment												β												α																																																																																																																																																																																																																																																																																																																																																																																															
0.98492	0.99184	0.99993	0.99978	0.99904	0.99971	0.98669	0.99272	0.99993	0.99985	0.99897	0.99971	0.00034	0.00013	0.00375	0.00178	0.00278	0.00046	0.00027	6.7E-05	0.00327	0.00165	0.00245	0.00032	-0.06586	-0.03492	-0.00763	-0.00382	-0.00078	-0.00028	-0.05856	-0.03106	-0.00671	-0.00357	-0.0009	-0.00036	-0.04142	-0.02265	0.01217	0.01317	-0.00316	-0.00079	-0.03671	-0.01996	0.01007	0.00753	-0.0031	-0.00079	0.73508	0.73583	0.48935	0.48825	0.24513	0.2447	0.73598	0.73395	0.48935	0.4925	0.2455	0.24638	0.4911	0.3915	0.3901	0.293	0.1952	0.0979	0.4911	0.3904	0.3906	0.2929	0.1957	0.0987	0.75	0.75	0.5	0.5	0.25	0.25	0.75	0.75	0.5	0.5	0.25	0.25	0.5	0.4	0.4	0.3	0.2	0.1	0.5	0.4	0.4	0.3	0.2	0.1	0.761	0.779	0.519	0.516	0.25398	0.2568	0.779	0.7699	0.514	0.521	0.254	0.252	0.515	0.409	0.408	0.303	0.202	0.101	0.503	0.41	0.406	0.302	0.202	0.102	0.7676	0.7817	0.5128	0.5179	0.2547	0.2574	0.7811	0.7706	0.5163	0.5225	0.2563	0.2538	0.52	0.412	0.411	0.308	0.204	0.103	0.509	0.413	0.41	0.306	0.207	0.103	Numerical												FEA												ANN												Experiment												β												α																																																																																																																																																																																																																																																																																																																																																																																																											
0.00034	0.00013	0.00375	0.00178	0.00278	0.00046	0.00027	6.7E-05	0.00327	0.00165	0.00245	0.00032	-0.06586	-0.03492	-0.00763	-0.00382	-0.00078	-0.00028	-0.05856	-0.03106	-0.00671	-0.00357	-0.0009	-0.00036	-0.04142	-0.02265	0.01217	0.01317	-0.00316	-0.00079	-0.03671	-0.01996	0.01007	0.00753	-0.0031	-0.00079	0.73508	0.73583	0.48935	0.48825	0.24513	0.2447	0.73598	0.73395	0.48935	0.4925	0.2455	0.24638	0.4911	0.3915	0.3901	0.293	0.1952	0.0979	0.4911	0.3904	0.3906	0.2929	0.1957	0.0987	0.75	0.75	0.5	0.5	0.25	0.25	0.75	0.75	0.5	0.5	0.25	0.25	0.5	0.4	0.4	0.3	0.2	0.1	0.5	0.4	0.4	0.3	0.2	0.1	0.761	0.779	0.519	0.516	0.25398	0.2568	0.779	0.7699	0.514	0.521	0.254	0.252	0.515	0.409	0.408	0.303	0.202	0.101	0.503	0.41	0.406	0.302	0.202	0.102	0.7676	0.7817	0.5128	0.5179	0.2547	0.2574	0.7811	0.7706	0.5163	0.5225	0.2563	0.2538	0.52	0.412	0.411	0.308	0.204	0.103	0.509	0.413	0.41	0.306	0.207	0.103	Numerical												FEA												ANN												Experiment												β												α																																																																																																																																																																																																																																																																																																																																																																																																																							
-0.06586	-0.03492	-0.00763	-0.00382	-0.00078	-0.00028	-0.05856	-0.03106	-0.00671	-0.00357	-0.0009	-0.00036	-0.04142	-0.02265	0.01217	0.01317	-0.00316	-0.00079	-0.03671	-0.01996	0.01007	0.00753	-0.0031	-0.00079	0.73508	0.73583	0.48935	0.48825	0.24513	0.2447	0.73598	0.73395	0.48935	0.4925	0.2455	0.24638	0.4911	0.3915	0.3901	0.293	0.1952	0.0979	0.4911	0.3904	0.3906	0.2929	0.1957	0.0987	0.75	0.75	0.5	0.5	0.25	0.25	0.75	0.75	0.5	0.5	0.25	0.25	0.5	0.4	0.4	0.3	0.2	0.1	0.5	0.4	0.4	0.3	0.2	0.1	0.761	0.779	0.519	0.516	0.25398	0.2568	0.779	0.7699	0.514	0.521	0.254	0.252	0.515	0.409	0.408	0.303	0.202	0.101	0.503	0.41	0.406	0.302	0.202	0.102	0.7676	0.7817	0.5128	0.5179	0.2547	0.2574	0.7811	0.7706	0.5163	0.5225	0.2563	0.2538	0.52	0.412	0.411	0.308	0.204	0.103	0.509	0.413	0.41	0.306	0.207	0.103	Numerical												FEA												ANN												Experiment												β												α																																																																																																																																																																																																																																																																																																																																																																																																																																			
-0.04142	-0.02265	0.01217	0.01317	-0.00316	-0.00079	-0.03671	-0.01996	0.01007	0.00753	-0.0031	-0.00079	0.73508	0.73583	0.48935	0.48825	0.24513	0.2447	0.73598	0.73395	0.48935	0.4925	0.2455	0.24638	0.4911	0.3915	0.3901	0.293	0.1952	0.0979	0.4911	0.3904	0.3906	0.2929	0.1957	0.0987	0.75	0.75	0.5	0.5	0.25	0.25	0.75	0.75	0.5	0.5	0.25	0.25	0.5	0.4	0.4	0.3	0.2	0.1	0.5	0.4	0.4	0.3	0.2	0.1	0.761	0.779	0.519	0.516	0.25398	0.2568	0.779	0.7699	0.514	0.521	0.254	0.252	0.515	0.409	0.408	0.303	0.202	0.101	0.503	0.41	0.406	0.302	0.202	0.102	0.7676	0.7817	0.5128	0.5179	0.2547	0.2574	0.7811	0.7706	0.5163	0.5225	0.2563	0.2538	0.52	0.412	0.411	0.308	0.204	0.103	0.509	0.413	0.41	0.306	0.207	0.103	Numerical												FEA												ANN												Experiment												β												α																																																																																																																																																																																																																																																																																																																																																																																																																																															
0.73508	0.73583	0.48935	0.48825	0.24513	0.2447	0.73598	0.73395	0.48935	0.4925	0.2455	0.24638	0.4911	0.3915	0.3901	0.293	0.1952	0.0979	0.4911	0.3904	0.3906	0.2929	0.1957	0.0987	0.75	0.75	0.5	0.5	0.25	0.25	0.75	0.75	0.5	0.5	0.25	0.25	0.5	0.4	0.4	0.3	0.2	0.1	0.5	0.4	0.4	0.3	0.2	0.1	0.761	0.779	0.519	0.516	0.25398	0.2568	0.779	0.7699	0.514	0.521	0.254	0.252	0.515	0.409	0.408	0.303	0.202	0.101	0.503	0.41	0.406	0.302	0.202	0.102	0.7676	0.7817	0.5128	0.5179	0.2547	0.2574	0.7811	0.7706	0.5163	0.5225	0.2563	0.2538	0.52	0.412	0.411	0.308	0.204	0.103	0.509	0.413	0.41	0.306	0.207	0.103	Numerical												FEA												ANN												Experiment												β												α																																																																																																																																																																																																																																																																																																																																																																																																																																																											
0.4911	0.3915	0.3901	0.293	0.1952	0.0979	0.4911	0.3904	0.3906	0.2929	0.1957	0.0987	0.75	0.75	0.5	0.5	0.25	0.25	0.75	0.75	0.5	0.5	0.25	0.25	0.5	0.4	0.4	0.3	0.2	0.1	0.5	0.4	0.4	0.3	0.2	0.1	0.761	0.779	0.519	0.516	0.25398	0.2568	0.779	0.7699	0.514	0.521	0.254	0.252	0.515	0.409	0.408	0.303	0.202	0.101	0.503	0.41	0.406	0.302	0.202	0.102	0.7676	0.7817	0.5128	0.5179	0.2547	0.2574	0.7811	0.7706	0.5163	0.5225	0.2563	0.2538	0.52	0.412	0.411	0.308	0.204	0.103	0.509	0.413	0.41	0.306	0.207	0.103	Numerical												FEA												ANN												Experiment												β												α																																																																																																																																																																																																																																																																																																																																																																																																																																																																							
0.75	0.75	0.5	0.5	0.25	0.25	0.75	0.75	0.5	0.5	0.25	0.25	0.5	0.4	0.4	0.3	0.2	0.1	0.5	0.4	0.4	0.3	0.2	0.1	0.761	0.779	0.519	0.516	0.25398	0.2568	0.779	0.7699	0.514	0.521	0.254	0.252	0.515	0.409	0.408	0.303	0.202	0.101	0.503	0.41	0.406	0.302	0.202	0.102	0.7676	0.7817	0.5128	0.5179	0.2547	0.2574	0.7811	0.7706	0.5163	0.5225	0.2563	0.2538	0.52	0.412	0.411	0.308	0.204	0.103	0.509	0.413	0.41	0.306	0.207	0.103	Numerical												FEA												ANN												Experiment												β												α																																																																																																																																																																																																																																																																																																																																																																																																																																																																																			
0.5	0.4	0.4	0.3	0.2	0.1	0.5	0.4	0.4	0.3	0.2	0.1	0.761	0.779	0.519	0.516	0.25398	0.2568	0.779	0.7699	0.514	0.521	0.254	0.252	0.515	0.409	0.408	0.303	0.202	0.101	0.503	0.41	0.406	0.302	0.202	0.102	0.7676	0.7817	0.5128	0.5179	0.2547	0.2574	0.7811	0.7706	0.5163	0.5225	0.2563	0.2538	0.52	0.412	0.411	0.308	0.204	0.103	0.509	0.413	0.41	0.306	0.207	0.103	Numerical												FEA												ANN												Experiment												β												α																																																																																																																																																																																																																																																																																																																																																																																																																																																																																															
0.761	0.779	0.519	0.516	0.25398	0.2568	0.779	0.7699	0.514	0.521	0.254	0.252	0.515	0.409	0.408	0.303	0.202	0.101	0.503	0.41	0.406	0.302	0.202	0.102	0.7676	0.7817	0.5128	0.5179	0.2547	0.2574	0.7811	0.7706	0.5163	0.5225	0.2563	0.2538	0.52	0.412	0.411	0.308	0.204	0.103	0.509	0.413	0.41	0.306	0.207	0.103	Numerical												FEA												ANN												Experiment												β												α																																																																																																																																																																																																																																																																																																																																																																																																																																																																																																											
0.515	0.409	0.408	0.303	0.202	0.101	0.503	0.41	0.406	0.302	0.202	0.102	0.7676	0.7817	0.5128	0.5179	0.2547	0.2574	0.7811	0.7706	0.5163	0.5225	0.2563	0.2538	0.52	0.412	0.411	0.308	0.204	0.103	0.509	0.413	0.41	0.306	0.207	0.103	Numerical												FEA												ANN												Experiment												β												α																																																																																																																																																																																																																																																																																																																																																																																																																																																																																																																							
0.7676	0.7817	0.5128	0.5179	0.2547	0.2574	0.7811	0.7706	0.5163	0.5225	0.2563	0.2538	0.52	0.412	0.411	0.308	0.204	0.103	0.509	0.413	0.41	0.306	0.207	0.103	Numerical												FEA												ANN												Experiment												β												α																																																																																																																																																																																																																																																																																																																																																																																																																																																																																																																																			
0.52	0.412	0.411	0.308	0.204	0.103	0.509	0.413	0.41	0.306	0.207	0.103																																																																																																																																																																																																																																																																																																																																																																																																																																																																																																																																																																																																												
Numerical																																																																																																																																																																																																																																																																																																																																																																																																																																																																																																																																																																																																																							
FEA																																																																																																																																																																																																																																																																																																																																																																																																																																																																																																																																																																																																																							
ANN																																																																																																																																																																																																																																																																																																																																																																																																																																																																																																																																																																																																																							
Experiment																																																																																																																																																																																																																																																																																																																																																																																																																																																																																																																																																																																																																							
β																																																																																																																																																																																																																																																																																																																																																																																																																																																																																																																																																																																																																							
α																																																																																																																																																																																																																																																																																																																																																																																																																																																																																																																																																																																																																							

Table 7.3. Comparing the results of modal analysis between Fuzzy Controller, numerical, FEA, ANN and Experimental

Crack inclination (θ) 15°										Crack inclination (θ) 0°																															
0.99981	0.99999	0.99817	0.99908	0.99852	0.99966	0.99992	0.99999	0.99809	0.99893	0.99846	0.99968	RFNF		0.99483	0.99714	0.99215	0.99609	0.99992	0.99998	0.99491	0.99703	0.99182	0.99582	RSNF		0.98514	0.99162	0.99993	0.99993	0.99897	0.99978	0.98529	0.9914	0.99993	0.99985	0.9989	0.99978	RTNF			
0.00034	0.00013	0.00375	0.00186	0.00269	0.0006	0.00034	0.00013	0.00391	0.00187	0.00259	0.0006	RFMD		-0.06545	-0.0371	-0.00757	-0.00382	-0.00088	-0.00019	-0.06516	-0.03827	-0.00788	-0.00394	RSMID		-0.04119	-0.02377	0.01086	0.00767	-0.00328	-0.00073	-0.04052	-0.02445	0.00928	0.01222	-0.00328	-0.00073	RTMD			
0.72	0.751	0.451	0.43	0.198	0.22	0.71	0.658	0.418	0.41	0.212	0.21	Triangular Fuzzy MF		0.44	0.34	0.32	0.26	0.154	0.06	0.45	0.385	0.301	0.25	Trapezoidal Fuzzy MF		0.729	0.761	0.462	0.435	0.21	0.230	0.731	0.698	0.426	0.423	0.221	0.221	Gaussian Fuzzy MF			
0.447	0.352	0.35	0.262	0.185	0.061	0.459	0.389	0.324	0.255	0.101	0.061	Bell-Shaped Fuzzy MF		0.737	0.769	0.472	0.441	0.232	0.241	0.742	0.725	0.435	0.232	Hybrid Fuzzy MF		0.452	0.364	0.389	0.275	0.195	0.069	0.479	0.391	0.356	0.267	0.111	0.072	ANN			
0.741	0.772	0.482	0.450	0.242	0.249	0.748	0.734	0.452	0.456	0.239	0.242	Numerical		0.465	0.386	0.398	0.283	0.199	0.075	0.485	0.399	0.389	0.279	FEA		0.752	0.781	0.492	0.498	0.482	0.253	0.752	0.745	0.482	0.501	0.246	0.251	Experiment			
0.497	0.389	0.399	0.298	0.2	0.09	0.502	0.409	0.395	0.301	0.187	0.101			0.497	0.389	0.399	0.298	0.2	0.09	0.502	0.409	0.395	0.301	0.187			0.497	0.389	0.399	0.298	0.2	0.09	0.502	0.409	0.395	0.301	0.187				
0.772	0.781	0.513	0.518	0.256	0.251	0.781	0.775	0.518	0.5122	0.2575	0.257			0.511	0.435	0.408	0.309	0.201	0.101	0.509	0.408	0.4	0.309	0.2068			0.73688	0.73313	0.49	0.49375	0.24563	0.24625	0.73125	0.72938	0.4875	0.49125	0.24625	0.245			
0.4894	0.3906	0.3898	0.2933	0.1963	0.0988	0.4875	0.392	0.389	0.294	0.195	0.0985			0.75	0.75	0.5	0.5	0.25	0.25	0.75	0.75	0.5	0.5	0.25	0.25			0.4894	0.3906	0.3898	0.2933	0.1963	0.0988	0.4875	0.392	0.389	0.294	0.195	0.0985		
0.75	0.4	0.4	0.3	0.2	0.1	0.5	0.4	0.4	0.3	0.2	0.1			0.5	0.4	0.4	0.3	0.2	0.1	0.5	0.4	0.4	0.3	0.2	0.1			0.75	0.4	0.4	0.3	0.2	0.1	0.5	0.4	0.4	0.3	0.2	0.1		
0.7743	0.7826	0.5138	0.521	0.2594	0.258	0.7838	0.7799	0.52	0.5125	0.2588	0.2575			0.7743	0.7826	0.5138	0.521	0.2594	0.258	0.7838	0.7799	0.52	0.5125	0.2588	0.2575			0.7743	0.7826	0.5138	0.521	0.2594	0.258	0.7838	0.7799	0.52	0.5125	0.2588	0.2575		
0.517	0.441	0.41	0.312	0.207	0.103	0.515	0.411	0.41	0.311	0.207	0.104			0.517	0.441	0.41	0.312	0.207	0.103	0.515	0.411	0.41	0.311	0.207	0.104			0.517	0.441	0.41	0.312	0.207	0.103	0.515	0.411	0.41	0.311	0.207	0.104		

7.8. Summary

An artificial neural network (ANN) model with six inputs and three outputs has been developed for crack identification in cracked cantilever beam elements. The training data for the developed neural network model have been derived from theoretical, finite element and experimental analysis. The results obtained from the neural network model for crack parameters are very closer to the experimental results; therefore the neural network model can be effectively used for inclined crack identification in cracked cantilever beam structures. The comparison the results between different fuzzy controllers and ANN model, it is concluded that the predicted results from ANN controller are nearer to the experimental results as compared to the developed intelligent fuzzy controllers.

CHAPTER 08

INSTALLATION AND DESCRIPTION OF EXPERIMENTAL SETUP FOR IDENTIFICATION OF CRACK

- 8.1. Introduction**
- 8.2. Detail specifications of the vibration measuring instruments**
- 8.3. Experimental procedure and its architecture**

CHAPTER 08

INSTALLATION AND DESCRIPTION OF EXPERIMENTAL SETUP FOR IDENTIFICATION OF CRACK

Experimental Analysis plays a key role in the research field. Experimental Analysis is being carried out to justify the validation of theoretical analysis, finite element analysis and different intelligent techniques projected in the chapter 6 to 7 for identification of crack. For the analysis, the experimental setup is made to determine the natural frequencies and mode shapes to observe the response of cantilever beam with the presence of inclined crack. The experimental setup is discussed in detail in the subsequent sections of this chapter.

8.1. Introduction




The experimental analysis has been carried out to measure the natural frequencies and mode shapes of the inclined crack cantilever beam. Experiments have been performed on the cracked beam structures with different crack location, crack depth and crack inclination to validate the results obtained from theoretical, finite element and other artificial intelligent techniques used for inclined crack detection as discussed in the previous chapters of the thesis. This chapter briefly describes the systematic procedures adopted for experimental investigation and the required instrumentation for measuring the vibration characteristics of the cantilever beam structures.



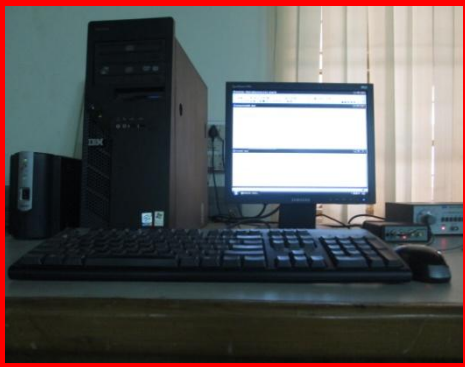

8.2. Detail specifications of the vibration measuring instruments

Experiments have been performed using the developed experimental set up (Table 8.1) for calculating the dynamic response (natural frequencies and amplitude of vibration) of the cantilever beam specimens made from Aluminum with dimension 800mm*60mm*6mm. During the experiment the cracked and un-cracked beams have been vibrated at their 1st, 2nd and 3rd mode of vibration by using an exciter and a function

generator. The vibrations characteristics of the beams correspond to 1st, 2nd and 3rd mode of vibration have been recorded by placing the accelerometer along the length of the beams. The signals from the accelerometer which contains the vibration parameters such as natural frequencies and mode shapes are analyzed and shown on the vibration indicator. The Table 8.1 shown below gives the detail specifications of the instruments used in the current experimental analysis.

Table 8.1. Specifications of the instruments used in the experimental set up

SL NO	Name of the Instrument	
1	<p>Vibration Analyzer</p> <p>Type : 3560L Product Name : Pocket front end Make : Bruel & kjaer Frequency : 7 Hz to 20 Khz ADC Bits : 16 Channels : 2 Inputs, 2 Tachometer Input Type : Direct/CCLD</p>	
2	<p>Accelerometer</p> <p>Type : 4513-001 Make : Bruel & kjaer Sensitivity : 10mv/g-500mv/g Frequency Range : 1Hz-10KHz Supply voltage : 24volts Operating temperature Range : -50⁰C to +100⁰C</p>	
4	<p>Vibration Exciter</p> <p>Type : 4808 Force rating 112N (25 lbf) sine peak) Frequency : 5Hz to 10 kHz First axial resonance : 10 kHz Acceleration : 700 m/s² (71 g) Continuous 12.7 mm (0.5 in)</p>	
3	<p>Power Distribution</p> <p>220V power supply, 50Hz</p>	

<p>5</p>	<p>Power Amplifier</p> <p>Type : 2719</p> <p>Power Amplifier : 180VA</p> <p>Make : Bruel & kjaer</p>	
<p>6</p>	<p>Test Specimen-beam</p> <p>Cracked (Multiple crack) cantilever beams made from Aluminum with dimension 800mmx60mmx6mm</p>	
<p>7</p>	<p>Vibration Indicator (PULSE Lab shop software)</p> <p>PULSE LabShop Software Version 12</p> <p>Make : Bruel & kjaer</p>	
<p>8</p>	<p>Function Generator</p> <p>Model : FG200K</p> <p>Frequency</p> <p>Range : 0.2Hz to 200 KHz</p> <p>Output Level : 15Vp-p into 600 ohms</p> <p>Rise/Fall Time : <300nSec</p>	

8.3. Experimental procedure and its architecture

The authenticity of the results obtained from theoretical, finite element and AI based techniques for inclined crack identification have been established by measuring the dynamic response of the undamaged and cracked Aluminum beam specimen through experimentation. The test specimen made from Aluminum is of 800 mm length and has a

cross section of 60mmx6 mm. The free end of the beam specimen was excited by an appropriate signal from the function generator, which was amplified by the amplifier. The cantilever was excited at first three modes of vibration, and the corresponding natural frequencies and mode shapes were recorded by the hard ware support i.e. miniature accelerometer by suitable positioning, data acquisition system and tuning the vibration generator at the corresponding resonant frequencies. Finally, the analysis of the vibration parameters from the intact and cracked beam were done by the PULSE Lab shop Software loaded in the laptop of the vibration analyzer.



Fig. 8.1. Complete view of the experimental setup

CHAPTER 9

CONCLUSION AND FUTURE WORK

- 9.1. Contribution**
- 9.2. Conclusion**
- 9.3. Application**
- 9.4. Scope for Future Work**

Reference

Publications

Appendix

CHAPTER 10

CONCLUSION AND FUTURE WORK

In the present work, identification of inclined crack in structural elements from the measured vibration parameters has been emphasized. During the crack detection, numerical method, finite element method and experimental method have been implemented to simulate the actual working condition. The measured natural frequencies and mode shapes at different modes of vibration, with different crack parameters, have been used to improve inverse techniques based AI techniques such as Fuzzy logic, Neural Network techniques for identification of relative crack location, relative crack depth and crack inclination angle.

10.1. Contributions

For identification of inclined crack, an analytical method has been developed on the basis of stress intensity factors and strain energy release rate to determine the effect of crack location, crack depth and crack inclination angle on changes of vibration signatures. Finite element method and experimental method have also been taken out on the inclined crack beam element to measure the effect of cracks on the vibration signatures of the beam. Different AI techniques have been composed for inclined crack identification using Fuzzy Inference System (FIS) and Artificial Neural Network (ANN).

10.2. Conclusions

Based on the results obtained from various techniques for identification of inclined crack on the cantilever beam structure, the following conclusions are drawn:

- ❖ Due to the changes in the crack parameters (crack location, crack depth and crack angle) there is always a significant change in the vibration parameters (natural frequencies and mode shapes).
- ❖ The results of the crack parameters have been obtained from the comparison of the results of the un-cracked and cracked cantilever beam during the vibration analysis. It is

also observed that analytical, finite element and experimental analysis are in good agreement.

❖ From the inspection of the mode shapes of the inclined cracked cantilever beam with different crack location, crack depth and crack inclination, the magnitude of deviation in mode shapes increases with increase in crack depths.

❖ When the crack location and crack inclination are constant, but the crack depth increases:

The natural frequency of the cracked beam decreases with increase the crack depth. The amplitude at crack location decreases with increase the crack depth for each mode shape.

❖ The crack depth and crack inclination are constant, but crack location increases from cantilever end:

When the crack location increases, the natural frequency also increases. At particular crack location of a beam, the amplitude is minimum w.r.t. other beams having a different crack location.

❖ The crack inclination angles are valid up to 45° for examining the transverse vibration. The crack location in the cantilever beam can be projected for crack size of more than 10% of depth.

❖ It has also been seen from experimental examples that the determination of the crack location is more precise than the determination of the crack size.

❖ The error increases as the crack position from the fixed end or the crack inclination angle increases. The maximum error is predicted up to 5% of all the cases calculated. The values found from FEA are in a good match with experimental values.

❖ The calculated vibration parameters from the first three modes of the cantilever beam model and the corresponding relative crack parameters have been used to design the fuzzy inference system (FIS) for inclined crack identification in structural elements.

❖ The FIS has six inputs and three outputs. The fuzzy controllers are based on fuzzy triangular, fuzzy trapezoidal, fuzzy Gaussian, fuzzy Bell-shaped and fuzzy hybrid membership functions. Results obtained from different fuzzy controllers, it has been found that, the developed fuzzy inverse models forecast the crack parameters more rapidly and

accurately than the theoretical and finite element analysis. Experimental results are also carried out for verifying the results from fuzzy controllers.

❖ The results obtained from different fuzzy controllers, it is observed that fuzzy model with Gaussian, Bell-shaped and hybrid membership function gives better results than the fuzzy model with triangular and trapezoidal membership function. So, these intelligent fuzzy controllers can be successfully used for structural health monitoring.

❖ An artificial neural network (ANN) model with six inputs and three outputs has been developed for crack identification in cracked cantilever beam elements. The training data for the developed neural network model have been derived from theoretical, finite element and experimental analysis. The results obtained from the neural network model for crack parameters are very closer to the experimental results; therefore the neural network model can be effectively used for inclined crack identification in cracked cantilever beam structures.

❖ The comparison the results between different fuzzy controllers and ANN model, it is concluded that the predicted results from ANN controller are nearer to the experimental results as compared to the developed intelligent fuzzy controllers.

10.3. Applications

❖ The developed intelligent techniques used for crack diagnosis are non-destructive in nature, so these intelligent techniques can be used for online condition monitoring of engineering systems.

❖ For crack diagnosis which uses optimization and Artificial Intelligence technique can be used for handling inverse engineering applications.

❖ The intelligent techniques developed for crack diagnosis can be used for online condition monitoring of various engineering structures like cantilever type bridges, beams, turbine shafts, cantilever type cranes, marine structures, nuclear plant, biomedical engineering applications, etc.

Scope for Future Work

- ❖ The artificial intelligent techniques may be developed to design in complex engineering structures.
- ❖ The application of the artificial intelligent techniques may be extended for multiple damage detection in bi material and composite material elements.
- ❖ More robust hybrid techniques may be developed and employed for fault detection of various vibrating parts in dynamic systems such as cone crusher, railway tracks, overhead cranes, oil rigs, turbine shafts etc.
- ❖ The artificial intelligence techniques may be embedded and integrated with the vibrating systems to make on line condition monitoring easier.

REFERENCES

- [1] Doebling, S.W., Farrar, C.R., Prime, M.B., “A summary review of vibration-based damage identification methods”, *Shock and Vibration Digest*, vol.30, no. 2, pp. 91–105, 1998.
- [2] Y. Narkis, “Identification of crack location in vibrating simply supported beams,” *Journal of Sound and Vibration*, vol. 172, no. 4, pp. 549-558, 1994.
- [3] P.C. Muller, J. Bajkowski and D. Soffker, “Chaotic Motions and Fault Detection in a Cracked Rotor,” *Nonlinear Dynamics*, Kluwer Academic Publishers, vol. 5, pp. 233-254, 1994.
- [4] S. Chinchalkar, “Determination of crack location in beams using natural frequencies,” *Journal of Sound and Vibration*, vol. 247, no. 3, pp. 417–429, 2001.
- [5] M.H.F. Dado and O. Abuzeid, “Coupled transverse and axial vibratory behaviour of cracked beam with end mass and rotary inertia,” *Journal of Sound and Vibration*, vol. 261, pp. 675–696, 2003.
- [6] Ohseop Song, Tae-Wan Ha, Liviu Librescu, “Dynamics of anisotropic composite cantilevers weakened by multiple transverse open cracks,” *Engineering Fracture Mechanics*, vol. 70, pp.105–123, 2003.
- [7] Luna Majumder and C.S. Manohar, “A time-domain approach for damage detection in beam structures using vibration data with a moving oscillator as an excitation source,” *Journal of Sound and Vibration*, vol. 268, pp.699–716, 2003.
- [8] Hai-Ping Lin, “Direct and inverse methods on free vibration analysis of simply supported beams with a crack,” *Engineering Structures*, vol. 26, pp. 427–436, 2004.
- [9] E. Douka and L.J. Hadjileontiadis, “Time – frequency analysis of the free vibration response of a beam with a breathing crack,” *NDT&E International*, vol. 38, pp. 3–10, 2005.
- [10] S. Loutridis, E. Douka and L.J. Hadjileontiadis, “Forced vibration behaviour and crack detection of cracked beams using instantaneous frequency,” *NDT&E International*, vol. 38, pp. 411–419, 2005.
- [11] S.S. Law and Z.R. Lu, “Crack identification in beam from dynamic responses,” *Journal of Sound and Vibration*, vol. 285, pp. 967–987, 2005.
- [12] T.G. Chondros, “Variational formulation of a rod under torsional vibration for crack identification,” *Theoretical and Applied Fracture Mechanics*, vol. 44, pp. 95–104, 2005.

- [13] T.G. Chondros and G.N. Labeas, "Torsional vibration of a cracked rod by variational formulation and numerical analysis," *Journal of Sound and Vibration*, vol. 301, pp. 994–1006, 2007.
- [14] J.A. Loya, L. Rubio and J. Fernandez-Saez, "Natural frequencies for bending vibrations of Timoshenko cracked beams," *Journal of Sound and Vibration*, vol. 290, pp. 640–653, 2006.
- [15] E. Viola, P. Ricci and M.H. Aliabadi, "Free vibration analysis of axially loaded cracked Timoshenko beam structures using the dynamic stiffness method," *Journal of Sound and Vibration*, vol. 304, pp. 124–153, 2007.
- [16] R.O. Curadelli, J.D. Riera, D. Ambrosini and M.G. Amani, "Damage detection by means of structural damping identification," *Engineering Structures*, vol. 30, pp. 3497-3504, 2008.
- [17] B. Faverjon and J.-J. Sinou, "Identification of an open crack in a beam using an a posteriori error estimator of the frequency response functions with noisy measurements," *European Journal of Mechanics A/Solids*, vol. 28, pp. 75–85, 2009.
- [18] Jinhee Lee, "Identification of multiple cracks in a beam using natural frequencies," *Journal of Sound and Vibration*, vol. 320, pp. 482–490, 2009.
- [19] H.W. Shih, D.P. Thambiratnam and T.H.T. Chan, "Vibration based structural damage detection in flexural members using multi-criteria approach," *Journal of Sound and Vibration*, vol. 323, pp. 645–661, 2009.
- [20] M. Behzad, A. Ebrahimi and A. Meghdari, "A Continuous Vibration Theory for Beams with a Vertical Edge Crack," *Transaction B: Mechanical Engineering*, Vol. 17, No. 3, pp. 194-204, 2010.
- [21] Michael Ryvkin and Leonid Slepyan, "Crack in a 2D beam lattice: Analytical solutions for two bending modes," *Journal of the Mechanics and Physics of Solids*, vol. 58, pp. 902–917, 2010.
- [22] Mousa Rezaee and Reza Hassannejad, "Damped free vibration analysis of a beam with a fatigue crack using energy balance method," *International Journal of the Physical Sciences*, Vol. 5(6), pp. 793-803, 2010.
- [23] RS Prasad, SC Roy and KP Tyagi, "Effect of Crack Position along Vibrating Cantilever Beam on Crack Growth Rate," *International Journal of Engineering Science and Technology*, Vol. 2(5), pp. 837-839, 2010.

- [24] Mousa Rezaee and Reza Hassannejad, "Free Vibration Analysis of simply Supported beam with breathing Crack Using Perturbation method," *Acta Mechanica Solida Sinica*, Vol. 23, No. 5, pp. 459-470, 2010.
- [25] Mousa Rezaee and Reza Hassannejad, "A New Approach to Free Vibration Analysis of a Beam with a Breathing Crack Based On Mechanical Energy Balance Method," *Acta Mechanica Solida Sinica*, Vol. 24, No. 2, pp. 185-194, 2011.
- [26] K. Mazanoglu and M. Sabuncu, "A frequency based algorithm for identification of single and double cracked beams via a statistical approach used in experiment," *Mechanical Systems and Signal Processing*, vol. 30, pp. 168–185, 2012.
- [27] Tianxin Zheng and Tianjian Ji, "An approximate method for determining the static deflection and natural frequency of a cracked beam," *Journal of Sound and Vibration*, vol. 331, pp. 2654–2670, 2012.
- [28] Wang-Ji Yan, Wei-Xin Ren and Tian-Li Huang, "Statistic structural damage detection based on the closed-form of element modal strain energy sensitivity," *Mechanical Systems and Signal Processing*, vol. 28, pp. 183–194, 2012.
- [29] Mostafa Attar, "A transfer matrix method for free vibration analysis and crack identification of stepped beams with multiple edge cracks and different boundary conditions," *International Journal of Mechanical Sciences*, vol. 57, pp. 19–33, 2012.
- [30] Ameneh Maghsoodi, Amin Ghadami and Hamid Reza Mirdamadi, "Multiple-crack damage detection in multi-step beams by a novel local flexibility-based damage index," *Journal of Sound and Vibration*, vol. 332, pp. 294–305, 2013.
- [31] Mehdi Behzad, Amin Ghadami, Ameneh Maghsoodi and Jack Michael Hale, "Vibration based algorithm for crack detection in cantilever beam containing two different types of cracks," *Journal of Sound and Vibration*, vol. 332, pp. 6312–6320, 2013.
- [32] B. P. NANDWANA and S. K. MAITI, "Modelling Of Vibration Of Beam In Presence Of Inclined Edge Or Internal Crack For Its Possible Detection Based On Frequency Measurements," *Engineering Fracture Mechanics*, Vol. 58, No. 3, pp. 193-205, 1997.
- [33] P.N. Saavedra and L.A. Cuitino, "Crack detection and vibration behavior of cracked beams," *computers and structures*, vol. 79, pp. 1451-1459, 2001.
- [34] E. Viola, L. Federici and L. Nobile, "Detection of crack location using cracked beam element method for structural analysis," *Theoretical and Applied Fracture Mechanics*, vol. 36, pp. 23-35, 2001.

- [35] D.Y. Zheng and N.J. Kessissoglou, "Free vibration analysis of a cracked beam by finite element method," *Journal of Sound and Vibration*, vol. 273, pp. 457–475, 2004.
- [36] Murat Kisa and M. Arif Gurel, "Modal analysis of multi-cracked beams with circular cross section," *Engineering Fracture Mechanics*, vol. 73, pp. 963–977, 2006.
- [37] Murat Kisa and M. Arif Gurel, "Free vibration analysis of uniform and stepped cracked beams with circular cross sections," *International Journal of Engineering Science*, vol. 45, pp. 364–380, 2007.
- [38] G.P. Potirniche, J. Hearndon, S.R. Daniewicz, D. Parker, P. Cuevas, P.T. Wang and M.F. Horstemeyer, "A two-dimensional damaged finite element for fracture applications," *Engineering Fracture Mechanics*, vol. 75, pp. 3895–3908, 2008.
- [39] H.B. Dong, X.F. Chen, B. Li, K.Y. Qi and Z.J. He, "Rotor crack detection based on high-precision modal parameter identification method and wavelet finite element model," *Mechanical Systems and Signal Processing*, vol. 23, pp. 869–883, 2009.
- [40] A. Ariaei, S. Ziaei-Rad and M. Ghayour, "Vibration analysis of beams with open and breathing cracks subjected to moving masses," *Journal of Sound and Vibration*, vol. 326, pp. 709–724, 2009.
- [41] Aysha Kalanad and B. N. Rao, "Detection of crack location and size in structures using improved damaged finite element," *IOP Conf. Series: Materials Science and Engineering*, vol. 10, pp. 012054, 2010.
- [42] Celalettin Karaagac, Hasan Ozturk and Mustafa Sabuncu, "Crack effects on the in-plane static and dynamic stabilities of a curved beam with an edge crack," *Journal of Sound and Vibration*, vol. 330, pp. 1718–1736, 2011.
- [43] Yue Cheng, Zhigang Yu, Xun Wu and Yuhua Yuan, "Vibration analysis of a cracked rotating tapered beam using the p-version finite element method," *Finite Elements in Analysis and Design*, vol. 47, pp. 825–834, 2011.
- [44] Aysha Kalanad and B.N. Rao, "Improved two-dimensional cracked finite element for crack fault diagnosis," *Computer Assisted Methods in Engineering and Science*, Copyright © 2012 by Institute of Fundamental Technological Research, Polish Academy of Sciences, vol. 19, pp. 213–239, 2012.
- [45] Kurt J. Hall and Gabriel P. Potirniche, "A three-dimensional edge-crack finite element for fracture mechanics applications," *International Journal of Solids and Structures*, vol. 49, pp. 28–337, 2012.
- [46] Mihir Kumar Sutar, "Finite Element Analysis of A Cracked Cantilever," *International Journal of Advanced Engineering Research and Studies*, E-ISSN2249–8974.

- [47] LI Bing, CHEN Xuefeng, and HE Zhengjia, “Three-Steps-Meshing based Multiple Crack Identification for Structures and Its Experimental Studies,” Chinese journal of mechanical engineering, vol. 26, no. 1, pp. 1-7,2013.
- [48] Irshad A Khan and Dayal R Parhi, “Finite Element Analysis of Double Cracked Beam and its Experimental Validation,” Procedia Engineering, vol. 51, pp. 703 – 708, 2013.
- [49] A. S. Bouboulas and N. K. Anifantis, “Three-dimensional finite element modeling of a vibrating beam with a breathing crack,” Arch Appl Mech, vol. 83, pp. 207–223, 2013.
- [50] M. Silani, S. Ziaei-Rad and H. Talebi, “Vibration analysis of rotating systems with open and breathing cracks,” Applied Mathematical Modelling, vol. xxx, pp. xxx–xxx, 2013.
- [51] Sazonov E.S., Klinkhachorn P., “Fuzzy logic expert system for automated damage detection from changes in strain energy mode shapes, Nondestructive Testing and Evaluation”, 8(1), 2002, pp.1 – 17.
- [52] Y. M. Kim, C.K. Kim and G. H. Hong, “Fuzzy set based crack diagnosis system for reinforced concrete structures, Computer sand Structures”, 85, pp.1828–1844, 2007.
- [53] T. Boutros and M. Liang, “Mechanical fault detection using fuzzy index fusion, International Journal of Machine Tools & Manufacture”, 47, pp. 1702–1714, 2007.
- [54] M. Chandrashekhar and Ranjan Ganguli, “Damage assessment of structures with uncertainty by using mode- shape curvatures and fuzzy logic, Journal of Sound and Vibration”, 26, pp. 939–957,2009.
- [55] A. K. Dash, D.R. Parhi, “Development of an inverse methodology for crack diagnosis using AI technique”, International Journal of Computational Materials Science and Surface Engineering (IJCMSSE), 2011, Vol. 4(2), pp.143-167.
- [56] V. Sugumaran and K.I. Ramachandran, “Fault diagnosis of roller bearing using fuzzy classifier and histogram features with focus on automatic rule learning”, Expert Systems with Applications, 2011, Vol. 38(5), pp.4901-4907.
- [57] S. Suresh, S.N. Omkar, R. Ganguli and V.Mani, “Identification of crack location and depth in a cantilever Beam Using a Modular Neural Network Approach, Smart Materials and Structures”, 13, pp. 907-916,2004.
- [58] M. Mehrjoo, N. Khaji, H. Moharrami and A. Bahreininejad, “Damage detection of truss bridge joints using Artificial Neural Networks”, Expert Systems with Applications, 35, pp. 1122–1131, 2008.

- [59] H. Das, D.R. Parhi, "Application of neural network for fault diagnosis of cracked cantilever beam" World Congress on Nature and Biologically Inspired Computing, Coimbatore, 2009; article no-5393733, pp 1303-1308.
- [60] G. Paviglianiti, F. Pierri, F. Caccavale and M. Mattei, "Robust fault detection and isolation for proprioceptive sensors of robot manipulators", *Mechatronics*, 20, 162–170, 2010.
- [61] I. Eski, S. Erkaya, S. Savas, S. Yildirim, "Fault detection on robot manipulators using artificial neural networks, *Robotics and Computer-Integrated Manufacturing*", 27 ,pp. 115–123, 2011.
- [62] D.R. Parhi, A. K. Dash, "Application of neural network and finite element for condition monitoring of structures", *Proceedings of the Institution of Mechanical Engineers, Part C: Journal of Mechanical Engineering Science*, 2011, Vol. 225, pp. 1329-1339.
- [63] Tada, H., Paris, P.C and Irwin G.R., 1973. *The stress analysis of cracks hand book*. Del Research Corp. Hellertown, Pennsylvanian.
- [64] D. R. Parhi, "Navigation of mobile robot using a fuzzy logic model. *Journal of Intelligent and Robotic Systems: Theory and Applications*, 42, pp. 253-273, 2005.
- [65] T. Takagi and M. Sugeno, "Fuzzy identification of systems and its application to modelling and control, *IEEE Trans. on Systems, Man, Cybernetics*, 15(1), pp.116-132, 1985.
- [66] A. K. Dash, D. R. Parhi, "Multiple Damage Identification of Beam Structure using Vibration Analysis and Artificial Intelligence Techniques", Ph.D. thesis, NIT Rourkela.

PUBLICATION

INTERNATIONAL CONFERENCE

- Presented a paper title “Numerical and Experimental Verification of a Method for Prognosis of Inclined Edge Crack in Cantilever Beam Based On Synthesis of Mode Shapes” in 2nd International Conference on Innovations in Automation and Mechatronics Engineering (ICIAME 2014), G H Patel College of Engineering & Technology, Vallabh Vidyanagar, Gujarat, 7th -8th, March, 2014.
- Presented a paper title “An Inverse Fuzzy Controller for Diagnosis of Inclined Edge Crack in Cantilever Beam Based on Frequency Response” in International Conference on Innovation in Design, Manufacturing and Concurrent Engineering (IDMC 2014), NIT Rourkela, Rourkela, Odisha, 1st -3rd, March 2014.
- Presented a paper title “Fault Diagnosis of Inclined Edge Crack Cantilever Beam based on Frequency Response and FEA” in 4th Nirma University International Conference on Engineering (NUiCONE 2013), Nirma University, Ahmedabad, 28th - 30th November, 2013.
- “A New Reactive Hybrid Membership Function in Fuzzy Approach for Identification of Inclined Edge Crack in Cantilever Beam Using Vibration Signatures” in International Mechanical Engineering Congress (IMEC 14), NIT Tiruchy, Tiruchirappalli, Tamil Nadu, 13rd – 15th, June, 2014. (Accepted)
- “Automatic Design of Fuzzy Rules using GA for fault Detection in Cracked Structures” in International Mechanical Engineering Congress (IMEC 14), NIT Tiruchy, Tiruchirappalli, Tamil Nadu, 13rd – 15th, June, 2014. (Accepted)

INTERNATIONAL JOURNAL

- Ranjan K. Behera, Dayal R. Parhi, “Fault Diagnosis of Inclined Edge Crack Cantilever Beam based on Frequency Response and FEA”, Procedia Engineering. (In Press)
- Ranjan K. Behera, Anish Pandey, Dayal R. Parhi, “Numerical and Experimental Verification of a Method for Prognosis of Inclined Edge Crack in Cantilever Beam Based On Synthesis of Mode Shapes”, Procedia Technology. (In Press)
- Ranjan K. Behera, Sasmita Sahu, Dayal R. Parhi, “A New Reactive Hybrid Membership Function in Fuzzy Approach for Identification of Inclined Edge Crack in Cantilever Beam Using Vibration Signatures”, Applied Mechanics and Materials. (Accepted)
- Sasmita Sahu, Ranjan K. Behera, Dayal R. Parhi, “Automatic Design of Fuzzy Rules

using GA for fault Detection in Cracked Structures”, Applied Mechanics and Materials. (Accepted)

- Dayal R. Parhi, Ranjan K. Behera, “Validation of results obtained from different types of fuzzy controllers for diagnosis of inclined edge crack in cantilever beam by vibration parameters”, Journal of Mechanical Design and Vibration. (communicated)
- Dayal R. Parhi, Ranjan K. Behera, Adik R. Yadao, “A review on vibrational parameters according to variation of crack parameters in the dynamic structures like beam”, International Journal of Applied Artificial Intelligence in Engineering System. (communicated)
- Dayal R. Parhi, Ranjan K. Behera, Adik R. Yadao, “Damage Detection of Inclined Edge Crack Cantilever Beam by Means of Both Analysis of Finite Elements and Synthesis of Mode Shapes Method”, International Journal of Applied Artificial Intelligence in Engineering System. (communicated)

APPENDIX

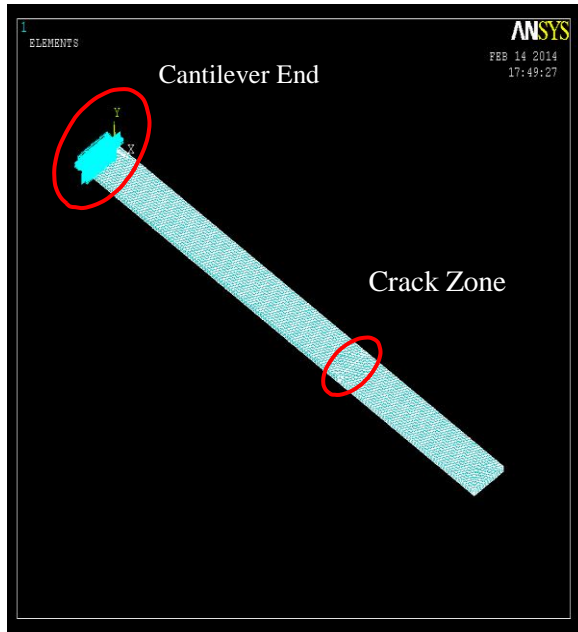


Fig.3. Finite element mesh model of the cracked beam

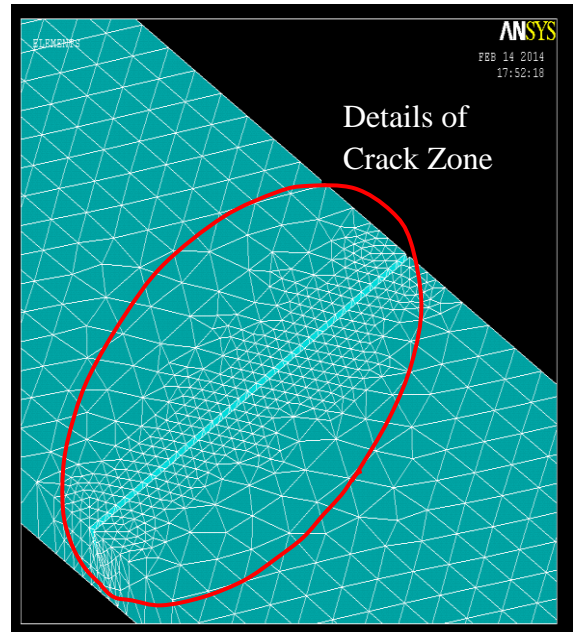


Fig.4. Magnified view at the crack zone

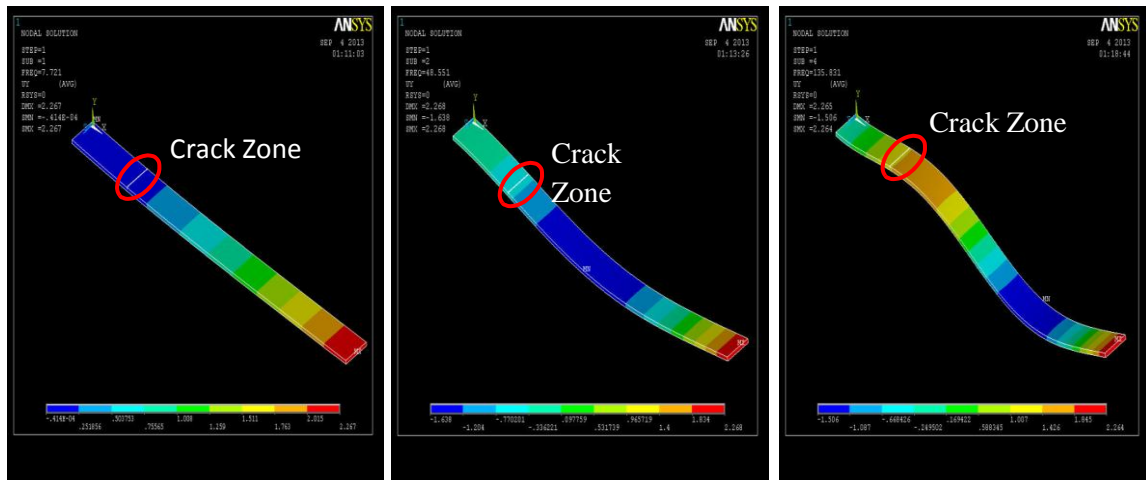


Fig.5. illustrates the mode shape variation of (a) 1st, (b) 2nd and (c) 3rd mode cantilever beam with crack at $\beta = 0.3$, $\alpha = 0.35$ and $\theta = 35^\circ$ respectively.